SESSION XII

OPEN END

Thursday, August 15, 1974
CHAIRMAN: Melvin W. First

ECONOMIC COMPARISON OF AN IMPROVED NUCLEAR FILTER SYSTEM CONSIDERING SPACE, OPERATION, TESTING, AND MAINTENANCE COSTS
J.R. Edwards, T. Hickey

THE EFFECT OF VARIOUS POLYMER BINDERS ON THE RADIATION RESISTANCE OF GLASS FIBER HEPA FILTER MEDIA
I.M. Hutten, E.C. Oswecki

ENHANCEMENT OF FILTER MEDIA PERFORMANCE BY CORONA-FREE ELECTRIC FIELDS
H.F. Bogardus, R.C. Clark
J.K. Thompson, G.H. Fielding

CHARACTERIZING SAND GRAINS TO OPTIMIZE FILTER PERFORMANCE
G.A. Schurr, J.E. Johnston

A CONSIDERATION OF THE SIGNIFICANCE OF CARBON-14 DISCHARGES FROM THE NUCLEAR POWER INDUSTRY
P.J. Magno, C.B. Nelson
W.H. Ellett

RESPIRATORY QUALITY ASSURANCE PROGRAM AT ROCKY FLATS
C.D. Skaats

THE BEHAVIOR OF FISSION GAS HOLDUP BEDS DURING NORMAL STARTUP, ACCIDENTAL LOSS OF REFRIGERATION, AND SPILLAGE OF CHARCOAL
Dwight Underhill

HEPA FILTERS FOR OFF-GAS SYSTEMS OF BWR UNITS
Robert Avery

A STUDY OF MOISTURE SEPARATORS FOR FINE PARTICLE WATER-AIR-STREAM SERVICE
Wayne L. Smith

RADIOIODINE SORPTION ON ACTIVE CARBONS FROM LIQUID PHASE
Z. Vuković, O. Janković,
Lj. Knezevic, A. Svabić

ECONOMIC COMPARISON OF AN IMPROVED NUCLEAR FILTER SYSTEM CONSIDERING SPACE, OPERATION, TESTING AND MAINTENANCE COSTS

James R. Edwards
Flanders Filters Inc., Kingston, North Carolina

Thomas N. Hickey
CVI Corporation, Columbus, Ohio

Abstract

The development of an all-welded charcoal adsorber design for increased system iodine removal efficiency has provided certain other unique advantages of particular interest to nuclear power plant personnel involved in health/safety, operation, maintenance, testing and space allocation for nuclear filter systems.

The design features providing these unique advantages have been refined and tested and are available and installed on operating reactors as a standard filter system trademarked HECA by the CVI Corporation.

Health/safety aspects of the system are improved through the use of a unique pneumatic conveying system which eliminates the need for entrance of maintenance personnel into the filter housing during removal and replacement of spent charcoal and; thereby, minimizes radiation exposure of occupational personnel.

Operational and maintenance costs, after capital investment, for nuclear filter systems being of particular interest to utility operations management are compared with conventional iodine adsorber systems. The material cost savings in charcoal replacement with the system can exceed capital investment costs for given operating conditions.

Testing and retest for by-pass leakage location and correction experiences are described and comparisons drawn between the HECA system and conventional designs.

Space allocation improvements for actual nuclear filter system installations are described using the HECA system in conjunction with Flanders 1500 CFM "Superflow" absolute filter modules.

Features of the separatorless absolute superflow filter that complement the like design features of the all-welded HECA charcoal adsorber are described and operational and test data are presented.

I. Introduction

A considerable amount of effort has been directed by industry and regulatory towards the improvement in reliability and contaminant removal performance of Nuclear Filter/Adsorber Systems.

Performance and reliability are, of course, prime criteria, especially for nuclear filter systems designated as engineered safety features. However, also important are other criteria such as ease of operation, testing and maintenance[1] and minimum radiation exposure to occupational personnel[2].

This paper, presented in two parts, discusses in Part One a High Efficiency Charcoal Adsorber (HECA^{TM}) System which demonstrates significant improvements in the foregoing criteria, in comparison with filter/adsorber systems utilizing the conventional drawer or tray type adsorber cells.

In addition, by combining the HECA^{TM} Adsorber System with separatorless, high efficiency particulate filter elements as manufactured by Flanders Filter, Inc., it is possible to reduce the cross sectional area of the filter assembly normal to direction of flow by 50 percent per volumetric unit of air flow.

The performance and advantages of this Superflow Filter are discussed in detail in Part Two of this paper.

II. Health/Safety

The exposure of maintenance personnel during adsorbent change-out with the HECA^{TM} system, relative to a conventional system, can be illustrated by discussion of the schematic diagrams shown on Figure 1.

Refering to Figure 1, the interconnections and equipment required are shown schematically for both removing used adsorbent (carbon) and for refilling the system beds.

The arrangement shown provides a pneumatic conveying system which is negative in pressure with respect to the occupational area for both fill and drain modes of operation.

During drain operation (Figure 1 A), the used carbon is removed from the adsorbent bed assembly and transferred to the disposal container via a flexible conduit after first having passed through a separator for removal of the heavier fines.

The separator exhaust air and remaining adsorbent fines are then ducted to bag filters and finally through a high efficiency absolute filter for completion of removal of particulates prior to discharge from the exhaust turbine.

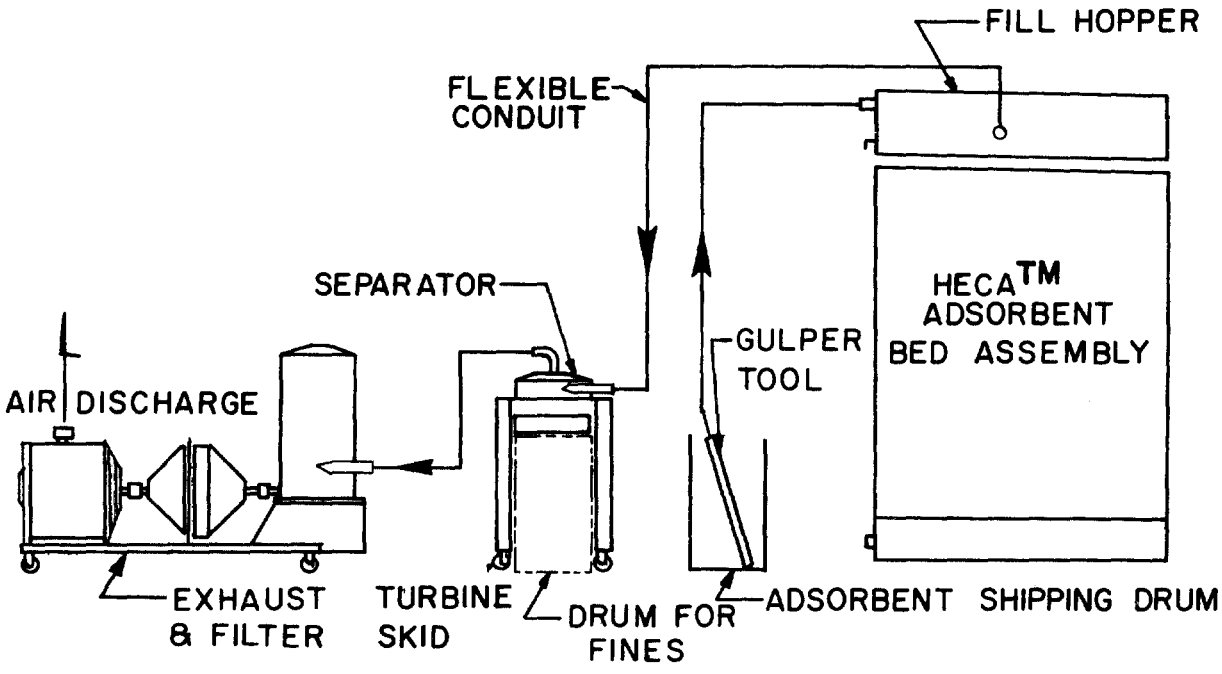

FIG. I-B FILLING MODE

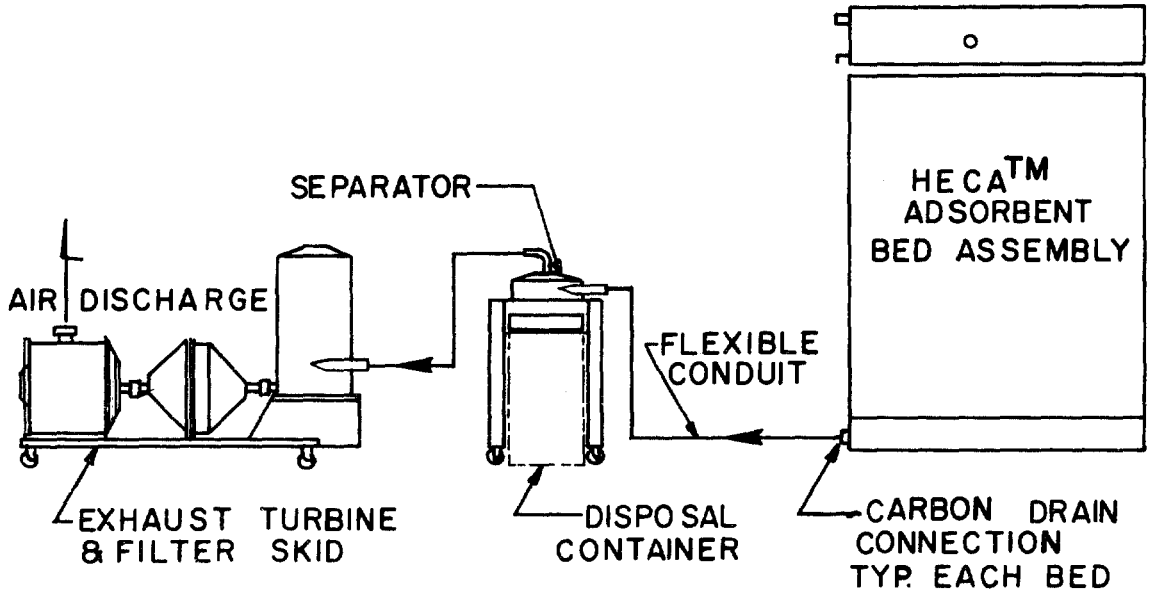

FIG. I-A DRAIN MODE

ADSORBENT CHANGE SYSTEM SCHEMATICS

FIGURE 1

The arrangement described will allow the complete removal of all adsorbent from the filter bed assembly without the need for entry of maintenance personnel into the filter housings. Further, and if required, installation of the interconnecting flexible conduit can be replaced with permanent ducting and shielding to separate the bed assemblies from a remote operator area.

The filter bed fill or adsorbent replacement operation is accomplished with the interconnections shown on Figure 1 B using the same equipment and, in addition, a "gulper tool" for administering the rate of conveying new adsorbent from the shipping drum to a fill hopper. The fill hopper acts as a batch holding plenum and controls distribution and filling density of the replacement adsorbent to the filter bed assembly.

Again, as in the case of drain operation, the system pressure is negative and all air for conveyance of the adsorbent is filtered prior to discharge.

The operations just described are contrasted with "change-out" of a larger conventional normal ventilating filter unit, which involves personnel in protective garments working within a housing on scaffolds and ladders using hoisting equipment for handling 80 to 90 pound adsorber trays. This contrast represents a significant improvement in maintenance operating conditions and reduction to potential exposure.

III. Operation/Maintenance

The adsorbent material operating costs of this improved nuclear filter system concept are compared with those of a conventional filter system on Figure 2.

The unit cost data shown on Figure 2 are not and are not intended to be exact or current figures for adsorbent material per pound costs or adsorber tray unit costs. The unit cost data shown is, however, representative of cost differences that have existed, on large order quantities, for the materials being compared.

The following assumptions were made in comparing the systems as shown on Figure 2.

Assumptions

1. Example system consists of four 16,000 CFM circulating units for $^{131}I_2$ and $CH_3{}^{131}I$ removal, tray type vs. HECA (two-inch carbon beds).

2. Each tray type unit contains 48 cells or a total of 192 cells.

3. Each HECA^{TM} type unit contains 2350 lbs of carbon or a total of 9400 lbs carbon.

ADSORBER MATERIAL COST COMPARISON FOR
FILTER SYSTEM OPERATION,
HECA™ VERSUS CONVENTIONAL SYSTEM

Material Category Cost Comparisons

	Conventional Type	HECA™	Savings
1. Inventory Cost (Emergency Change)			
Conventional Type - 48 trays x $275/tray	$ 13,200		
HECA - 2350 lbs charcoal at $1.80/lb		$ 4,230	
			$ 8,970
2. Initial Routine Change Cost			
Conventional Type - 4 units x 48 trays/unit x $275	$ 52,800		
HECA - 4 units x 2350 lbs/unit x $1.80/lb		$ 16,920	
			$ 35,880
3. Second and Subsequent Routine Changes			
Conventional Type:			
a) Refurbished Trays 4 units x 48 trays x 2/3 x $125/cell	$ 16,000		
b) Replacement Trays 4 units x 48 trays x 1/3 x $275/cell	17,600		
HECA - 4 units x 2350 lbs/unit x $1.80/lb		$ 16,920	
			$16,680
4. Number of Subsequent Changes			
$\frac{\text{40 yrs (plant life) - 3 yrs (initial change)}}{\text{3 yrs/change}}$ =			
12.3 changes/plant life (minimum)			
Conventional Type - 12.3 changes x $33,600/change	$413,280		
HECA - 12.3 changes x $16,920/change		$208,116	
			$205,164
TOTAL MATERIALS	$512,880	$246,186	$266,694 (1)

(1) Average savings on HECA over 40 yr. plant life at today's cost. A more accurate comparison would be these cost increments compounded at a percent/year.

FIGURE 2.

4. Facility will inventory sufficient stock (trays or bulk carbon) to provide non-routine (emergency) change capability for 25% of the circulation capacity.

5. Used tray type cells will be returned to the supplier for refurbishment and when radioactively contaminated will be emptied of carbon, decontaminated and crated for shipment by facility personnel.

6. Tray type cells have an average life of 3 changes due to wear and tear from handling, draining, filling, decontamination, crating, shipping and qualification testing operations.

7. Routine carbon changes will be performed on all units at least every 3 years.

8. Plant life is 40 years.

The cost comparisons that are tabulated on Figure 2 illustrate the net material savings in dollars for each of the categories of facility maintenance operations listed.

For example, the total material savings involved in Categories 1 and 2, "Inventory and Initial Routine Change" costs, can equal one fourth the equipment costs for a given class of systems.

The "Inventory Costs," Category 1, for a ventilating system having a variety of unit capacities would require "emergency change" capability associated with the largest unit capacity involved. Typically, a ventilating system includes units of the 30 to 40 thousand CFM capacity.

Category 3 a) and b), "Subsequent Routine Changes" accounts for the replacement tray cost savings that can be realized by performing the operations listed in Assumption 5 and returning the trays to the supplier for refurbishment.

The "useful life" stated in Assumption 6 might be argued as arbitrary since three changes can be exceeded with due care; however, three changes is fairly representative of an average useful life for tray refurbishment.

"Number of Subsequent Changes," Category 4, accounts for the total number of subsequent adsorbent changes that will occur during the plant life based on Assumptions 7 and 8.

The costs associated with this category can be much greater than shown if the ventilating air being processed is high in humidity or contains above average amounts of contaminants which would act to poison the adsorbent and its impregnant.

The maintenance labor costs associated with leak testing adsorber beds are difficult to compare quantitatively between the improved system (HECA^{TM}) and a conventional system. Variations in efficiency, skill and dedication to detail of maintenance/test personnel, who are responsible for actual performance of adsorbent "change-out" operations and subsequent testing, prevent any attempt at an absolute comparison such as tabulated in Figure 2 for material costs.

However, certain qualitative comparisons can be stated, between this improved system and a conventional system, upon which positive statements can be made. Figures 3 and 4 are typical sections of normal ventilating system housings which have been constructed utilizing the HECA^{TM} adsorber beds (Figure 3) and the conventional tray/cell adsorber construction (Figure 4).

Refering to Figure 4, the photograph shows the down stream side of a nominal 42,000 CFM rated tray-type adsorber mounting rack within a housing section. The tray mounting rack shown has provisions for approximately 126 tray-type adsorber cells, each of which is individually sealed by gaskets against the rack sealing face.

With trained maintenance personnel and extreme attention to detail, it is possible to replace this quantity (126) of trays and not experience detectable leaks during subsequent performance testing. When leakage does occur, however, detection is quite simple by comparison to the tedious and time consuming task of leak location, correction and retesting.

Refering to Figure 3, the photograph illustrates the all-welded sealing face of a typical comparably sized HECA^{TM} adsorber bed section.

The unit shown is approximately the same in physical size as the 42,000 CFM unit shown in Figure 4. However, all surfaces acting as seals and not guarded against by-pass leakage by adsorbent are stainless parent metal or nonstructurally loaded seal welds.

Therefore, the probability of leakage and the expenditure of the time and effort involved in leak location, correction and retest is extremely low and the possibility of unscheduled and costly periods of down time are, therefore, considerably less likely.

IV. Space

The costs associated with facility building space requirements for the HECA^{TM} improved nuclear filter system capability can be compared with a conventional system by again refering to Figures 3 and 4.

A nuclear filter system duct as shown in Figure 4 (rated at 42,000 CFM utilizing conventional tray adsorber cells) will, with the aid of Superflow

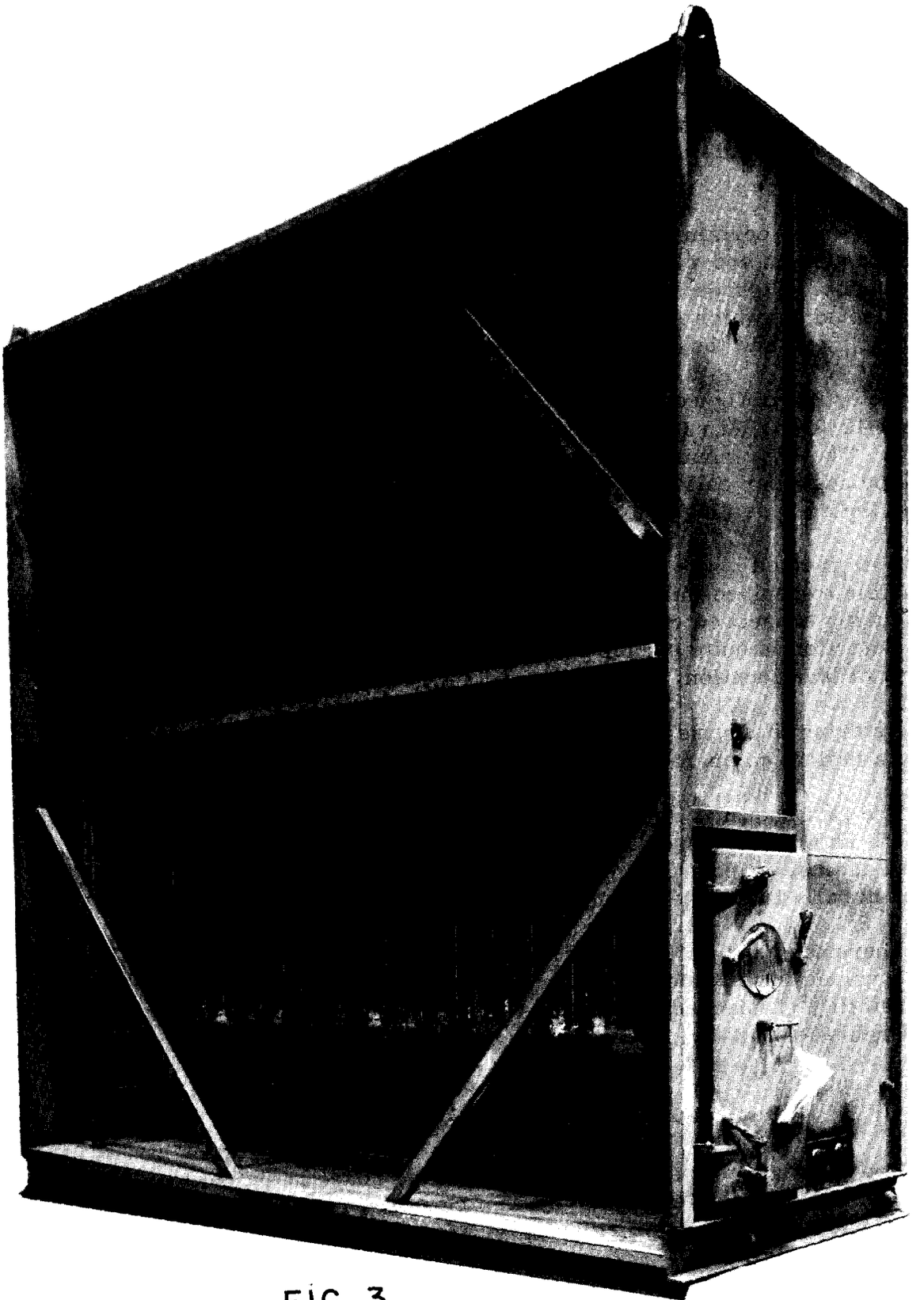

FIG 3

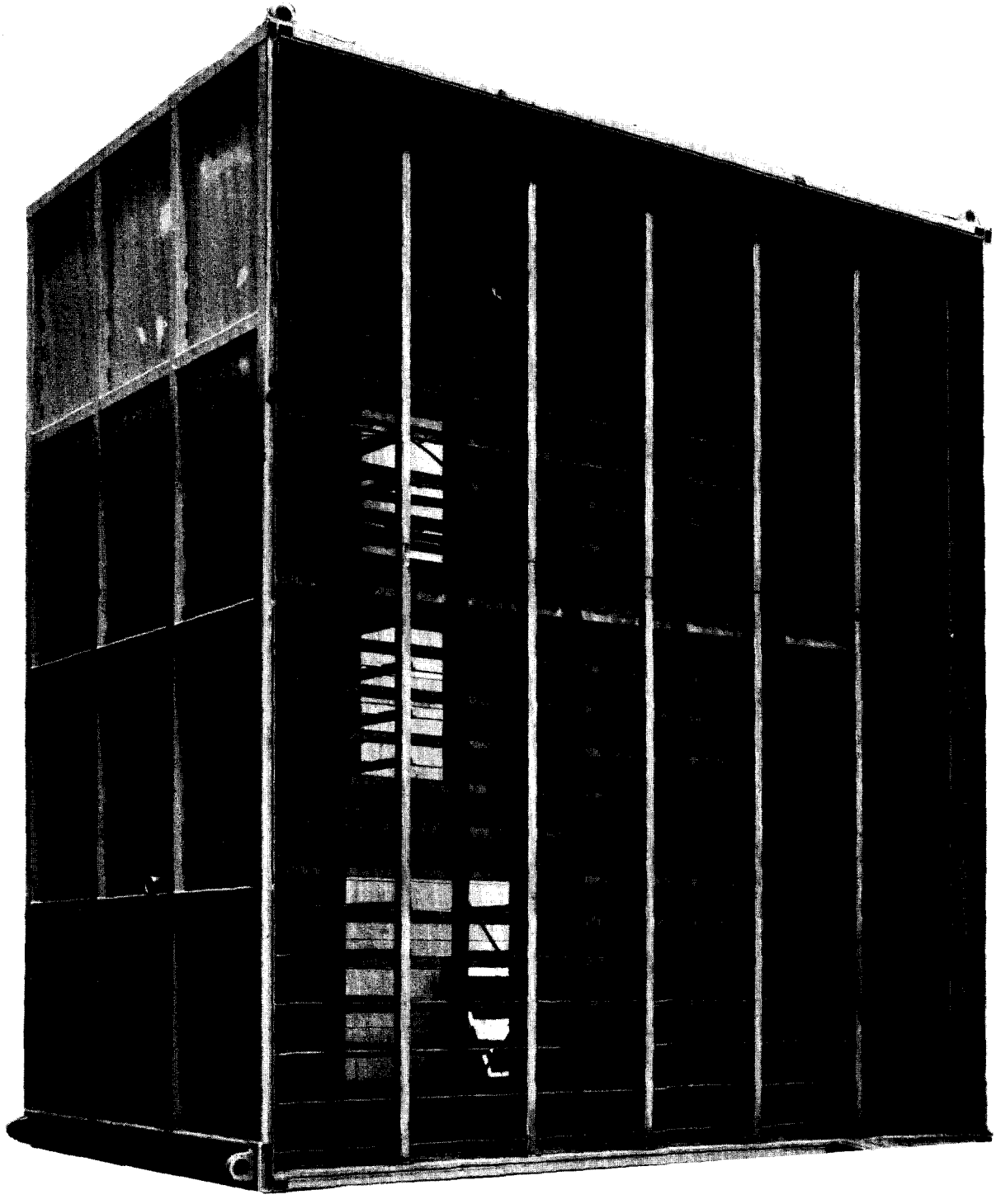

FIG 4

particulate filters and two-inch bed depth HECA units as shown in Figure 3, process 63,000 CFM of ventilating air under identical conditions and with equal performance.

The performance capability of the Superflow High Efficiency Particulate Filter will allow an increase in flow capacity of up to 50 percent for HECA™ nuclear filter system housings whose performance requirements are compatible with two-inch adsorber bed thicknesses. Increases in flow capacity, using a HECA™/Superflow combination, are proportionately less for adsorber bed thickness requirements up to six inches in depth.

The space savings capability with this improved filter system combination can reflect a significant cost savings when applied to building space allocations for nuclear filtering system requirements.

V. Summary

The data and discussions put forth in this paper all relate to comparisons which effect costs after capital investment as well as maintenance operations which bear on personnel health/safety considerations.

Some of the comparisons made, such as material cost savings, can be presented in a specific manner; others are qualitative and dependent upon judgement and cannot be reduced to a precise tabulation of costs. However, the savings are significant even on a quantative basis.

As more operating experience and data is gained from the various HECA™ systems that have and soon will be installed, specific cost comparisons will be reported for the various flow capacities and applications.

References

1. USAEC, Regulatory Guide 1.52, "Design, Testing and Maintenance Criteria for Atmosphere Cleanup System Air Filtration and Adsorption Units of Light-Water-Cooled Nuclear Power Plants."

2. USAEC, Regulatory Guide 8.8, "Information Relevant to Maintaining Occupational Radiation Exposure as Low as Practicable (Nuclear Reactors)."

3. Parish, H.C., Schuerman, L.E., and Siegwarth, D.P., "Development and Performance Evaluation of an Improved Standby Gas Treatment System for Enrico Fermi - Unit 2, " 13th Air Cleaning Conference.

TheHEPA filter must be considered in any attempt to reduce the size of an ESF, to reduce operating and maintenance costs, and to facilitate the ease of testing the system.

The usual parameters assigned to a HEPA filter have to be altered. That is, the flow rate must be increased without decreasing the efficiency and dust holding capacity of the HEPA filter. The pressure drop must remain unchanged.

The parameters assigned to Flanders SUPERFLOW meet those criteria. That is, the flow rate is increased, the efficiency, pressure drop, and physical size remain unchanged, and the dust holding capacity increased significantly.

The following table compares the characteristics of the SUPERFLOW and the conventional separator type HEPA filter.

	FLOW (CFM)	PRESSURE DROP	MAXIMUM DOP PENETRATION	DUST HOLDING CAPACITY APPROXIMATE (ASHRAE DUST)
SUPERFLOW	1500	1.0	0.03%	550 Gms.
Separator Type	1200	1.0	0.03%	950 Gms.

Flanders SUPERFLOW is compatible with extended carbon beds such as CVI's HECA. It is capable of a higher flow rate than conventional HEPA filters, because its design utilizes more of the surface area of the filter medium. A high volume per filter means that systems of high capacity can be built and placed in a smaller space.

The SUPERFLOW reduces operating and maintenance costs since it lasts longer than conventional separator type filters.

The SUPERFLOW is constructed by molding the glass paper into self-supporting corrugations. A SUPERFLOW filter pack, compared to a separator type filter, is shown in figure 5.

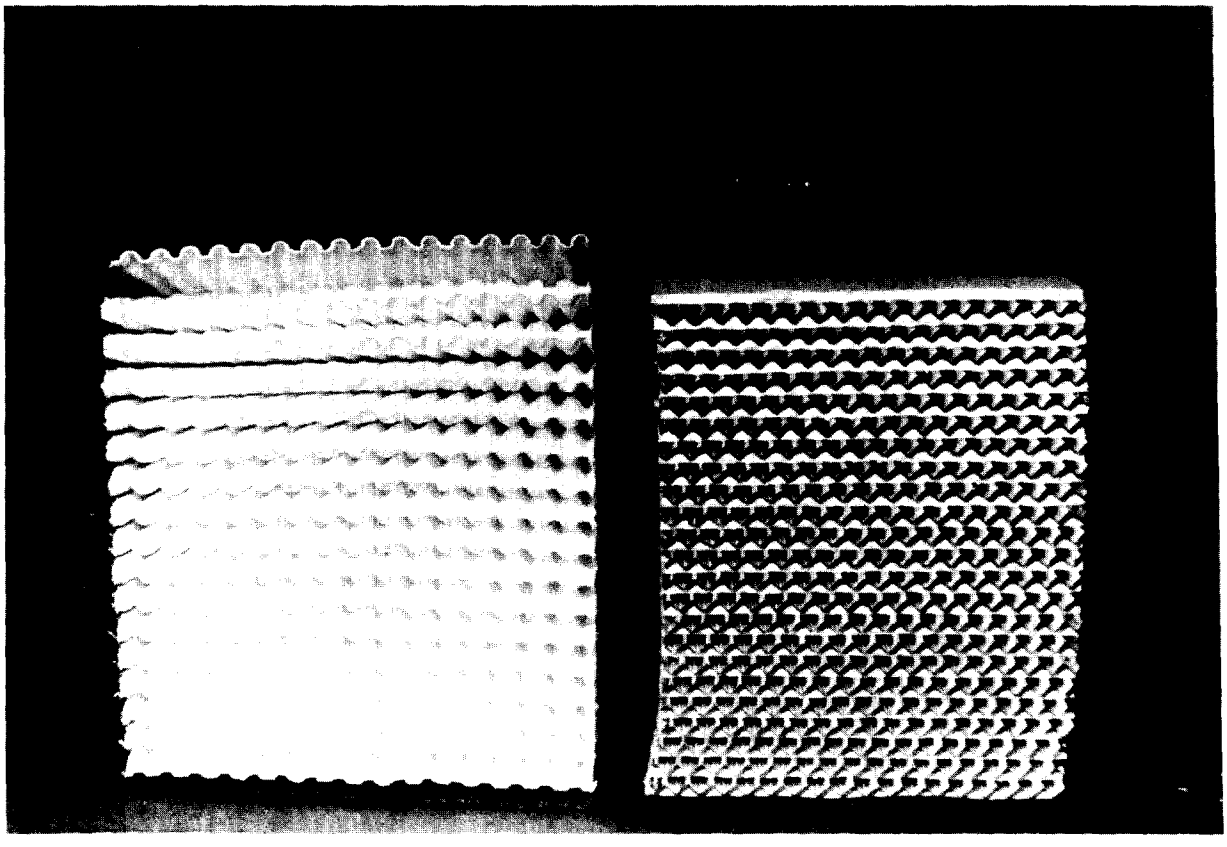

Figure 6 is another slide showing the SUPERFLOW.

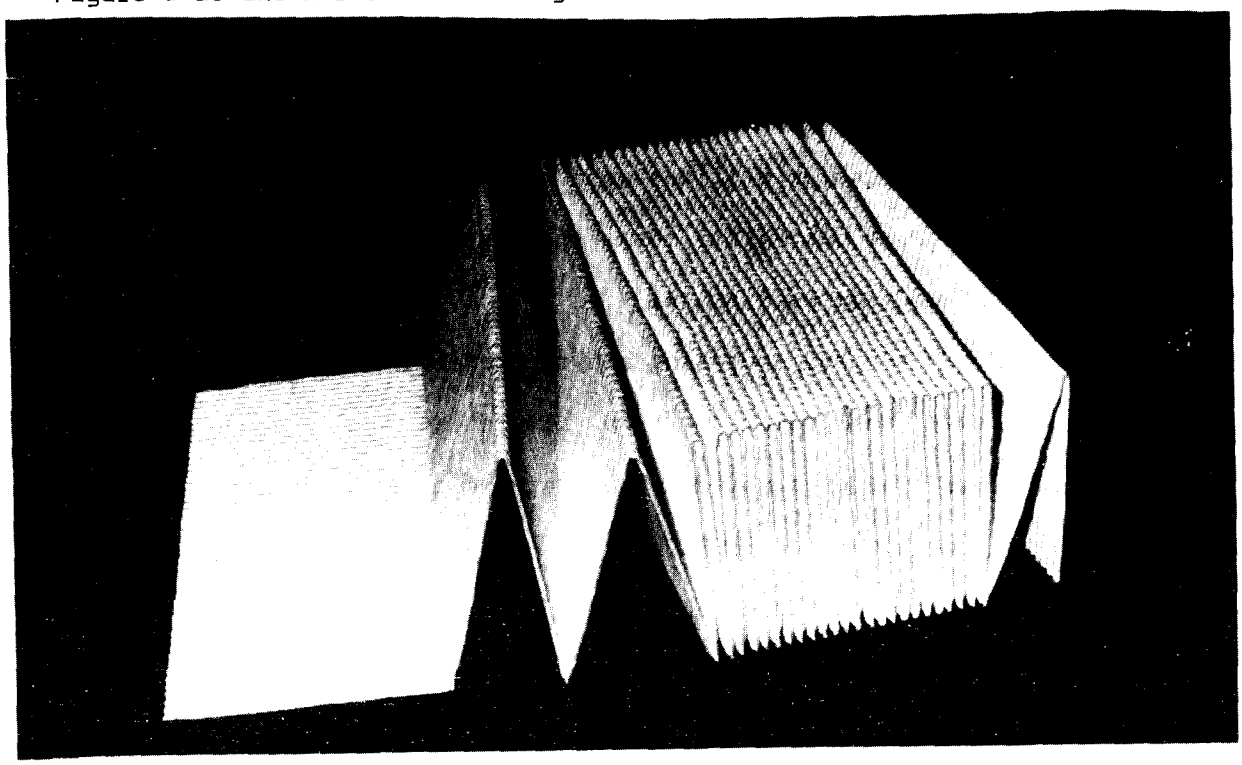

Figure 7 shows a comparison of the medium after a filter has been artifically loaded with a standard test dust.

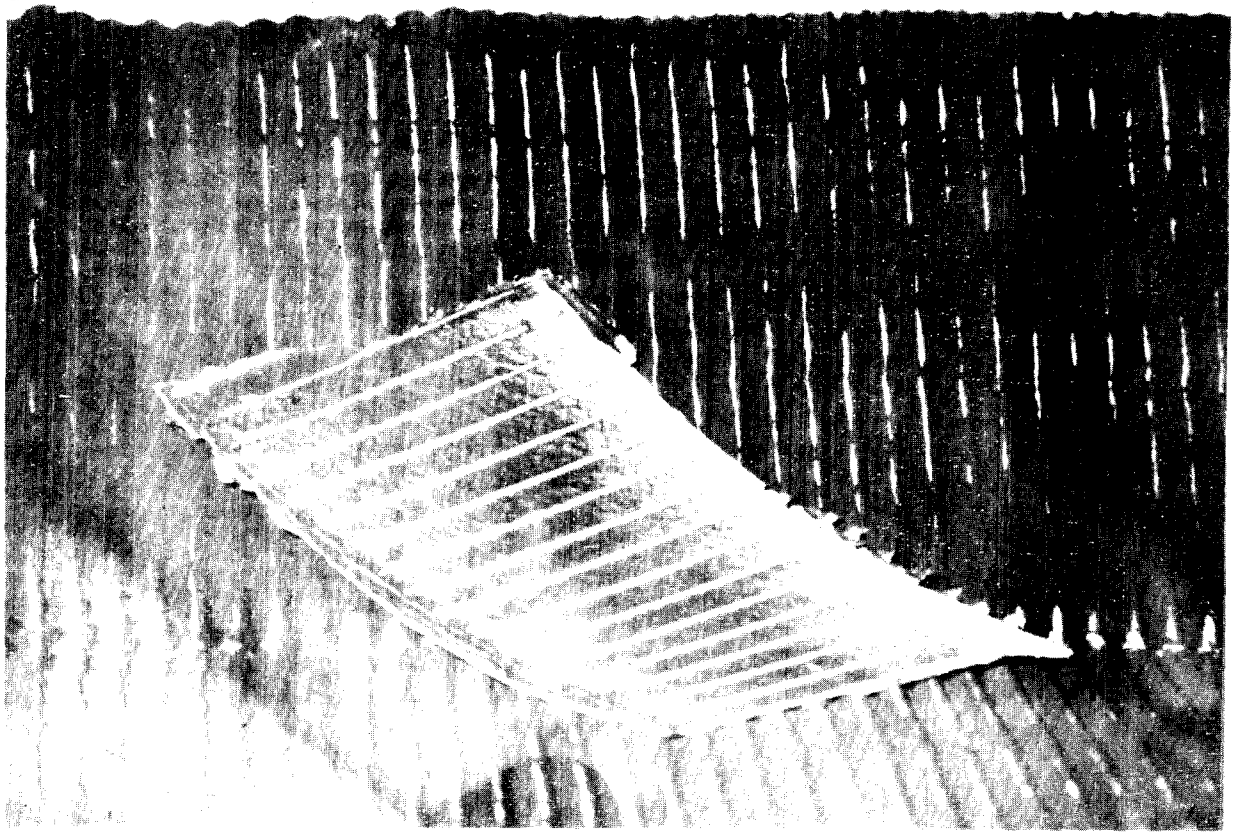

This figure also shows that there is more usable area in the SUPERFLOW than in the Separator type filter. Note the white streak areas in both types. This accounts for the higher flow rate and the higher dust holding capacity. Figure 8 shows a comparison of flow, or impedance curves.

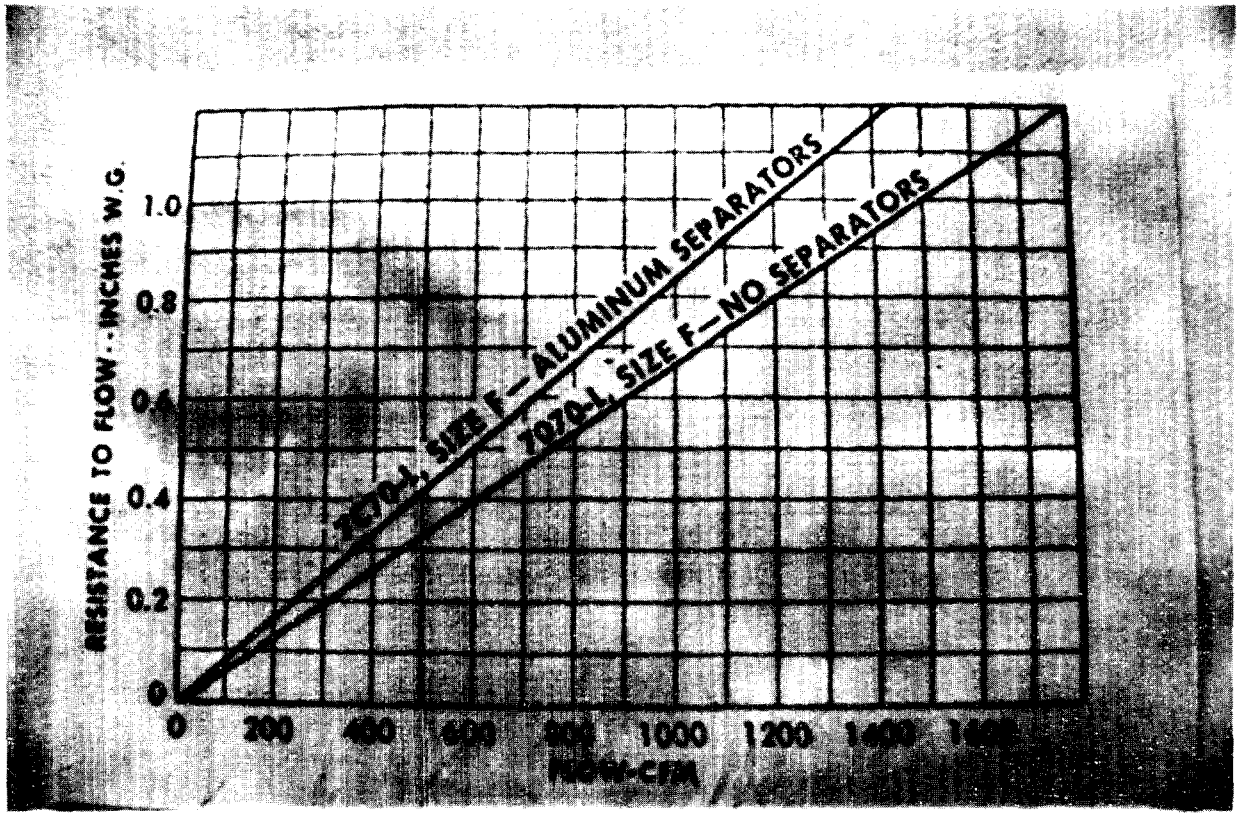

Note that at 1.0 in. w.g., the SUPERFLOW is rated at 1500 CFM, and the Separator is rated at 1200 CFM. This is a 25% greater flow rate in a filter which meets every standard that the separator type meets.

Figure 9 shows a comparison of dust holding curves.

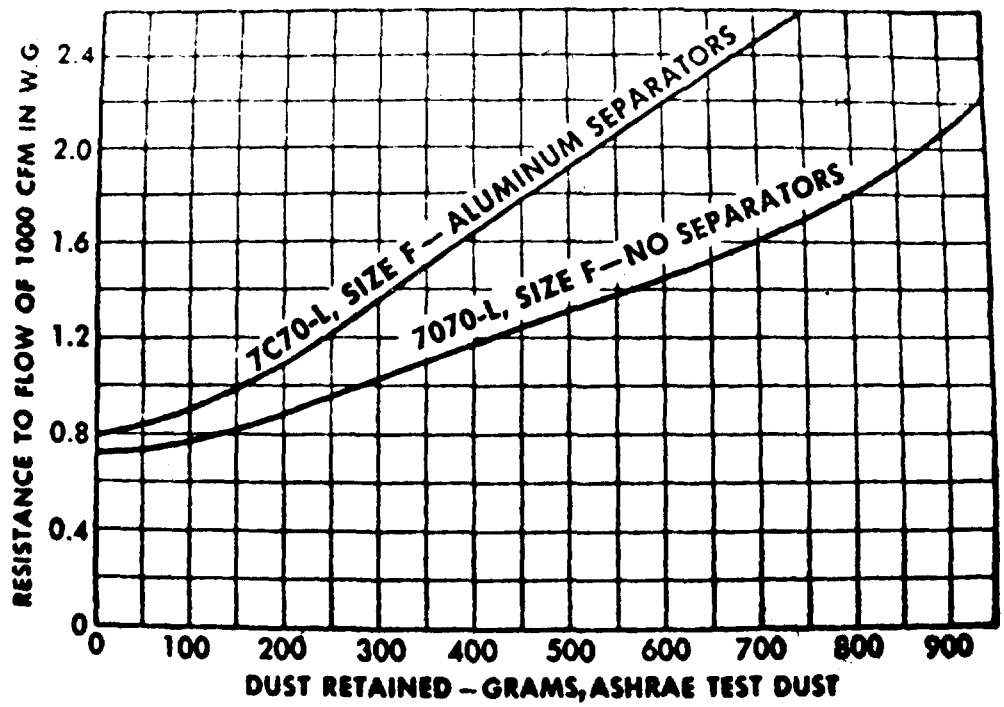

Note that at 2.0 in. w.g., the SUPERFLOW holds approximately 950 gms. of standard test dust, and the separator type holds approximately 550 gms. This is almost 75% more dust holding capacity — or about 75% longer life.

We can summarize these facts by saying:

1. With the use of the SUPERFLOW and compatible associated equipment, a system can be designed to have the same flow rate, and be about 25% smaller in volume.

2. The elimination of the separator reduces asbestos related problems with asbestos separators, possibility of hydrogen explosions with aluminum separators. It also reduces inventory problems for the consumer since one type of filter can be used for any application. For example, containment filters must use no aluminum, and control room filters must use no asbestos.

3. The smaller bank will hold more dust, so that another advantage will be longer life. Consider a system requiring 12,000 CFM:

A bank of 12 conventional separator type filters is capable of 12,000 CFM at 1.0 in.w.g. and will hold about 6600 gms. of standard dust.

A bank of only 9 SUPERFLOW filters will yield 12,000 CFM at 1.0 in.w.g and will hold about 8100 gms.

Even with the smaller system, the bank should last 23% longer $\left(\frac{8100 - 6600}{6600}\right)$.

4. Longer life and fewer filters mean less down time, less exposure of person personnel to radioactively loaded filters, and less disposal problems.

5. The SUPERFLOW is lighter, so it is easier to handle in changing filters.

Another innovation by Flanders is the Fluid Seal concept.

The Fluid Seal eliminates gaskets and provides a positive leak-free method of mounting a HEPA filter to a frame.

The Fluid Seal is simply a 3/8" wide x 3/4" deep channel in the HEPA filter frame which is filled with a silicone grease, and a mating flange on the framing system. The filter is placed so that the flange merely penetrates the grease, creating the seal.

Figure 10 shows the groove and flange just prior to being sealed (right photo) and the one on the left shows the two parts mated.

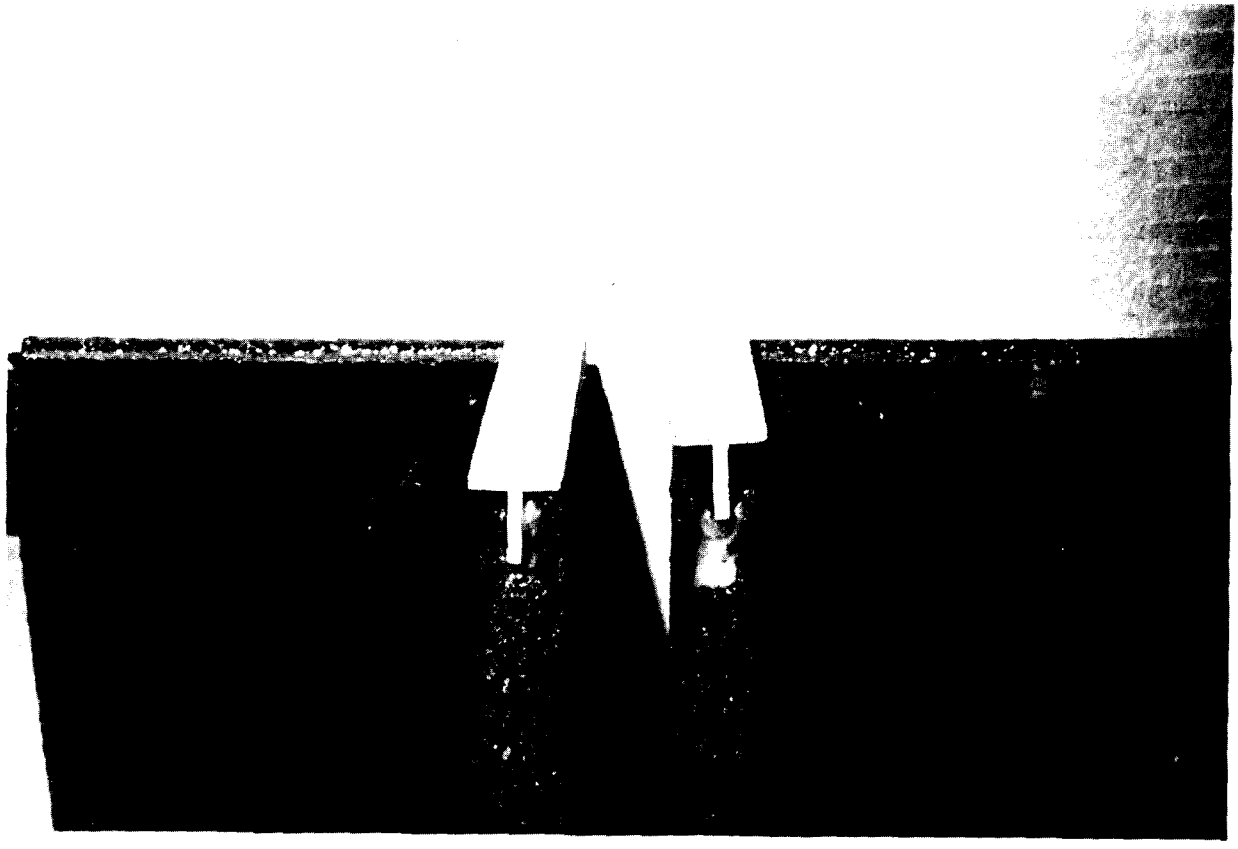

These facts presented can be summarized as follows:

1. The Fluid Seal creates a permanent seal independent of compression.

2. The Fluid Seal eliminates the need for compression equipment, and in turn, makes any bagging-out easier.

3. The Fluid Seal provides a quicker method of mounting and dismounting of a filter, which reduces personnel exposure time in the dust system environment.

4. The Fluid Seal eliminates gasket relaxation and gasket set.

Thank you very much.

THE EFFECT OF VARIOUS POLYMERIC BINDERS ON THE RADIATION RESISTANCE OF GLASS FIBER HEPA FILTER MEDIA

I. M. Hutten and E. C. Oswecki
C. H. Dexter Division
Dexter Corporation
Windsor Locks, Connecticut

Abstract

Glass fiber HEPA filter media bonded with various polymeric materials were exposed to several levels of radiation dosage from an electron beam source. The effects on water repellency, tensile strength, DOP filtration efficiency and organic content were noted. All media suffered degradation at the highest levels of radiation dosage ($7X10^8$ rads). However, at intermediate levels, radiation resistance was affected by the type of binder. Greatest resistance to radiation was exhibited by media bonded with a phenylated polysiloxane resin. Cross-linking polymers such as polystyrene and SBR displayed improvement in some properties, such as in water repellency and tensile strength, at low levels of radiation exposure ($< 2X10^8$ rads), however degraded at higher levels of exposure. Filtration properties such as DOP efficiency and resistance to air flow did not appear to be greatly affected by radiolysis.

Introduction

HEPA filters are installed in airborne-activity confinement systems of nuclear installations to provide environmental protection against the rare possibility of a nuclear accident by filtering out radioactive debris that might result from such an accident. The basic medium in these filters is a paper-like structure composed of glass microfibers. The properties are well specified in MIL-F-51079A[1]. This specification includes requirements for strength and water repellency properties that can only be achieved by incorporating an organic binder into the glass microfiber structure. To assure fire resistance, MIL-F-51079A limits the binder content to 5% maximum based on organic ash analyses. Despite this limitation on binder content, the media manufacturers have developed HEPA media that more than satisfy the requirements of MIL-F-51079A.

In recent years, the Atomic Energy Commission has become concerned about the radiolysis effects on HEPA media. This concern is based on the premise that unless the media is radiation-resistant the combination of radioactive debris and steam that might be released during an accident could cause radioactive degradation of the HEPA filter and subsequent failure. As a result, a new specification, MIL-F-0051079B(EA)[2] is being considered to include requirements for radiation resistance. The proposed specification stipulates that HEPA media must still retain certain levels of tensile strength and water repellency after exposure to $0.8X10^8$ rads of gamma radiation. Wullaert et al[3] reports insignificant change in the flexural strength of borosilicate glass when exposed to an electron beam dosage of $2.5X10^8$ rads. This suggests that the glass fiber component of HEPA media will not be a problem with respect to the proposed requirements for radiation resistance. Of more concern are the organic binders in the media. Data presented by Jones[4]

suggests that the rate of degradation of water repellency and tensile strength properties of HEPA media may very well relate to the type of binder used in the media.

This study was undertaken to investigate a number of polymeric materials that might be used as binders in HEPA media and to determine how they affected the radiation resistance of the media. The polymers investigated are listed and described in Table 1. The polymers were all supplied under manufacturers trade names, therefore the structure of the suspected or possible repeating unit listed for each polymer was deduced by a combination of infrared analysis and the manufacturer's description of the product.

Irradiation of Polymers - Review

There is considerable literature concerning the radiolysis effects on various polymeric materials. It is beyond the scope of this presentation to delve into the intricate and complex radiation chemistry of the various polymers, however, a few generalities do emerge. It is quite evident that two major types of reactions that occur when polymers are bombarded with radiation are cross-linking and scission. The theories of these two reactions have been discussed in detail by Charlesby[5]. Cross-linking is combining of branches of adjacent molecules in the polymer, whereas scission is the breakdown of the backbone of the polymer molecule into smaller segments. Other types of reactions such as oxidation or peroxide formation also occur; however, these are often intermediate steps to the cross-linking or scission reactions. In some polymers, the two reactions--cross-linking and scission--may be competing, the dominating reaction depending on whichever is greater: the cross-linking rate or the scission rate. Cross-linking may be considered as a positive effect that enhances the properties of the polymer such as its strength, whereas scission is often considered as being synonymous with degradation of the polymer. Kircher[6] points out that even polymers which initially cross-link will tend to degrade at sufficiently high doses of radiation. King et al[7] indicates that aromatic structures in a polymer lend radiation stability because they absorb radiation and stabilize the resonance structure of the molecule. King argues that the aromatic is more effective in stabilizing the structure if it is part of a side chain rather than part of the main chain of the polymer molecule. Bovey[8] notes that chain scission will predominate in vinyl polymers containing in their main chain a quarternary carbon that does not bear a hydrogen atom. This is particularly true if one of the substituents is a methyl group that may cause a steric strain on the carbon-to-carbon bonds of the main chain.

Table 2 lists the relative radiation resistance of some polymers. This is data extracted from another publication by King et al[9]. The data indicates polystyrene to be one of the most stable of high polymers when exposed to radiation. It will be noted from Table 1 that polystyrene is a polymer that contains an aromatic benzene attached to the main chain but not part of the main chain. Other polymers, such as polyester (Mylar film), polycarbonate, and the phenolics, that contain an aromatic in their main chain are less radiation resistant. Low on the list of polymers of Table 2 are polymethyl methacrylate and Teflon, which contain non-hydrogen bearing quarternary carbons in their main chain. In the case of Teflon, the substituents on the quarternary carbons are halogens, such as chlorine and fluorine. The fluoroethylene polymers are generally recognized as being very poor in radiation resistance. Table 2 lists the silicones as next to polystyrene in terms of radiation resistance. Warrick[10] suggests that silicones with a high level of phenyl linkages attached to the main chain would be particularly resistant to radiation, especially when compared to their methylated counterparts. In another publication, Warrick et al[11] reports that phenylated siloxane rubbers with 80% phenylation can absorb more than five times as much radiation as conventional dimethyl siloxanes for equal damage. Undoubtedly, the

silicone rubber that is listed low on Table 2 is of the dimethyl siloxane type. Generally, the elastomers and rubbers are reported as being less radiation resistant than their high polymer plastic counterparts. This would explain why SBR is low on the list of Table 2 polymers despite the fact that it has phenyl groups attached to its main chain structure.

It will be noted that Table 2 does not state the type of radiation exposure; whether it be alpha, beta, or gamma radiation. King et al[9] argues that damage to a polymer by radiation is generally dependent on total dose absorbed regardless of type of radiation. In support, Charlesby[12] states "It has been repeatedly confirmed that the major reactions in polymers whether produced by fast electrons, x-rays or gamma rays, or mixed radiation including neutrons from atomic reactors, depend primarily on the total energy absorbed and sometimes on the radiation intensity, but rarely, if ever, on the type of radiation or its source."

Experimental Procedures

A. Preparation of Specimens

Specimens for irradiation experiments were all prepared from a uniform lot of untreated HEPA media produced on a production machine. The untreated paper had the following properties:

Basis Weight	54 lb/3000 ft^2
Thickness	.016 inches
DOP Penetration	.005% at 320 cm/min
Pressure Drop	33 mm H_2O at 320 cm/min

In addition, the untreated paper contained 2.0% by weight of a cellulosic binder. This was to prevent the glass sheet from disintegrating when exposed to the solvent of the polymer binder solution.

The untreated sheets, 8-1/2x11 inches, were impregnated by submerging the sheets into a solution of the polymer prepared by adding the polymer resin to an appropriate solvent. Solution concentrations were carefully controlled so as to achieve the desired polymer content for the sheet. After the sheet was immersed in the polymer solution, it was run through a size press to remove excess solution. A size press is a set of squeeze rolls very much like the clothes wringers on old-fashioned washing machines. After squeezing out excess solution, the sheets were dried on a steam-heated can drier. During drying, the sheets were flipped over several times so that one side, then the other, was in contact with the surface of the drier. This back-and-forth flipping over of the sheet during drying helped insure a uniform polymer resin impregnation throughout the thickness of the sheet.

B. Irradiation Experiments

The sheets were irradiated by exposure to an electron beam source located at the Windsor Nuclear Corporation in South Windsor, Connecticut. The beam is developed from a 3 MEV Van de Graaf generator. Figure 1 is a view looking up at the generator vessel. The pipeline coming straight down from the vessel contains the electron beam. A scanning device in this line distributes the ionizing radiation uniformly over a 15-inch wide crossection, one inch wide, at the bottom of the line. The beam scans the 15-inch wide crossection at a frequency of 200 cycles/sec.

On the exposure side of the radiation beam, Windsor Nuclear has an assortment of power-driven conveyors for the various commercial jobs this company performs. The one chosen for these studies was a back-and-forth type that passed the specimens back and forth through the beam until the desired radiation dosage was achieved. The specimens were mounted in a wooden box-like structure containing eight-inch deep slots, 1/16" wide, cut into each side of the box from the top. Sheets were mounted into the structure by sliding each end of the sheet into a slot on either side of the box as demonstrated in the photograph of Figure 2. The slots were cut at a 15° angle to the vertical so that the surface of each specimen would see the radiation when passing underneath the beam. The parallel slots were cut at 1/2" intervals, which allowed as many as 60 sheet specimens to be irradiated in the box shown in Figure 2. The conveyor drove the box-like structure with its specimens through the beam at a rate of 12 inches/minute, as demonstrated in Figure 3. For these experiments, the 3 MEV generator was regulated to generate a beam current of 1.0 milliamperes. The radiation exposure of the specimens was estimated to be 10^7 rads per pass. During irradiation, the specimens were cooled by a fan air current to prevent overheating. In some experiments, a fine wire thermocouple was imbedded in a specimen to measure temperature rise during irradiation. Generally the specimens would reach temperature peaks of approximately 250 - 270°F. when directly under the beam and then cool off to 120 - 130°F. prior to the next pass. It cannot be assured that the thermocouple was indicating the exact temperature of the specimen since the thermocouple was imbedded in a good insulating media and quite possibly its material had a different rate of radiation absorption than did the glass fiber media around it.

C. Testing of Irradiation Specimens

After irradiation, sheet specimens were tested for properties in accordance with methods spelled out in MIL-F-51079A. Properties in this specification that were tested were tensile strength, percent combustibles (a measure of organic content) and D.O.P. penetration and pressure drop at an air flow of 320 cm/min. In addition, sheets were tested by two different water repellency methods described as follows:

1. Water Burst Height - This is the water repellency method specified in MIL-F-51079A. The procedure involves screw-clamping a HEPA specimen to a compartment which contains an inlet water valve and has attached a glass column for measuring water height. After the specimen is clamped in place, water is charged to the compartment so that the water level in the column rises at a rate of 12 inches/minute, the height of the water level above the specimen being the water pressure exerted against the specimen. The water level is increased until water is seen to either penetrate the media or the media bursts under the pressure of the water. The former case is a measure of the water repellency of the sheet. Some highly water repellent sheets will burst before water penetrates and this will be an indication of the burst strength of the media as well as its water repellency. Values reported are the average of two tests on each sheet; one with the wire (smooth) side of the media against the water, the other with the felt (rough) side against the water.

2. Penetration Time - This method developed by Jones[4] of the Atomic Energy Commission involves using the same apparatus as described in 1. above. Water is charged to a 6-inch head above the specimen, then timed until the first drop of water penetrates the specimen. The water level is then increased as described in 1. above until the specimen bursts. As in 1. above, values reported are the average of the wire side and felt side. For reasons of time economy, penetration time tests were limited to 10-minute durations. Values greater than 10 minutes are reported as 600+ seconds.

Discussion of Results

A. Effect of Polymer Type

The effects of radiation on media bonded with the various polymers are tabulated in Tables 3 through 6. The most revealing evidence is in Table 3, which indicates the effect on water burst height, and Table 4, indicating the effect on tensile strength.

The data of Table 3 is plotted in Figure 4. Quite clearly, the water burst height test indicates the silicone polymer as the most radiation resistant binder. After exposure to $7X10^8$ rads, the media bonded with the silicone is the only one to have a measurable burst height. Phenol formaldehyde appears to be the least radiation resistant binder for HEPA media; however, this may relate to the low polymer content of this particular set of specimens. It should also be noted that these specimens were thermally cured prior to irradiation. Two of the polymers--polystyrene and the styrene-butadiene copolymer (SBR)--show improvement at the lower levels of radiation dosage ($0.5X10^8$ rads). The indication is that at the lower level of radiation exposure a cross-linking effect predominates to improve the burst height properties of media bonded with these two polymers. The properties of the sheet bonded with the SBR polymer are so poor prior to irradiation that it appears that the lower level of radiation dosage has a curing or "vulcanizing" effect on the polymer.

Figure 5 plots the average tensile strength* data in Table 4 normalized to percent of maximum value for each polymer. Note that the maximum value is not necessarily the initial value. The most resistant media again appears to be the sheet bonded with the silicone polymer. All of the media show sharp declines in tensile strength at approximately $1X10^8$ rads. Interestingly enough, the specimens bonded with the phenol formaldehyde resin, which had the poorest performance by the water burst height measurement appear to be among the better in terms of retaining tensile strength after radiation exposure. There are several other interesting features that reveal themselves in the plots of Figure 5.

1. The polymer binders that appear best to retain tensile strength properties after prolonged levels of radiation exposure are the thermosetting or cross-linking resins--silicone, phenol formaldehyde, and SBR.

2. At radiation dosages less than $2.0X10^8$ rads, the polystyrene bonded sheet appears to have the slowest rate of degradation; however, at higher dosages it is degraded as much if not more than the thermosetting resins. Polystyrene, although considered as a linear thermoplastic, is known to have good cross-linking properties under irradiation. For a discussion of the radiation induced cross-linking of polystyrene, see Parkinson et al[13].

3. Three polymers--polyester, polycarbonate, and polyphenylene oxide--that are considered as linear thermoplastics and suspected of not having many cross-linking properties show poorer performance than the thermosetting resins in retaining tensile strength of the media they bond.

4. The media containing the polyacrylate binder show the steadiest decline in tensile strength with increasing levels of radiation. The polyacrylate polymer is the only one in this study not containing an aromatic or phenyl grouping in its polymer structure. Bovey[8] lists the

* Average Tensile Strength = $\frac{\text{MD Tensile Strength + CD Tensile Strength}}{2}$

polyacrylates as cross-linking polymers; however, Charlesby[5] notes that degradation is occurring simultaneously. Based on the data of Figure 5, degradation appears to be the dominating reaction.

5. Sheets bonded with the three thermosetting resins--silicone, phenol formaldehyde, and SBR--all achieve maximum tensile strength after exposure to $0.5X10^8$ rads, suggesting that the cross-linking effect is improving the tensile properties of these sheets at the lower level of radiation. Sheets bonded with the linear thermoplastic polymers, polyester, polyphenylene oxide, and polyacrylate show a steady decline in tensile strength from their initial values prior to exposure. The one anamoly is the polycarbonate bonded sheets. Although polycarbonate is not suspected of being a strong cross-linker, the sheets it bonds show improvement in tensile strength after exposure to $0.5X10^8$ rads.

6. At $0.5X10^8$ rads, the SBR bonded sheets showed the greatest improvement in tensile strength over its initial un-irradiated values, again suggesting that this binder may have been "vulcanized" at the lower level of radiation.

In comparing the two sets of data, water burst height and tensile strength, it will be noted that the sharpest declines for all of the polymers, with the possible exception of silicone, occur at approximately $1X10^8$ rads for both sets of data. At the highest levels of radiation the water burst height values degrade to essentially zero, whereas even after $7X10^8$ rads the specimens are retaining from 30 to 60% of their maximum tensile strength properties. If water burst height can be considered as a measure of water repellency, one explanation as to why this property appears more readily degraded than the tensile strength property may be considered in terms of what happens to the binder when it is applied to the untreated web. Some of the binder will form very thin films over the surface of the glass microfibers. The rest of the binder will collect as thicker beads or nodules at the fiber intersections. It can be reasonably argued that the thin films coating the fiber surfaces contribute to the water repellency of these surfaces, whereas the thicker beads at the fiber intersections affect the tensile strength of the web. When exposed to radiation, the very thin films on the fiber surfaces will be more quickly degraded than the thicker nodules at the fiber intersections. Correspondingly, the water repellency of the media would therefore be more quickly degraded than the tensile strength.

Table 5 is a presentation of how irradiation effects the filtration properties of the various media bonded with different polymers. The filtration test measures the efficiency of the media in filtering generated smoke particles of dioctyphthalate (DOP). The apparatus, the Q-127 DOP smoke generator, also provides a means for measuring the pressure drop across the media as it is filtering the DOP smoke. The smoke particles are estimated to be 0.3 microns in diameter. The standard air flow rate for this test is 320 cm/minute (10.5 ft/second).

The data of Table 5 suggests very little change in the filtration properties of the media at all levels of radiation dosage. There is some indication that at the highest levels of radiation dosage, $7X10^8$ rads, there may be some improvement in the filtration properties, that is, lower DOP penetration and/or lower pressure drop. This effect appears to be most significant with the media bonded with the polyacrylate binder. Based on the data of Table 5, this indication cannot be considered statistically conclusive; however, the authors have observed that unbonded HEPA media has better filtration properties than media bonded with a polymer, particularly if the polymer is water repellent. It may be that at the highest levels of radiation dosage the polymer is so degraded that the media acts as if it were an unbonded media.

Table 6 is an attempt to study what happens to the organic content of the media when exposed to radiation. The intent here was to provide some assurance that, although the polymers may be affected by the radiation, they were not being burnt off due to the thermal energies created by the irradiation. The organic content, expressed as percent combustibles, is determined by ashing the specimens at 1000°F. for 5 minutes. The percent combustibles include not only the polymer content of the media but also the 2.0 percent cellulosic binder in the untreated specimens prior to polymer impregnation. The polymer content reported in Tables 3 - 6 are based on the combustible content of the specimens prior to irradiation less the 2.0 percent cellulosic binder content. The data in Table 6 indicates small change in percent combustibles through all levels of radiation dosage. The small changes that are indicated suggest that the percent combustibles may be increasing with increasing levels of radiation dosage. This effect appears most significant with the phenolic treated sheet. Phenol formaldehyde is known to oxidize when irradiated in the presence of oxygen.

B. Effect of Polymer Content

A second study was conducted with four of the polymers mentioned above to determine the effect of polymer content in the HEPA sheet. The properties studied were water burst height and tensile strength. In addition, the irradiated sheets were also studied for water penetration time, a test not included in the first study because at that time the authors were not yet aware of the test. It should be pointed out that the water burst height values reported in this second study are a little different than those reported in the first study because in the second study the burst heights were measured on the media after they had been tested for water penetration time. The latter procedure gives somewhat lower results.

The four binders studied for the effect of polymer content were the silicone, polystyrene, polyester and polyacrylate polymers. The results are presented in Figure 6, showing the effect on water burst height, Figure 7, showing the effect on average tensile strength, and Table 7, showing the effect on water penetration time.

The data indicates that higher polymer content does increase media resistance to radiation simply because there is more polymer to be degraded. Judging from the relative parallelity of the curves in Figures 6 and 7, it does appear that the rate of degradation appears roughly the same regardless of polymer content. Figure 6 confirms that the silicone binder is the slowest to degrade and is by far the most radiation resistant with respect to the water burst height property. The polystyrene bonded sheet never does have high burst height values; however, the cross-linking effect is noted by the improvement at $0.5X10^8$ rads. The two sheets bonded with polyester and polyacrylate show sharp degradation at approximately $1X10^8$ rads, thus confirming the observations of the previous study.

The effects of polymer content on tensile strength plotted in Figure 7 includes data from Figure 5 of the first study for three of the resins--polystyrene, polyester, and polyacrylate. Figure 7 continues to support the argument that higher polymer content increases resistance to radiation degradation but not the rate of degradation. The cross-linking effect of the silicone resin is still evident at $0.5X10^8$ rads. It is interesting to note that after leveling out at $2X10^8$ rads the tensile strength of the silicone treated sheets begins to slowly increase with increasing radiation dosage. This suggests a secondary cross-linking effect that was not observed in the previous study. One possible explanation for the difference between the two studies is that the silicone polymer used for the second study was taken from a different lot than used for the first

study, and therefore may have had a different profile in its resistance to radiation. The effects on the other three polymers are consistent with what was observed in the first study except for the sheet bonded with the highest level of polyester content. Similar to a result previously reported for the polycarbonate polymer, the polyester curve suggests a cross-linking effect at the lower levels of radiation. Because of this result this experiment was suspect and repeated, and the same result obtained. The curve plotted is the average of the two experiments. For three of the binders--polyester, polystyrene and silicone--there is a levelling-out effect at the higher radiation dosages. Increasing the radiation dosage does not continue to decrease tensile strength. On the other hand, the sheet bonded with the polyacrylate polymer shows a monotonously continuing degradation with increasing radiation dosage.

The water penetratiom times listed in Table 7 indicates that this water repellency property is the one most adversely affected by radiation. Again, the higher the polymer content the more resistant is the sheet to ultimate degradation. The specimens bonded with the silicone resin are quite clearly the most superior with respect to radiation resistance. It is quite obvious that the polystyrene resin is not the best binder for obtaining water repellent media; however, it is improved at low levels of radiation dosage.

C. Comparison of Beta Radiation Versus Gamma Radiation

It will be noted that the electron beam source used in this study is a beta radiator, whereas proposed MIL-F-0051079B(EA) spells out gamma radiation as the means for testing HEPA media. References to the literature earlier in this paper clearly indicated that the radiation effect on polymers is related to the dosage and not the source, nevertheless a study was undertaken to correlate the two radiation sources. The authors provided samples to L. Jones of the Savannah River Laboratory for correlation studies between the two types of irradiators. Three sets of samples with three different polymer compositions (A, B and C) were prepared. A portion of each set of samples was irradiated to $1.0X10^8$ rads at the electron beam source located in the Windsor Nuclear facility. Another portion from the same set of samples were gamma irradiated by Jones using a Cobalt 60 source located at the Savannah River Laboratory. Table 8 is a tabulation of Jone's results presented to the Government - Industry Committee on Filters, Media and Testing during their meeting at the 12th AEC Air Cleaning Conference held in Oak Ridge, Tennesee in August 1972[14]. The results suggest that the degradation of all three sets of samples by either means of irradiation were similar. It was the general conclusion of the meeting that the two types of irradiators--beta and gamma--had similar effects on HEPA media[15].

Summary and Conclusions

It is quite apparent that different polymer binders have different effects on the radiation resistance of HEPA media. Although the literature and the data of Table 1 suggests that polystyrene is one of the most stable of all high polymers, the results of this study clearly indicate that silicone adds considerably more radiation resistance and stability to the media. Polystyrene does appear to have cross-linking effects and degrades slowly at low levels of radiation dosage. It appears to be the type of binder that inherently adds relatively poor water repellency properties to HEPA media. The silicone used in this study is a thermosetting resin with phenylated side branches. The data supports the previously mentioned arguments by Warrick[10,11] that this type of polymer has very good radiation resistance. HEPA media bonded with thermosetting polymers appear better able to retain their tensile strength properties at high levels of

radiation exposure than do HEPA media bonded with polymers classified as linear thermoplastics. The thermosetting resins all show cross-linking effects at low levels or radiation. The presence of an aromatic in the polymer structure does appear to stabilize the tensile strength property and level out the rate of tensile strength degradation at high levels of radiation dosage. The polyacrylate polymer is the only one in this study that does not contain an aromatic and is the only one to continuously degrade in tensile strength at all levels of radiation exposure.

Regardless of binder, the water repellency properties of HEPA media appear to be more readily degraded than the tensile strength properties. One possible explanation is that this may be due to distributional effects of the polymer in the fiber matrix of the HEPA media. Increasing polymer content does increase resistance to radiation; however, this is simply because there is more polymer to be degraded; the rate of degradation remains unchanged.

Filtration properties as expressed by DOP penetration and pressure drop do not appear to be greatly affected by increasing radiation dosage. This supports a previous finding by Cheever et al[16] who studied the effects of high level gamma radiation on finished HEPA filters. At the highest levels of radiation dosage--$7X10^8$ rads--this study mildly suggests that filtration properties may be slightly improved. If this is true, the suspicion is that this may relate to radiation degradation of the surface properties of at least some of the polymers.

The organic content of the media bonded with the various polymers has a slight tendency to increase with increasing radiation dosage. The suspected cause is oxidation.

The presentation of Jone's results supports previous contentions in the literature that the radiation dosage and not the source of radiation is the primary cause of polymer degradation.

It should be mentioned that it is quite possible that HEPA media bonded with any of the polymers included in this study still may not satisfy all the requirements of MIL-F-51079A or its proposed revision that includes requirements for radiation resistance. For example, the silicone polymer, despite its superior radiation resistance, is a stiff rigid material. Media bonded with this polymer will probably not possess the flexing characteristics to satisfy the military specification. What may be necessary is the formulating or blending of different polymeric materials to achieve the best compromise of properties.

Acknowledgements

The authors wish to acknowledge C. H. Dexter Division of Dexter Corporation for permission to present this paper.

The authors also wish to acknowledge Maurice Gaddua of Windsor Nuclear Corporation whose advice and suggestions were so helpful in conducting the radiation experiments.

References

1. MIL-F-51079A, Military Specification Filter Medium, Fire-Resistant, High-Efficiency, 31 March 1970.

2. MIL-F-0051079B(EA), Military Specification Filter Medium, Fire-Resistant, High-Efficiency, 29 March 1974.

3. R. A. Wullaert, R. J. Burian, J. B. Melehan, M. Kangilaski and J. E. Gates, "Effect of radiation on ceramic materials", Chapter 6, Effects of Radiation on Materials and Components, J. F. Kircher and R. E. Bowman, Editors, Reinhold Publishing Corp., New York, 1964 (p 372).

4. L. R. Jones, "Effects of radiation on reactor confinement system materials", Proceedings of the Twelfth AEC Air Cleaning Conference, Oak Ridge, Tennessee (pp 655-676), Aug. 28-31, 1972.

5. A. Charlesby, Atomic Radiation and Polymers, Pergamon Press, New York, 1960.

6. J. F. Kircher, "Basic concepts of radiation effects", Chapter 1, Effects of Radiation on Materials and Components, J. F. Kircher and R. E. Bowman, Editors, Reinhold Publishing Corp., New York, 1964, (pp 11-48).

7. R. W. King, N. J. Broadway, R. A. Mayer and S. Palinchok, "Polymers", Chapter 3, Effects of Radiation on Materials and Components, J. F. Kircher and R. E. Bowman, Editors, Reinhold Publishing Corp., New York, 1964, (pp 84-166).

8. F. A. Bovey, The Effects of Ionizing Radiation on Natural and Synthetic High Polymers, Interscience Publishers Inc., New York, 1958.

9 R. W. King, N. J. Broadway, and S. Palinchok, The Effect of Nuclear Radiation on Elastomeric and Plastic Components and Materials, AD267890, Radiation Effects Information Center, Battelle Memorial Institute, Columbus, Ohio. Distributed by National Technical Information Center, Springfield, Va., 1 Sept. 1964 (pp 12-14).

10. E. L. Warrick, "Effects of radiation on organopolysiloxanes", Ind. Eng. Chem., Vol. 47 p. 2388 (1955).

11. E. L. Warrick, D. J. Fisher, and J. F. Zack, Jr., "Radiation resistant silicones", Third Semiannual Radiation Effects Symposium, Vol. 5, Oct. 28-30, 1958.

12. A. Charlesby, "Effect of radiation on behavior and properties of polymers" Chapter 10, Effect of Radiation on Materials, J. J. Harwood, H. H. Hausner, J. C. Morse, and W. G. Rauch, Editors, Reinhold Publishing Corp., New York, 1958 (pp 261-286).

13. W. W. Parksinson, C. D. Bopp, D. Binder and J. E. White, "A comparison of fast neutron and γ-irradiation of polystyrene, I. Cross-linking rates", J.Phys.Chem., Vol. 69, pp 828-833, (1965).

14. L. R. Jones, Presentation to Government-Industry Meeting on Filters, Media and Media Testing, Twelfth AEC Air Cleaning Conference, Oak Ridge, Tennessee, Aug. 28-31, 1972.

15. W. L. Anderson, "Government-Industry meeting on filters, media and media testing", Proceedings of the Twelfth AEC Air Cleaning Conference, Oak Ridge, Tennessee, (pp 731-737), Aug. 28-31, 1972.

16. C. L. Cheever, C. H. Youngquist, P. R. Hirsch, J. C. Hoh, D. S. Janetka and H. R. Fish, "Effects on high-level gamma radiation exposure of HEPA filters", Proceedings of the Twelfth AEC Air Cleaning Conference, Oak Ridge, Tennessee, (pp 638-645), Aug. 28-31, 1972.

Table 1

Polymers Investigated as Binders for HEPA Media in Irradiation Studies

POLYMER	DESCRIPTION	SUSPECTED OR POSSIBLE REPEATING UNIT
POLYCARBONATE	LINEAR THERMOPLASTIC	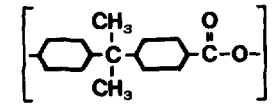
POLYESTER	LINEAR THERMOPLASTIC	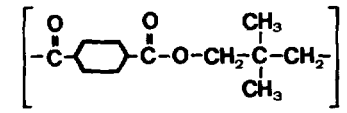
SILICONE	THERMOSETTING RESIN	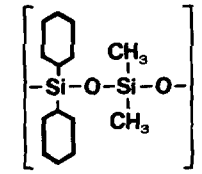
POLY (PHENYLENE OXIDE)	LINEAR THERMOPLASTIC	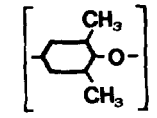
POLYACRYLATE	LINEAR THERMOPLASTIC MOSTLY POLY (ETHYL ACRYLATE)	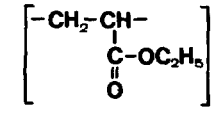
PHENOLFORMALDEHYDE (PHENOLIC)	THERMOSETTING RESIN THERMALLY CURED PRIOR TO RADIATION EXPOSURE	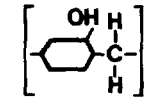
POLYSTYRENE	LINEAR THERMOPLASTIC	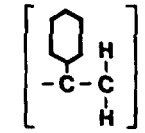
STYRENE-BUTADIENE COPOLYMER (SBR)	HIGH STYRENE THERMOSETTING RESIN STYRENE: BUTADIENE RATIO = 85:15	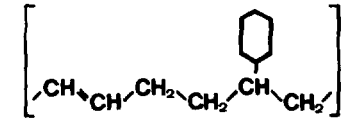

Table 2 Relative radiation resistance of some polymers.

Polymer	Type	Radiation Dosage Required for Threshold Damage * (rads)	Radiation Dosage Required for 25 per cent Damage ** (rads)
Polystyrene	Thermoplastic	8×10^8	$> 4 \times 10^9$
Silicone	Thermosetting	1×10^8	--
Polyvinyl Chloride	Thermoplastic	1.9×10^7	1.1×10^8
Polyethylene	Thermoplastic	1.9×10^7	9.3×10^7
Polyester - Mylar Film	Thermosetting	4.4×10^6	8.7×10^7
Polycarbonate	Thermoplastic	4.3×10^6	4.3×10^7
Phenolic	Thermosetting	2.7×10^6	1.1×10^7
Styrene Butadiene SBR (GR-S)	Elastomer	2.0×10^6	1.3×10^7
Polymethyl Methacrylate	Thermoplastic	8.2×10^5	1.1×10^7
Silicone Rubber	Elastomer	1.3×10^6	4.2×10^6
Teflon	Thermoplastic	1.7×10^4	3.7×10^4

* Threshold Damage - The dosage at which at least one property begins to change.

** 25 percent Damage - The dosage at which at least one property is changed by 25%.

Source: R. W. King, N. J. Broadway and S. Palinchok, The Effect of Nuclear Radiation on Elastomeric and Plastic Components and Materials, AD 267890, Radiation Effects Information Center, Battelle Memorial Institute, Columbus, Ohio. Distributed by National Technical Information Center, Springfield, Va., 1 Sept. 1964, Pages 12-14.

Table 3

Table 3 Effect of irradiation on HEPA media bonded with various polymers.

Water Burst Height (inches of H_2O)

Polymer	Polymer Content (%)	Radiation Dosage (x 10^{-8} rads) 0	0.5	1.0	2.0	3.0	7.0
Polycarbonate	4.4	35	31	6	3	3	0
Polyester	3.2	41	35	16	9	7	0
Silicone	3.2	50	45	35	34	33	13
Polyphenylene Oxide	3.4	50	40	26	6	4	0
Phenol-Formaldehyde	1.9	32	4	0	0	0	0
Polystyrene	2.0	5	15	15	8	6	0
Polyacrylate	3.1	35	27	16	8	6	0
Styrene-butadiene copolymer (SBR)	3.5	3	19	8	7	5	0

Table 4 Effect of irradiation on HEPA media bonded with various polymers.

Tensile strength - (Units: lb/in)

Polymer	Polymer Content (%)	Tensile Strength	Radiation Dosage ($X10^{-8}$ rads) 0	0.5	1.0	2.0	3.0	7.0
Polycarbonate	4.4	MD	5.0	5.9	5.6	2.8	2.7	2.9
		CD	4.2	5.6	4.5	2.7	2.0	2.3
		Avg.	4.6	5.8	5.1	2.8	2.4	2.7
Polyester	3.2	MD	5.5	3.7	3.5	3.5	4.2	3.4
		CD	5.3	3.0	3.1	2.1	4.1	1.7
		Avg.	5.4	3.4	3.3	2.8	4.2	2.6
Silicone	3.2	MD	4.6	6.1	4.8	4.3	3.6	3.2
		CD	4.5	4.5	3.3	3.3	3.5	3.0
		Avg.	4.6	5.3	4.1	3.8	3.6	3.1
Polyphenylene oxide	3.4	MD	8.5	5.9	5.5	3.5	3.5	2.3
		CD	4.7	4.9	4.9	2.7	2.5	2.2
		Avg.	6.6	5.4	5.2	3.1	3.0	2.3
Phenolformaldehyde	1.9	MD	5.4	7.8	5.3	--	4.5	3.5
		CD	3.0	3.8	2.5	--	2.3	3.3
		Avg.	4.2	5.8	3.9	--	3.4	3.4
Polystyrene	2.0	MD	2.9	2.5	2.3	2.2	1.7	1.6
		CD	1.8	0.6	1.8	1.1	0.8	0.8
		Avg.	2.4	1.6	2.0	1.7	1.3	1.2
Polyacrylate	3.1	MD	6.2	3.9	4.2	3.6	3.0	1.8
		CD	2.8	2.2	2.3	1.5	1.8	0.8
		Avg.	4.5	3.1	3.3	2.6	2.4	1.3
Styrene-butadiene copolymer (SBR)	3.5	MD	2.2	5.7	3.6	3.1	3.0	2.8
		CD	1.3	3.2	2.2	2.1	1.8	1.7
		Avg.	1.8	4.5	2.9	2.6	2.4	2.3

Table 5 Effect of irradiation on HEPA media bonded with various polymers.

DOP penetration and pressure drop @ 320 cm/min

Polymer	Polymer Content (%)	Property	Radiation Dosage ($X10^{-8}$ rads) 0	0.5	1.0	2.0	3.0	7.0
Polycarbonate	4.4	DOP (%)	.007	.004	.004	.005	.005	.003
		ΔP (mm H_2O)	35.5	37.0	37.7	38.6	34.1	34.8
Polyester	3.2	DOP (%)	.003	.003	.003	.004	.006	.005
		ΔP (mm H_2O)	34.0	34.3	34.8	35.6	35.2	32.4
Silicone	3.2	DOP (%)	.003	.005	.005	.005	.005	.004
		ΔP (mm H_2O)	36.7	37.3	37.6	37.2	37.3	35.8
Polyphenylene oxide	3.4	DOP (%)	.004	.003	.004	.005	.006	.006
		ΔP (mm H_2O)	37.3	37.8	37.6	37.2	37.3	35.1
Phenolformaldehyde	1.9	DOP (%)	.004	.002	.003	.003	.004	.003
		ΔP (mm H_2O)	34.8	34.6	34.7	35.0	35.1	34.4
Polystyrene	2.0	DOP (%)	.002	.002	.001	.003	.002	.002
		ΔP (mm H_2O)	38.1	38.0	36.8	37.3	37.6	34.9
Polyacrylate	3.1	DOP (%)	.005	.005	.006	.004	.007	.003
		ΔP (mm H_2O)	35.7	35.5	34.8	35.1	35.3	31.7

Table 6 Irradiation of HEPA media bonded with various polymers.

Combustibles (%)

Polymer	Polymer Content (%)	Radiation Dosage ($X10^{-8}$ rads) 0	0.5	1.0	2.0	3.0	7.0
Polycarbonate	4.4	6.4	6.8	6.9	6.1	4.1	7.0
Polyester	3.2	5.2	5.3	5.5	5.2	4.7	5.8
Silicone	3.2	5.2	5.5	5.1	5.3	5.4	6.3
Polyphenylene oxide	3.4	5.4	5.6	5.5	5.4	5.6	6.1
Phenolformaldehyde	1.9	3.9	4.0	4.1	4.2	4.3	4.8
Polystyrene	2.0	4.0	4.2	4.1	4.1	4.3	4.7
Polyacrylate	3.1	5.1	5.4	5.1	4.9	5.2	5.0

Note: % Combustibles minus 2% cellulose = Polymer Content

Table 7 Radiation resistance of HEPA media - Effect of polymer content on water penetration time (sec.).

Polymer	Polymer Content	Radiation Dosage ($X10^{-8}$ rads) 0	0.5	1.0	2.0	3.0	4.0	5.0
Silicone	2.2	600+	600+	600+	600+	132	40	2
	3.3	600+	600+	600+	600+	352	29	8
Polystyrene	4.5	4	43	120	2	3	0	0
	5.4	29	51	60	28	47	0	0
Polyester	4.0	600+	600+	115	40	0	0	0
	6.0	600+	572	363	98	35	6	0
Polyacrylate	3.9	600+	600+	30	0	0	0	0
	5.8	600+	600+	342	0	0	0	0

Table 8 Irradiation comparison tests.

Sample	Radiation Source	H_2O Pen. Time (sec)	Wet Strength (in. H_2O)	MD Dry Strength (#/in)	CD Dry Strength (#/in)
A	Control	>50,000	>30	5.2	4.0
A	WN	41	5	4.0	2.6
A	SRL	27	4	3.8	2.3
B	Control	>50,000	>30	4.5	4.4
B	WN	31	5.25	3.8	2.9
B	SRL	29	4.5	2.75	2.75
C	Control	>50,000	>30	2.5	1.5
C	WN	> 3,600	14.5	2.2	1.4
C	SRL	455 to >3600	7 - 13	2.0	1.2

Control — Sample prior to radiation exposure

WN — Sample irradiated to $1X10^8$ rads by electron beam source at Windsor Nuclear (beta radiation)

SRL — Sample irradiated to $1x10^8$ rads by Cobalt 60 source at Savannah River Laboratory (gamma radiation)

Source: Jones, L. R. presentation to Government-Industry Meeting on Filters, Media, and Filter Testing held during Twelfth AEC Air Cleaning Conference in Oak Ridge, Tennessee, August 28 - 31, 1972.

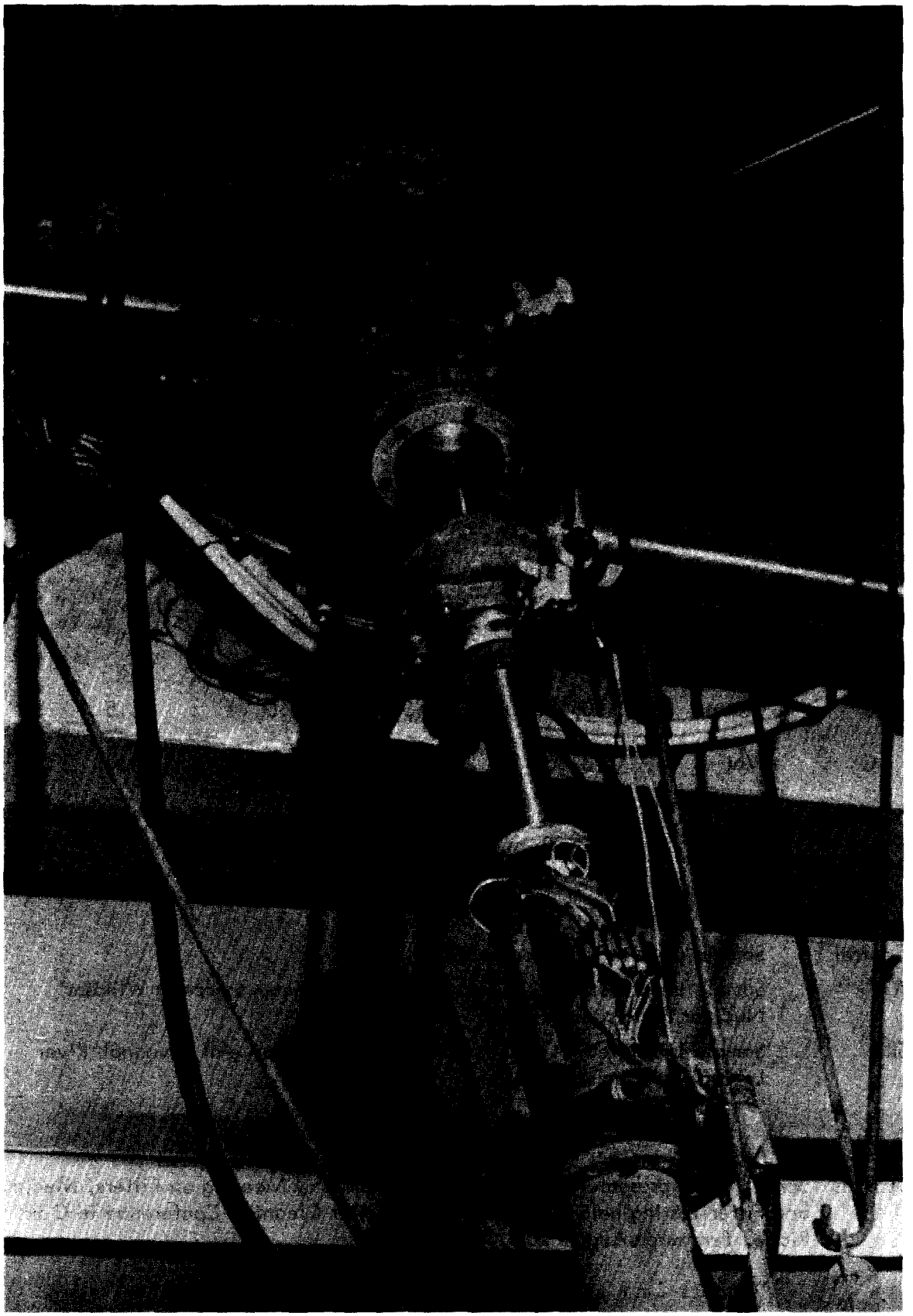

Figure 1 3 MEV Van de Graaf Generator at Windsor Nuclear

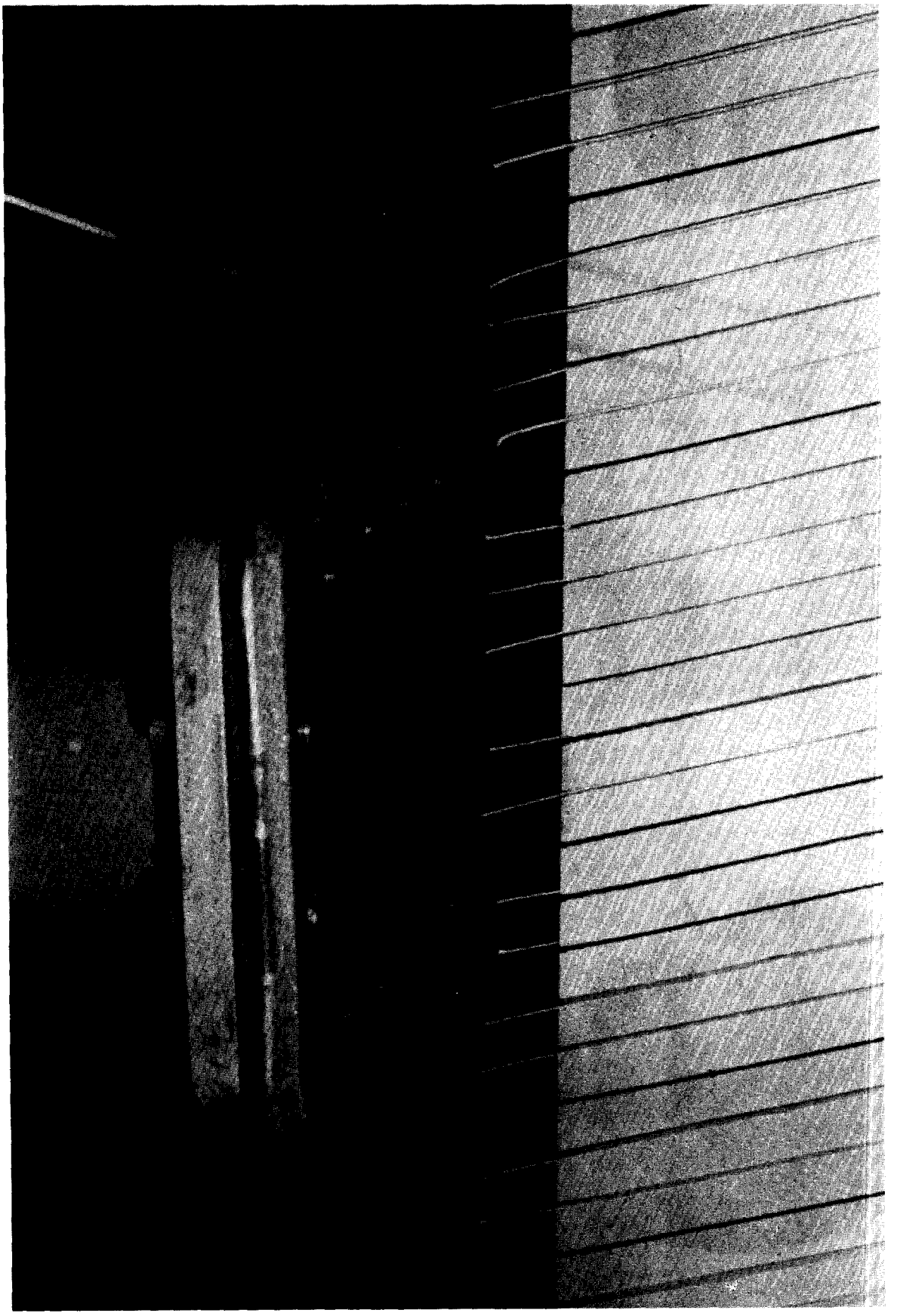

Figure 3 Electron Beam Irradiation of HEPA Specimens

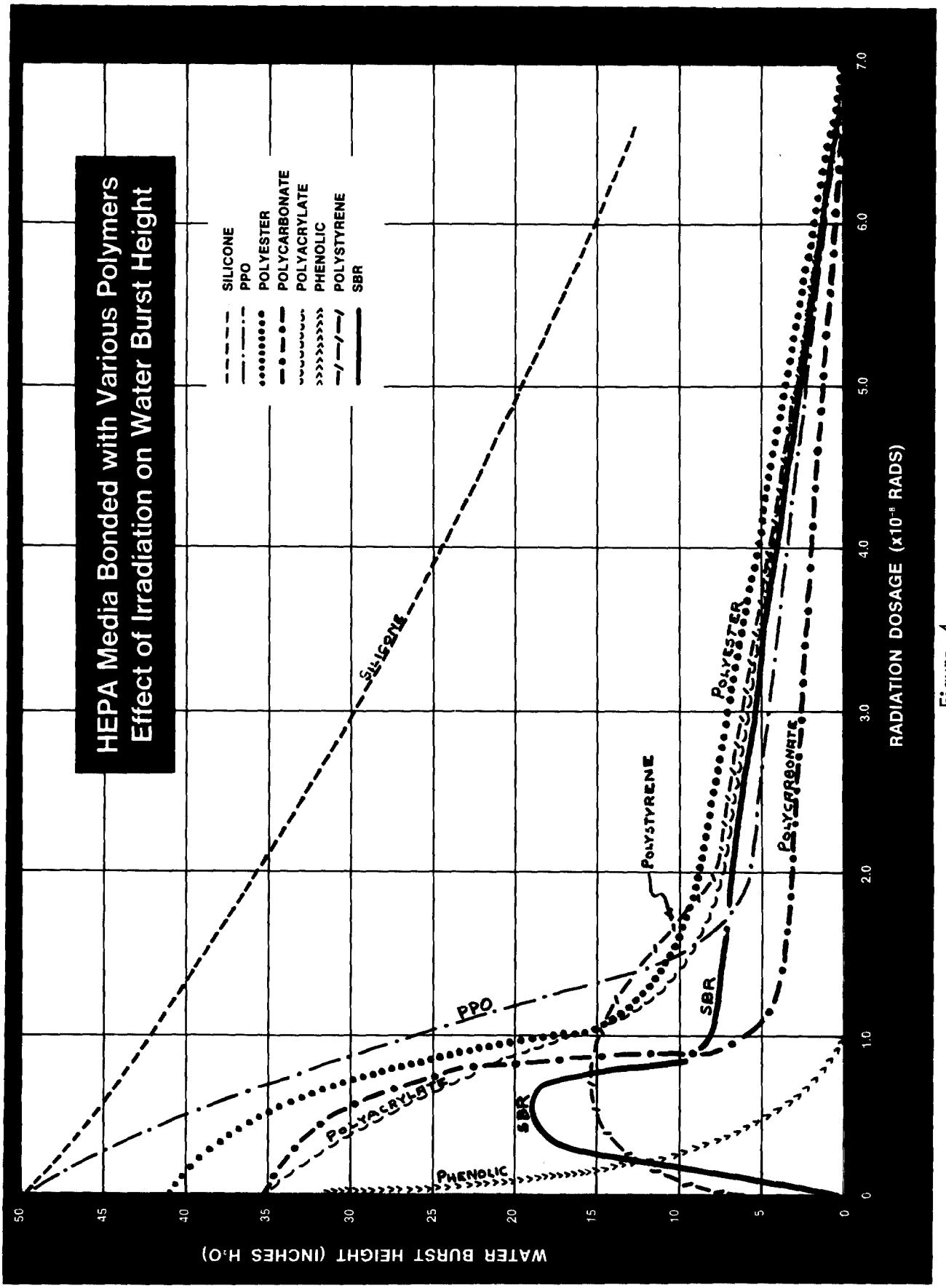
HEPA Media Bonded with Various Polymers
Effect of Irradiation on Water Burst Height
SILICONE
PPO
POLYESTER
POLYCARBONATE
POLYACRYLATE
PHENOLIC
POLYSTYRENE
SBR
WATER BURST HEIGHT (INCHES H₂O)
RADIATION DOSAGE (x10⁻⁸ RADS)
0
5
10
15
20
25
30
35
40
45
50
1.0
2.0
3.0
4.0
5.0
6.0
7.0
SILICONE
PPO
POLYESTER
POLYSTYRENE
POLYCARBONATE
SBR
POLYACRYLATE
PHENOLIC
SBR

Figure 4

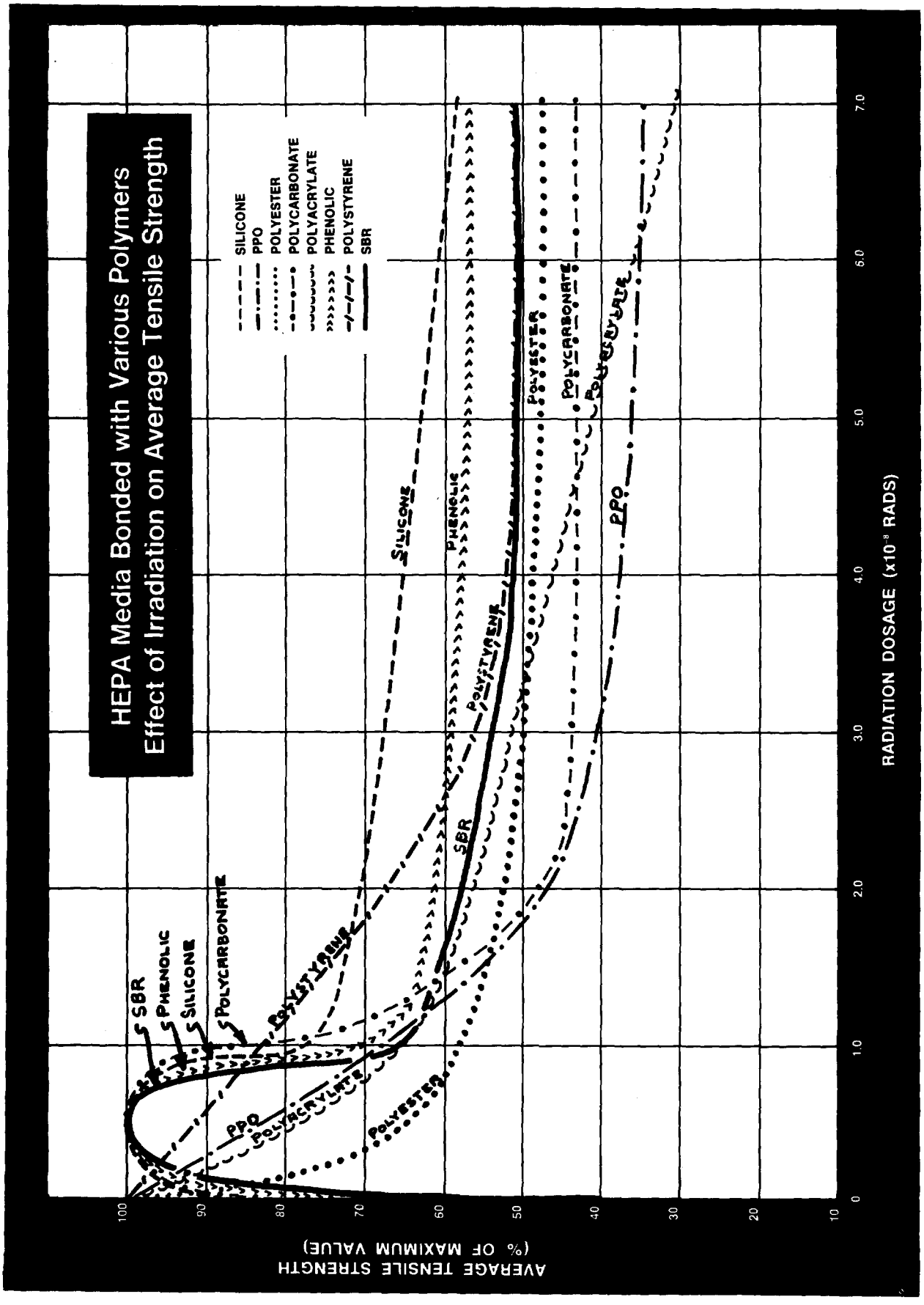
HEPA Media Bonded with Various Polymers
Effect of Irradiation on Average Tensile Strength
SILICONE
PPO
POLYESTER
POLYCARBONATE
POLYACRYLATE
PHENOLIC
POLYSTYRENE
SBR
AVERAGE TENSILE STRENGTH
(% OF MAXIMUM VALUE)
RADIATION DOSAGE (x10⁻⁸ RADS)
100
90
80
70
60
50
40
30
20
10
0
1.0
2.0
3.0
4.0
5.0
6.0
7.0

Figure 5

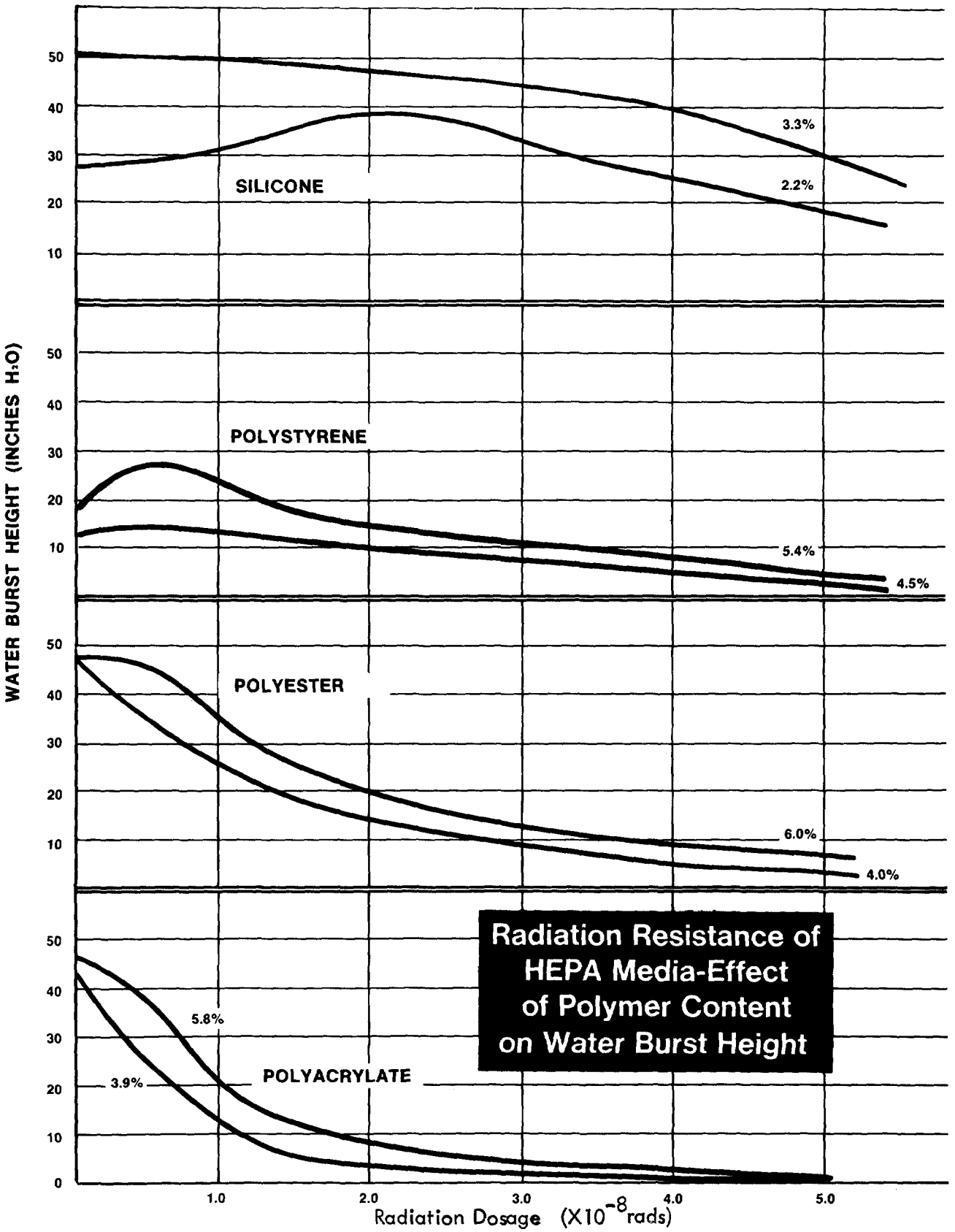
WATER BURST HEIGHT (INCHES H₂O)
SILICONE
3.3%
2.2%
POLYSTYRENE
5.4%
4.5%
POLYESTER
6.0%
4.0%
POLYACRYLATE
5.8%
3.9%
Radiation Resistance of HEPA Media-Effect of Polymer Content on Water Burst Height
Radiation Dosage (X10⁻⁸ rads)
0
10
20
30
40
50
1.0
2.0
3.0
4.0
5.0

Figure 6

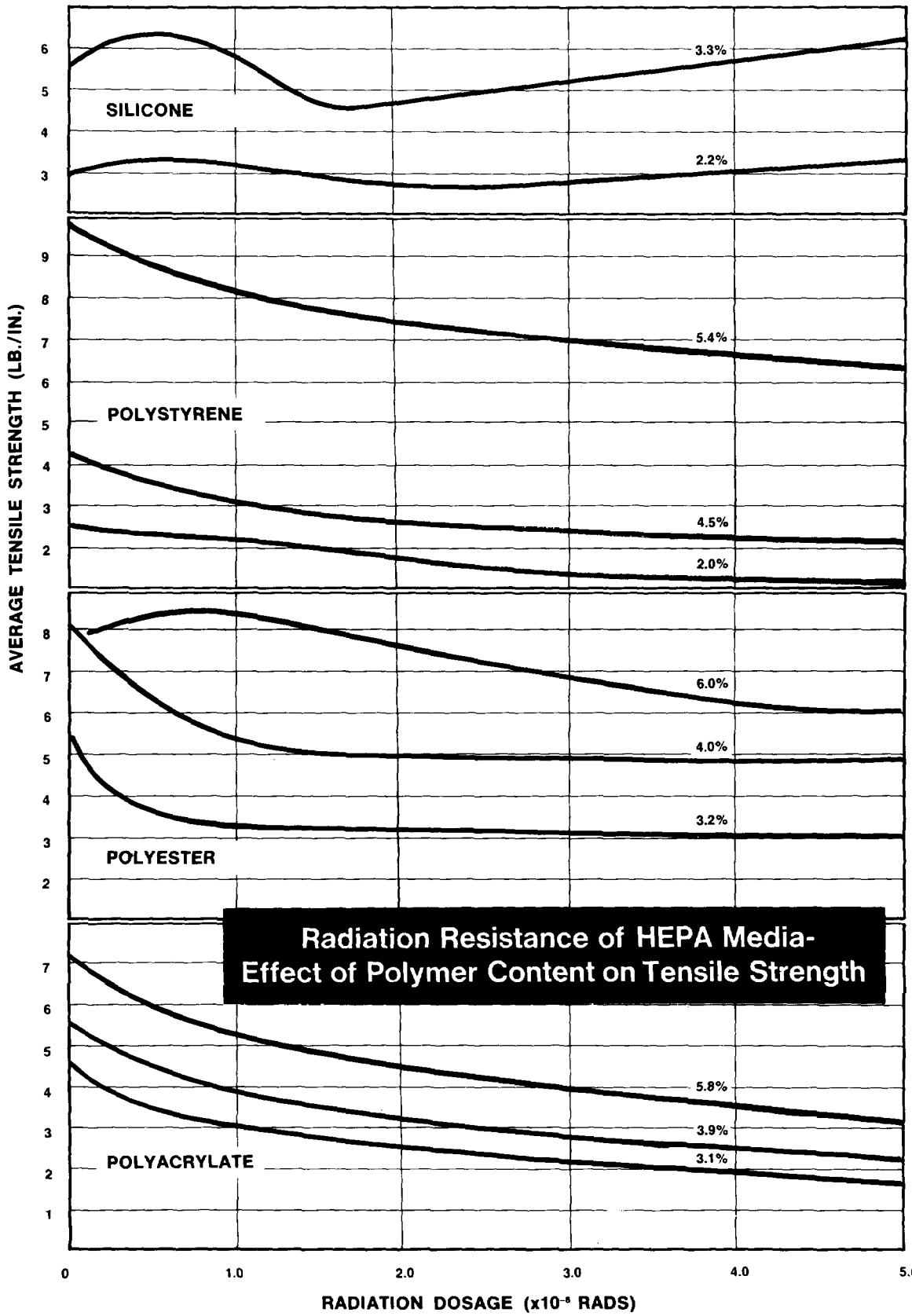
AVERAGE TENSILE STRENGTH (LB./IN.)
SILICONE
3.3%
2.2%
POLYSTYRENE
5.4%
4.5%
2.0%
POLYESTER
6.0%
4.0%
3.2%
POLYACRYLATE
5.8%
3.9%
3.1%
Radiation Resistance of HEPA Media-
Effect of Polymer Content on Tensile Strength
0
1.0
2.0
3.0
4.0
5.0
RADIATION DOSAGE (x10⁻⁶ RADS)

Figure 7

ENHANCEMENT OF FILTER MEDIA PERFORMANCE BY CORONA-FREE ELECTRIC FIELDS*

H. F. Bogardus, R. C. Clark, J. K. Thompson and G. H. Fielding
Chemical Dynamics Branch
Naval Research Laboratory
Washington, D. C. 20375

Abstract

Dielectrophoresis is the movement of uncharged particles in a nonuniform electric field. Aerosol dielectrophoresis occurs when an aerosol and a glass fiber filter medium are exposed together to an electric field. The aerosol particles are polarized by the field, and experience a dielectrophoretic force in the field nonuniformities caused by the glass fibers. Motion of the particles is in the direction of the higher electric field intensity. Since the highest intensity is at the fiber surface, the particles are deposited there.

Using a commercial fibrous glass filter medium between flat screen electrodes providing a field strength of 11 kv/cm, and at the manufacturer's rated pressure drop of 0.4 inch w.g., the filtration efficiency of the medium is increased from the normal 68 percent to 98 percent with a 0.3 micron aerosol, and from 78 to 99 percent for a one micron aerosol. This means that electrification decreases aerosol penetration of the medium by factors of 16 and 22, respectively. The results indicate the existence of a promising family of dielectrophoretic aerosol filters. Development has only begun, and the scope of the applications of dielectrophoretic filters will be determined by future scientific and engineering studies.

I. Background

In the science and technology of aerosol filtration, in addition to mechanical or aerodynamic effects, three major types of electrical processes or effects can be distinguished. The first is electrostatic precipitation, a well known and valuable commercial technique. In this process, corona-generated air ions, following the lines of force of the high-voltage corona field, deposit on aerosol particles and charge them electrically to a very high degree. The charged particles are then attracted to and deposited on a metallic electrode which establishes one pole of a high voltage field, which may be the corona field or a separate precipitating field. The second process is the coulombic deposition of slightly and fortuitously charged aerosol particles in a fibrous filter due to attractive forces between the particle charges and polarization charges induced on the fibers, and to other related effects. This process has no commercial significance, and is generally only a minor perturbation on the major filtration mechanisms of diffusion and inertial capture. The third process, which is the subject of this paper, is dielectrophoresis. This term coined by Pohl is used to provide a name clearly distinct from electrostatic precipitation, with which dielectrophoresis is occasionally confused(1).

*Work performed under USAEC Project Number WA6690-71 in FY74.

A dielectrophoretic filter operates on uncharged aerosol particles. Both the particles and the filter medium are simultaneously exposed to a strong and generally uniform electric field, i.e. a zero-gradient field, which charges neither particles nor medium but polarizes both. Additionally, the filter fibers distort the originally uniform electric field to produce an enormous number of microscopic nonuniformities in the field within the fiber mat. The distortion results from the fact that the dielectric constant of the fiber material (glass) is greater than that of the continuous medium (air). The electrical lines of force converge as they approach each fiber, and diverge as they leave it. Thus, there is an electric field gradient from each interfiber space to each fiber, and the uncharged but polarized aerosol particles experience an accelerating force in the direction of the higher field strength, i.e., up the gradient and toward the fiber.

Several features of the dielectrophoretic filtration process are worth noting or emphasizing at this point: (1) there is no net charge on the aerosol particles before, during, or after deposition; (2) the particles do not move to a metallic or conducting electrode, but to the field-distorting elements, the fibers; (3) the electrodes do not collect the particles, but serve only as the means to impress an external field on the filter medium and the aerosol particles; (4) the polarity of the impressed field is immaterial to the dielectrophoretic process, since the field gradients around each fiber are independent of field polarity; (5) dielectrophoretic filtration in a fibrous filter necessarily occurs simultaneously with ordinary diffusive and inertial deposition, and the observed filtration is the net effect of all mechanisms operating; (6) a dielectrophoretic aerosol filter is an extremely low-current and low-power device; after receiving its initial energy charge (acting as a capacitor), current flow is only that due to leakage through the glass fibers and deposited material.

The overall process of dielectrophoretic aerosol filtration is not only unfamiliar; its basic mechanism - the movement of an uncharged particle in a field gradient - is an uncommon one. An appreciation of this mechanism may be aided by a comparison to a magnetic analog, the deposition of iron filings on the poles of a magnet. Consider an uncharged aerosol particle in a uniform electric field, and a particle of iron in a uniform magnetic field. Neither particle experiences a net force, and neither particle moves (neglecting gravity, etc.). However, let the fields be rendered nonuniform in some way. Each particle is then forced toward the more intense region of its respective field, i.e., up the field gradient. In each of these highly analogous mechanisms, the force required to accelerate the particle comes through the conversion of potential into kinetic energy.

II. Introduction

The first reported work in the dielectrophoretic filtration of aerosols was a series of tests conducted by the Harvard University Air Cleaning Laboratory on a commercial prototype in 1954[2]. The factors by which electrification improved the performance of common glass fiber mats ranged from 1.5 to 6.5, or from 2 to 3, depending on test conditions. The device appeared to offer no particular

advantages in comparison with other filter types already in production and it was never marketed.

Thomas and Woodfin, in 1959, reported a study on a novel type of dielectrophoretic air filter consisting of alternating charged and grounded metal plates with the interplate spaces packed with glass fiber[3]. For a filter 14.5 inches deep (in the direction of the air stream), application of a field of 9.3 kv/cm resulted in a performance improvement of better than a factor of five in the air velocity range of 500-400 fpm. A similar filter one inch deep also showed "great improvement" when electrified, but the improvement factor could not be measured accurately.

In Rivers' theory paper of 1962, he refers to a device in which an electric field is applied essentially parallel to the plane of a laminated-paper filter medium, and perpendicular to the direction of air flow through the medium[4]. The design is outlined in Dahlman's 1950 U. S. patent[5]. Dahlman states that the efficiency of the laminated medium is increased from 20 percent to 90 percent by electrification, corresponding to a reduction in penetration by a factor of eight. This result was obtained with aerosol particles precharged in a corona; a smaller improvement would be expected with uncharged particles. The manufacturer of the device described by Rivers claims that electrification reduces penetration by a factor of 1.7.

Havlicek, in a 1961 paper, investigated theoretically and experimentally the relative merit - in dielectrophoretic aerosol filters - of a parallel vs. a perpendicular arrangement of air flow and electric field[6]. He concluded that the perpendicular geometry, which is the one used by Dahlman and by Thomas and Woodfin, is inferior. Havlicek's argument was that, in perpendicular orientation of air flow and electric field near a fiber surface, the maximum air velocity coincides with the maximum field gradient, and that the effect of the former tends to cancel that of the latter. The parallel geometry is therefore preferred. Havlicek also analyzed theoretically the magnitude of the forces between aerosol particles and the fibers of a dielectrophoretic filter.

Walkenhorst and Zebel reported, in 1964, on a dielectrophoretic aerosol filter comprised of 30 to 100 layers of nylon hosiery fabric with interspersed electrodes between every 10 layers[7]. Pressure losses were very low in comparison with conventional filters having similar filtration efficiency.

Extensive theoretical and model studies in dielectrophoretic filtration of aerosols have been reported by Zebel and by Walkenhorst, and are commented on by Davies[8,9,10,11,12].

While opinions may legitimately differ, we regard the filters of Dahlman and Thomas and Woodfin as suffering from the theoretical disadvantage noted by Havlicek. Similarly, it appears that the nylon mat filters are interesting and useful models not likely to be scaled up to commercially useful size.

In June, 1973, at the time the NRL one-man-year program for the Atomic Energy Commission was being forumulated, mathematical analyses

and geometrically-regular model studies in dielectrophoretic filtration appeared adequate in number and variety. The NRL effort was therefore slanted toward pragmatic ends. Specifically, it was designed to explore the dielectrophoretic filtration possibilities of existing commercial glass fiber filter media in a model of the simplest possible configuration using a parallel orientation of air flow and electric field.

Materials and Apparatus

A series of glass fiber filter media from a single manufacturer was selected for the NRL investigation. These were designated HP-15, HP-100 (two types) and HP-200. Each mat was an all-glass fiber material, 6.5 mm thick, but differing in fiber size and air flow characteristics. The HP-100 medium, which we have studied most extensively, was comprised of fiber sizes from 0.25 to several microns, with fibers of about one micron in diameter predominating. In normal use all three media are commonly fabricated into pleated or pocketed assemblies to increase the flow rate to pressure loss ratio above that for a flat sheet.

For support, 14 by 14 cm samples of the filter media were permanently cemented into 6.5 mm thick hardboard frames, 18 by 18 cm in outside dimensions. Prior to an experiment, flat stainless steel woven screen electrodes, 18 by 18 cm, were taped to each face of the hardboard frame. This filter package was then ready to be clamped between and taped into mating flanges in the air flow duct.

The flow system was basically a cylindrical aluminum duct, 10 cm in diameter and 250 cm long, fitted near the midpoint with round-to-square transitions and flanges to accept the filter package. Air flow in the duct was induced by a canister-type vacuum cleaner controlled by a variable autotransformer. Air flow was measured via the pressure drop across a standard flow nozzle mounted in the duct. A manometer registered the pressure loss in the filter. Two DOP aerosols were used: a thermally generated one of 0.3 micron particle diameter, and an air-atomized one of about one micron diameter. Aerosol concentrations before and after the filter were measured with a light-scattering photometer. Each aerosol sampling point was preceded in the duct by a set of six orifice plates for aerosol mixing.

One of the screen electrodes attached to the filter was supplied with DC voltage from a negative-polarity 0-20 kv power supply, the other electrode being grounded. Voltages were measured with a calibrated electrostatic voltmeter.

III. Experimental Procedure

The simple experimental procedure adopted involved the simultaneous measurement of filter penetration (or filter efficiency) and pressure loss in the filter, at a number of voltages and air flows. With the filter package and electrodes clamped airtight into the duct system, the lowest flow rate was established. In this condition, the electrode voltage was varied successively from 1 or 2 kv to 7 kv, and the unfiltered and filtered aerosol concentrations measured at each voltage. The air flow rate was then increased, and aerosol concentrations again measured at each voltage. The stepwise increase in air flow was continued to the level desired.

IV. Results

The experimental results obtained with the HP-100 filter medium are outlined in Figures 1 and 2. Qualitatively similar results were also obtained with the HP-15 and HP-200 media.

The information in Figures 1 and 2 has been processed into a single quantity of particular interest, the Dielectrophoretic Augmentation Factor (DAF), values for which are given in Tables I and II. The DAF is a direct indicator of the reduction in filter penetration which results from application of an electric field, all other experimental variables remaining constant. The DAF is calculated by dividing the filter penetration percentage at zero voltage by the penetration at the voltage of interest.

V. Discussion

Figures 1 and 2 show that, for both the 0.3 and one micron aerosols and the nonelectrified condition, filtration efficiency increases with increasing air velocity. This result indicates that the predominant filtration mechanism is inertial capture of the aerosol particles by the glass fibers. Further, at a pressure drop of one inch w.g. (45 cm/sec), the capture efficiency for the smaller aerosol is no longer increasing while that for the larger aerosol is still rising. This effect is in qualitative accord with the inertial capture mechanism and the relative particle masses.

With the application of an electric field to the filter medium and the aerosol, the change in efficiency with air velocity is in the opposite direction to that characteristic of the nonelectrified condition. This effect is to be expected, since, at higher air velocities through the filter, an aerosol particle is under the influence of any field micrononuniformity for a shorter time, and its probability of deposition in the filter is therefore reduced.

It is evident that the performance curves for the electrified condition continue to approach the nonelectric curve as the air velocity increases. At extremely high air velocities it may be assumed that the dielectrophoretic effect would be negligible, and pure inertial capture would prevail.

The dielectrophoretic augmentation factors of Tables I and II show very high values at the lowest air velocity, and, in fact, may become still higher as the air velocity approaches zero. Such figures may be of no practical significance. It is suggested that a consideration of Tables I and II take into account the fact that the HP-100 medium is designed for conventional use at a pressure drop of 0.4 inch w.g., corresponding to a face velocity of 21 cm/sec (41 fpm). At this flow rate and at an applied voltage of 7 kv an interpolation based on the data of Tables I and II shows that the DAF is 21 for 0.3 micron aerosol and 28 for 1.0 micron aerosol. New applications of this or other filter media employing the dielectrophoretic principle may, of course, use other standard air velocities resulting in other dielectrophoretic augmentation factors.

It should be emphasized that the NRL data reported here cannot be extensively generalized at the present time. Variables which

Table I - Dielectrophoretic Augmentation Factor as a Function of Voltage and of Pressure Loss in HP-100 Filter Medium (No. 6); 0.3 Micron Aerosol.

Applied Voltage, Kilovolts*	Filter Pressure Loss, inches w.g.							
	0.05	0.10	0.15	0.25	0.35	0.50	0.75	1.00
0	1	1	1	1	1	1	1	1
2	8	3	3	2	2	2	2	1
3.5	19	13	11	6	5	4	3	2
5	95	39	28	13	9	6	4	3
7	330	120	100	42	27	14	9	6

*Applied voltage x 1.54 = electric field strength in kv/cm.

Table II - Dielectrophoretic Augmentation Factor as a Function of Voltage and of Pressure Loss in HP-100 Filter Medium (No. 6); One Micron Aerosol.

Applied Voltage, Kilovolts*	Filter Pressure Loss, inches w.g.							
	0.05	0.10	0.15	0.25	0.35	0.50	0.75	1.00
0	1	1	1	1	1	1	1	1
2	30	6	4	3	2	2	2	1
3.5	110	30	18	10	6	4	3	2
5	300	95	50	20	13	8	5	3
7	1100	360	170	50	35	18	11	7

*Applied voltage x 1.54 = electric field strength in kv/cm.

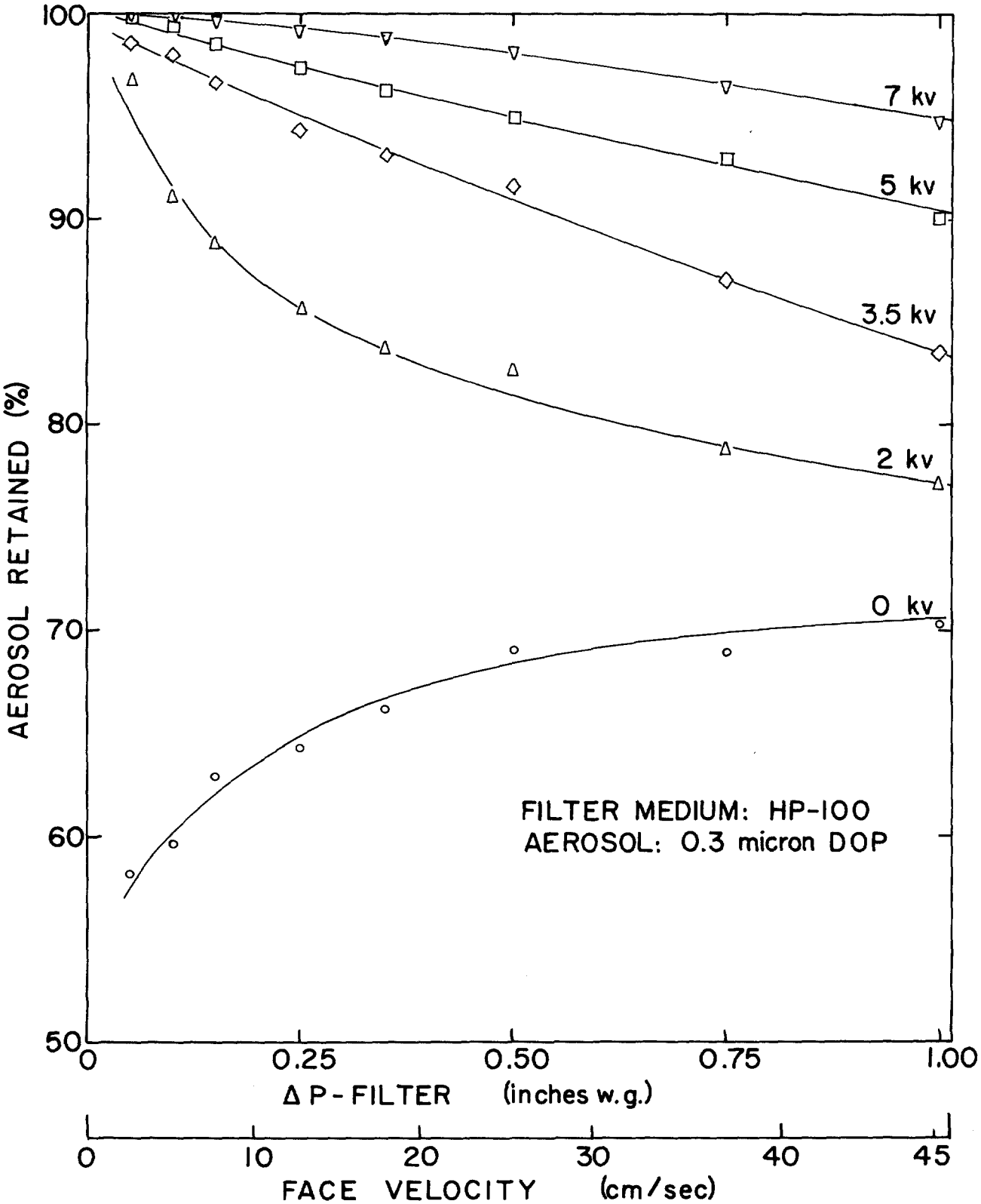

Figure 1 Dielectrophoresis effect in HP-100 medium; 0.3 micron DOP.

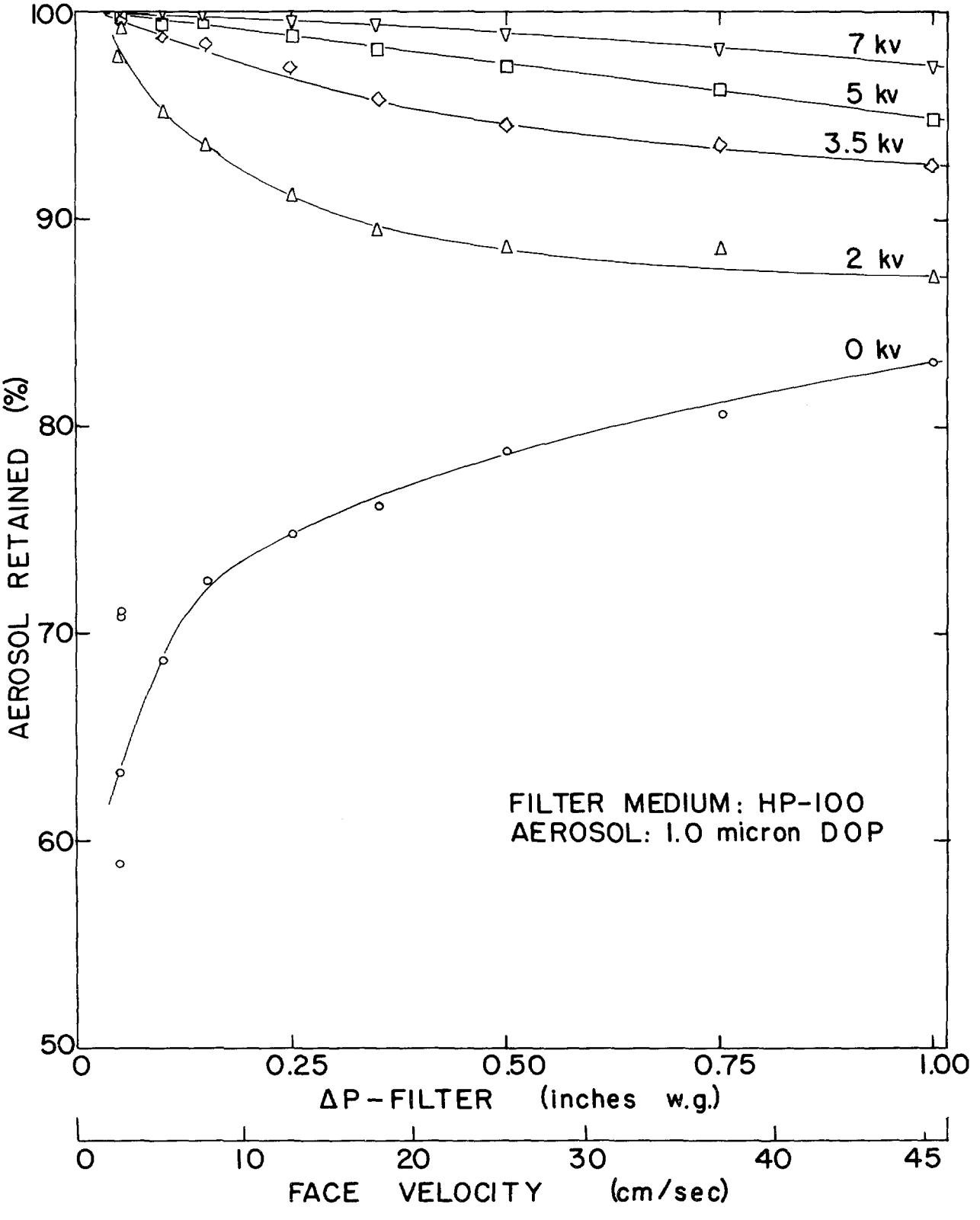

Figure 2 Dielectrophoresis effect in HP-100 medium; 1.0 micron DOP.

remain to be explored include aerosols of different sizes and materials, media of different fiber sizes or fiber size mixes, different fiber materials, different fiber coatings, and different fiber medium thicknesses. The results of introducing these variables cannot, in some cases, be predicted.

It may also be noted that the use of a planar filter configuration in our studies does not imply that this is the optimum arrangement for full sized filters. Typical means used in commercial filter installations to decrease filter pressure losses should be applicable to dielectrophoretic filters as well.

VI. Conclusions

The results of the NRL studies in FY74 on the dielectrophoretic augmentation of standard glass fiber filter mats are sufficiently impressive to convince us of the existence of a promising new direction for study in aerosol filtration. The dimensions of the application of the dielectrophoretic aerosol filter family cannot be foreseen at present, and in any case will depend on the scientific and engineering vigor and innovation applied to future work.

VII. References

(1) Pohl, H. A., "The Motion and Precipitation of Suspensions in Divergent Electric Fields", J. Appl. Phys. 22:869-871 (1951)
(2) Billings, C. E., Dennis, R., and Silverman, L., "Performance of the Model K Electro-Polar Filter", Harvard Air Cleaning Laboratory, Boston, Massachusetts, Report NYO-1592 (1954)
(3) Thomas, J. W. and Woodfin, E. J., "Electrified Fibrous Air Filters", AIEE Trans., Pt. II 78:276-278 (1959)
(4) Rivers, R. D., "Non-Ionizing Electrostatic Air Filters", ASHRAE Jnl: 37-40 (Feb. 1962)
(5) Dahlman, V., "Electrical Gas Cleaner Unit", USP 2,502,560 (1950)
(6) Havlicek, V., "The Improvement of Efficiency of Fibrous Dielectric Filters by Application of an External Electric Field", Int. J. Air and Water Poll. 4:225-236 (1961)
(7) Walkenhorst, W. and Zebel, G., "Concerning a New Dust Filter of High Separation Capacity and Low Flow Resistance", Staub 24:444-448 (1964)
(8) Zebel, G., "Deposition of Aerosol Flowing Past a Cylindrical Fiber in a Uniform Electric Field", J. Colloid Sci. 20:522-543 (1965)
(9) Zebel, G., "Improving the Separation Efficiency of Fiber Filters by Electrical Fields", Staub 26:18-22 (Engl. trans.) (1966)
(10) Zebel, G., "Aerosol Deposition on a Single Fiber Under the Influence of Electrical Forces, Part I", Staub: 29:21-27 (Engl. trans.) (1969).
(11) Walkenhorst, W., "Reflections and Research on the Filtration of Dust from Gases with Special Consideration of Electric Forces", Aerosol Science 1:225-242 (1970). See also Staub 29:1-13 (Engl. Trans.) (1969).
(12) Davies, C. N., "Problems in Aerosol Filtration", Filtration and Separation: 692-694 (Nov/Dec 1970)

DISCUSSION

RIVERS: It's certainly a pleasant thing to see an idea I worked on 20 years ago exhumed and given vigorous attention. However, I can't echo Wendell Anderson's remark yesterday that it's nice to see your results duplicated because you were far more successful at it than any of the experiments we ever ran. I was fishing around for some sort of explanation for the difference. We worked with aerosols that were pretty aged; namely, whatever was floating around outside the window. You used DOP smoke which is freshly generated and of course pressure generated aerosols tend to be charged even when the cloud does not have a net unbalanced charge. If this is so, you would be experiencing the usual type of precipitation in a field rather than purely dielectric radiation effects. We performed experiments like that and we got astounding improvements in glass fiber penetration. Did you do any investigation of the charge distribution?

FIELDING: Indirectly, Mr. Rivers. First, let me thank you for your courteous remarks. We were careful to say this is not new. We all stand on someone else's shoulders, you know. As to the charge of the particles, we plan to do a little more work on that. We have one bit of evidence. If the effect is predominantly dielectric, then the effectiveness should vary by the square of the voltage and if it's coulombic, it should vary by the first power of the voltage, as nearly as we can tell. It looks as though the dielectric effect is minor.

RIVERS: One other thing, I don't see the humidities at which you ran. These things have been quite successful in dry atmospheres, but they do fade out under high humidity operating conditions. Then, performance drops back to what it would be without any electric field applied.

FIELDING: Ours was 50 percent or less and we have not explored variations in the relative humidity.

FIRST: I was interested in looking at your filtration conditions. You said that the filter mat normally had a pressure drop of 0.4 in w.g. This indicates that it's a high velocity filter and yet your filtration velocity was exceptionally low for this kind of filter. It was around 10 fpm or, perhaps, even less. Does this mean that you have to have an extraordinarily long time for this effect to become manifested?

FIELDING: These filters, as perhaps most of you know, are tested over a range of air velocities and the face velocities at which the filter is operated commercially is 0.4 in w.g. This is about 41 fpm. Our range of velocities covers this. We mentioned at the end that the augmentation factors are on the order of 10 to 20 at rated velocity.

CHARACTERIZING SAND GRAINS TO OPTIMIZE FILTER PERFORMANCE

G. A. Schurr
J. E. Johnston

Engineering Service Division
E. I. du Pont de Nemours & Company
Newark, Delaware

Abstract

The operating performance of a deep-bed sand filter used for cleaning radioactive particulates from exhaust air is dependent upon the characteristics of the finest sand layer. This sand is usually specified on the basis of particle size distribution and air permeability. Recent studies have shown this specification is inadequate in providing a basis for selection of an optimum filter media. Sands obtained from different geographic deposits behave differently in the filter. The surface microstructure of the sand related to roughness or texture has been found to be an important variable in determination of the best sands for use as filter media.

Discussion

The deep-bed sand filters in use at the Savannah River Plant use 36 inches of "G" grade[1] sand to achieve their particulate collection capability. This sand is specified to have less than 2 percent coarser than 20 mesh and no more than 1 percent fines and dirt passing 50 mesh screen. A further restriction calls for 20-40 percent to be retained on 30 mesh screen. The air permeability as measured in a 24 inch bed under a superficial air flow of 5 ft/min is to be in the range from 2.4-4.0 inches H_2O under minimum packing density. This represents a stringent specification on the sand producer's equipment in trying to achieve high tonnage production rate.

In anticipation of additional filter construction, interested vendors were asked to submit samples produced to this specification. These silica sands were then tested in an eight inch square filter column to assess their air permeability and DOP filter collection efficiency. Results from these tests are tabulated in Table 1. Besides origin of the sand, the DOP collection efficiency and bed pressure drop for a 36 inch layer operated under a 5 ft/min flow velocity are shown.

While each sand was produced to the same specification, its particle collection efficiency as determined using a DOP aerosol smoke varied from 99.75-99.97%. This represents considerable latitude in performance where high collection efficiency is essential. While permeability readings ranged from 4.9 to 6.2 inches for these sands, there seems no correlation between high efficiency and high pressure drop. In fact, sand #5 has both the highest efficiency and lowest pressure drop - a desirable combination.

TABLE 1 - SAND CHARACTERISTICS

36" SAND - 5 FT/MIN FLOW VELOCITY

Ident.	Origin	ΔP, Inches H_2O	DOP Eff. %	Roughness Index
1	Texas	5.1	99.87	7.0
2	Wisconsin	5.6	99.90	5.0
3	Illinois	5.6	99.905	6.0
4	Iowa	5.0	99.95	10.0
5	Ohio	4.9	99.97	12.0
6	W. Virginia	5.1	99.97	15.0
7	N. Jersey	6.0	99.96	17.0
8	N. Jersey	6.2	99.94	18.0
9	Georgia	5.2	99.93	20.0
10	Illinois	5.6	99.75	3.5

The photomicrographs in Figure 1 show the general characteristics of the sand particles for the various samples. The shape factor (perimeter^2/area) is nearly constant for the ten samples. It had been suggested previously[2] that the surface roughness of the sand may be an important variable. A measure of surface roughness for these samples was obtained using a proprietary technique. The roughness indexes obtained are shown in Table 1. They range from 3.5 to 20.

The DOP filtration efficiency of 36 inches of sand at a 5 ft/min air flow velocity is shown plotted as a function of surface roughness in Figure 2. A strong correlation is shown relating filter efficiency and roughness. A roughness index near 12 appears optimum for the sands evaluated. In general, higher roughness up to a point appears to be advantageous.

Roughness of the sand surface is generally thought to affect packing density and thus air permeability. However, as shown by the graph of Figure 3, no correlation between permeability and roughness is apparent. In this case, the size distribution of the sand imposed by the specifications on the screening process may mask the effect of roughness on this parameter.

Conclusions

Size specification and air permeability alone are not sufficient to define an optimum sand for deep-bed air filtration. Actual testing of the candidate sands in small-scale filter columns, although laborious, is valuable in screening the relative merits of candidate sands. Results reported here indicate that surface roughness is an important variable in the relative collection efficiency. A sand specification based upon grain size, air permeability, and roughness more closely defines sands suitable for use in deep-bed, high-efficiency air filtration applications.

References

1. G. A. Schurr, D. B. Zippler, and D. C. Guyton, "Deep-Bed Filter Performance Tests." Proc. 12th AEC Air Cleaning Conference, August, 1972, pp. 596-616.

2. G. G. Brown, et al., Unit Operations, p. 216, John Wiley & Sons, Inc., New York (1950).

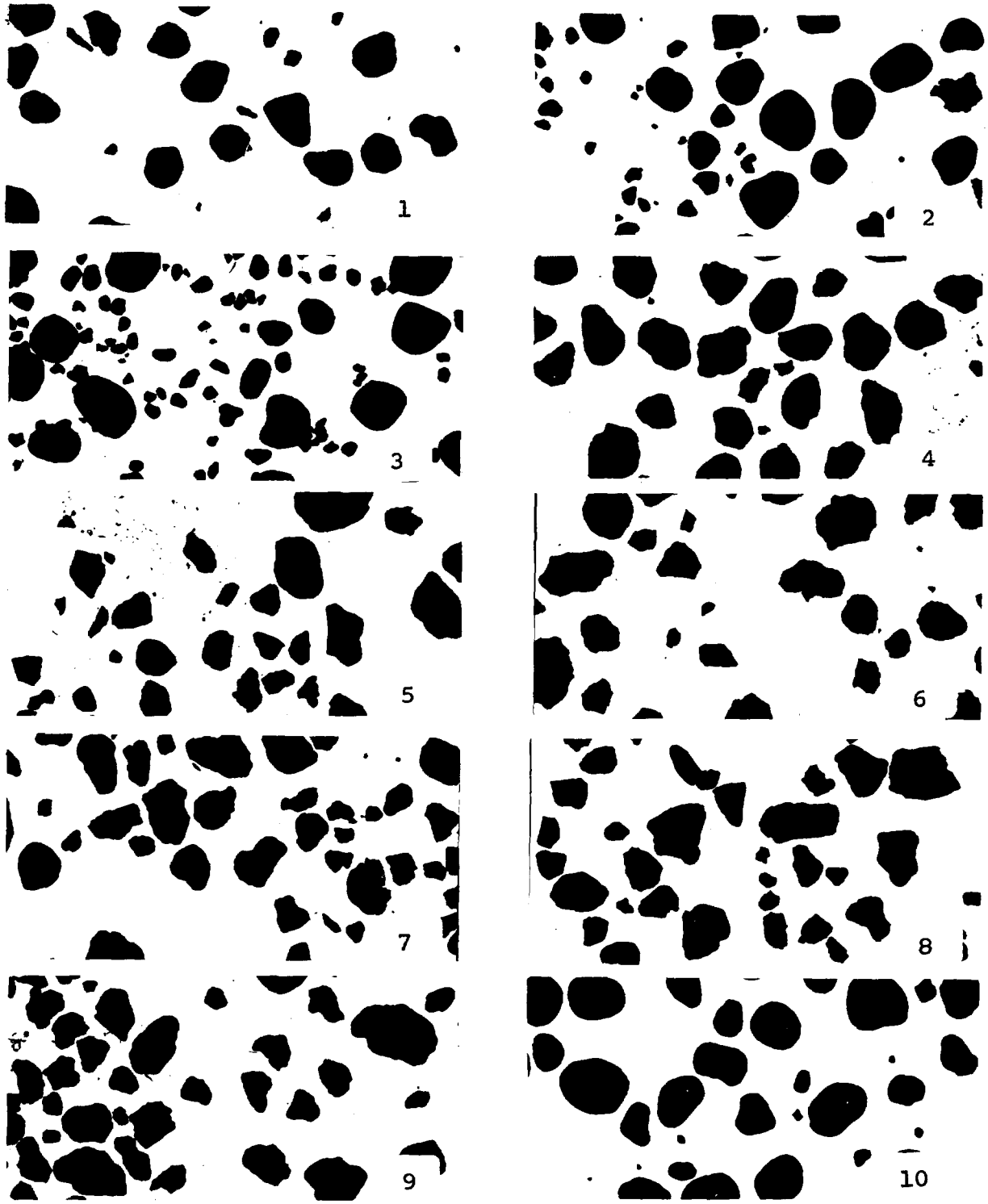

FIGURE 1 - SAND PARTICLES FROM DIFFERENT DEPOSITS
11.8 X MAGNIFICATION

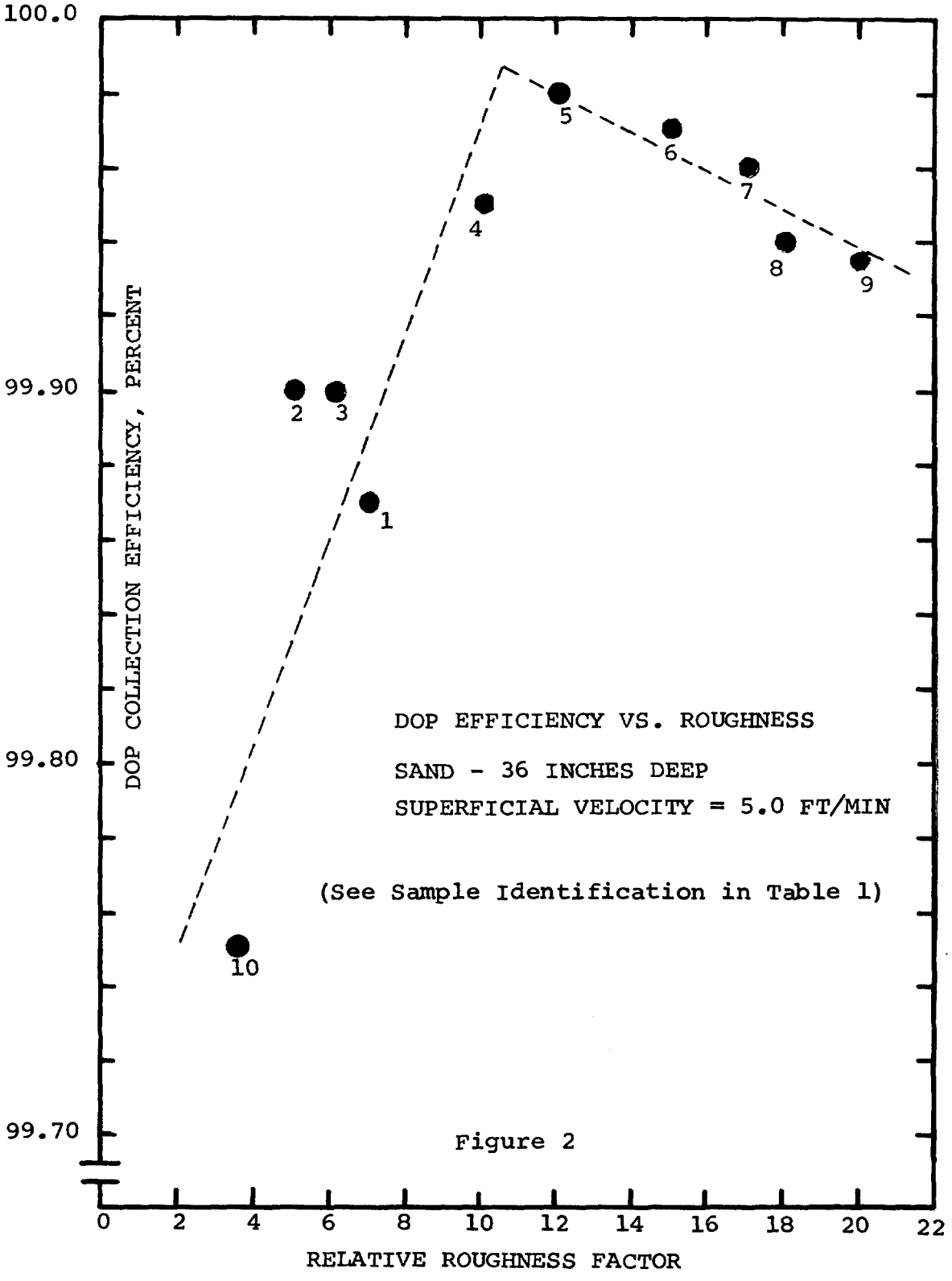
100.0
99.90
99.80
99.70
DOP COLLECTION EFFICIENCY, PERCENT
1
2
3
4
5
6
7
8
9
10
DOP EFFICIENCY VS. ROUGHNESS
SAND - 36 INCHES DEEP
SUPERFICIAL VELOCITY = 5.0 FT/MIN
(See Sample Identification in Table 1)
0
2
4
6
8
10
12
14
16
18
20
22
RELATIVE ROUGHNESS FACTOR

Figure 2

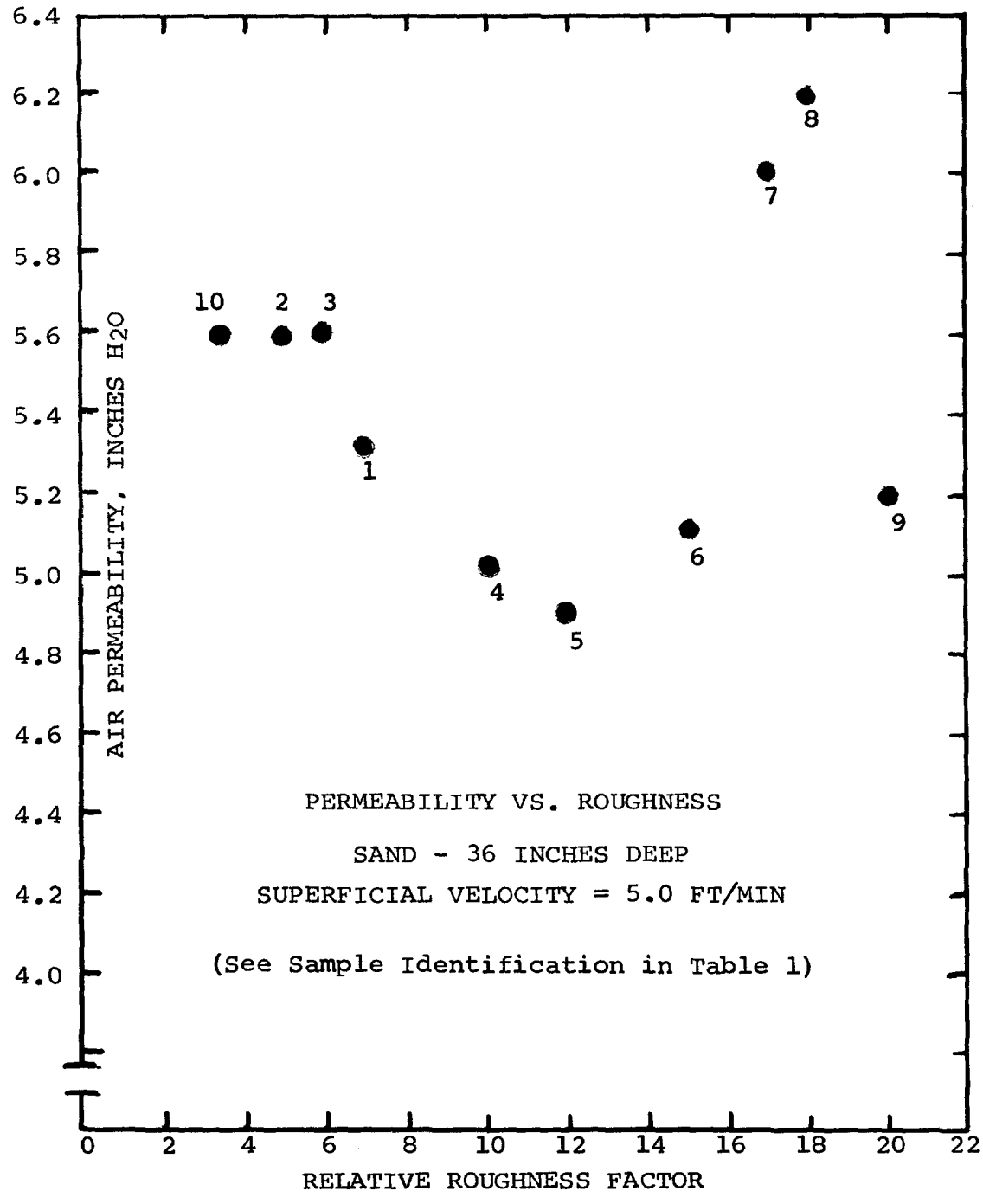
6.4
6.2
6.0
5.8
5.6
5.4
5.2
5.0
4.8
4.6
4.4
4.2
4.0
AIR PERMEABILITY, INCHES H2O
10
2
3
1
8
7
4
5
6
9
PERMEABILITY VS. ROUGHNESS
SAND - 36 INCHES DEEP
SUPERFICIAL VELOCITY = 5.0 FT/MIN
(See Sample Identification in Table 1)
0
2
4
6
8
10
12
14
16
18
20
22
RELATIVE ROUGHNESS FACTOR

Figure 3

DISCUSSION

FIRST: I don't think it's surprising that you get better efficiency with more surface because, with hot DOP aerosol, the principle removal mechanism is diffusion, as Dr. Jonas pointed out. Roughness is related to surface. This suggests that your roughness parameter is not well related to surface area. Perhaps, if some other roughness parameter were used, you would find that the curve would have a better shape.

SCHURR: On sand particles of this size, it would be very difficult to measure the differences in the surface area by any known technique. While, indeed, roughness is some measurement of the surface area, I don't think suitable quantitative methods are available because these are extremely large areas. We don't have a significant increase in surface due to roughness.

JORDAN: I would like to point out that we are using crushed sand in our sand filters. Does your investigation also include broken sand; I mean broken by mills, with a very high roughness?

SCHURR: Samples 5 and 10 are crushed aggregate; the others are weathered sand. The best and worst are crushed aggregate. It's not necessarily true that crushing provides any magic to make a better sand.

THE FOLLOWING QUESTIONS WERE ASKED IN WRITING AFTER THE CLOSE OF THE CONFERENCE:

MICHELS: Would you please comment on the reproducibility of the data? Figures 2 and 3 would imply that only single tests were conducted for each type of sand.

SCHURR: We ran many tests and our data are reproducible within ± 5%. There was a minimum of 200 particles measured to generate each point.

MICHELS: Would you please comment on methods for preparation of samples in the test apparatus? For example, were all samples loaded under identical conditions to develop maximum packing density prior to DOP testing?

SCHURR: Every sample of sand was carefully prepared. It never fell more than 4" and we made three separate loadings for each different sand tested. Results were reproducible to ± .01% in DOP efficiency. Minimum packing density was what we were looking for in all cases; not maximum packing density. Our minimum specification for preparing full scale sand filters is that sand will not fall more than 6 inches. There is no evidence of settling over the 20 year life of some of our filters.

MICHELS: Would non-uniform methods of sample preparation be partially responsible for differences in efficiency?

SCHURR: No. We made repetitive tests on sands from each deposit and they were remarkably uniform within each sand deposit.

MICHELS: Is the measured roughness constant for an entire lot of sand used for a filter?

SCHURR: We only built one filter since we started using this design method. We tested 100 lb. samples every two days as the filter was being constructed and the roughness remained uniform over entire period of packing. We took samples of sand as it was being deposited and tested DOP efficiency of small scale units. After the full-scale unit was packed, we tested it with DOP and the results agreed with the test specimens.

A CONSIDERATION OF THE SIGNIFICANCE OF CARBON-14 DISCHARGES FROM THE NUCLEAR POWER INDUSTRY

P. J. Magno, C. B. Nelson and W. H. Ellett
Office of Radiation Programs
Environmental Protection Agency
Washington, D. C. 20460

Abstract

Carbon-14 is produced in nuclear power reactors by a variety of nuclear reactions. This carbon-14 becomes a potential consitituent of reactor and reprocessing plant off-gas effluents. This presentation discusses the significance of these potential discharges and includes (a) an estimate of the amount of carbon-14 which may be produced, (b) projections of the tropospheric inventory which would result from continuous discharge of this carbon-14, and (c) a comparison of the whole-body doses from discharges of carbon-14 and krypton-85. This evaluation indicates a need to better define the amounts of carbon-14 discharged from the nuclear power industry.

I. Introduction

Carbon-14 is produced in nuclear power reactors by a variety of neutron reactions. The most important of these are as follows:

Reaction	Cross Section
$^{14}N\ (n,p)\ ^{14}C$	1.8 b
$^{17}O\ (n,\alpha)\ ^{14}C$	0.24 b
$^{13}C\ (n,\gamma)\ ^{14}C$	0.9 mb

This carbon-14 becomes a potential constituent of reactor and reprocessing plant off-gas effluents. Because of its long physical half-life (5730y) and its persistence in the environment, carbon-14 discharges from nuclear facilities will result in an increase in the inventory of this nuclide in the atmosphere. The purpose of this paper is to analyze the significance of these potential discharges.

II. Estimates of Carbon-14 Production

Carbon-14 production in nuclear reactors has received little attention and few actual measurements of the production rate of carbon-14 in reactors have been reported. However, recently a number of estimates of carbon-14 production rates have been reported (1-6). These estimates ranged from 30-40 Ci/GWe-yr for light water reactors (LWR) and fast breeder reactors (FBR) to 60-1000 Ci/GWe-yr for high temperature

IV. Dose Rates from Carbon-14

Figure 1 shows the projected individual whole-body dose rates for the period 1970-2020 from carbon-14 in the troposphere from (a) projected discharges from the nuclear industry and (b) natural production by cosmic rays. These dose rates were calculated utilizing the UNSCEAR (12) dose conversion factor 0.167 millirad/year per picocurie of carbon-14 per gram of carbon in the body. Following the UNSCEAR model we have assumed that the specific activity of carbon-14 in the body closely follows that in the troposphere (13).

The whole-body dose rate due to the naturally produced carbon-14 decreases by about 20 percent during this period due to an increase in the carbon dioxide content of the troposphere from the burning of fossil fuels. The dose rate due to projected discharges of carbon-14 from the nuclear industry would increase steadily during this period to a dose rate of about 0.8 millirad/yr in the year 2020.

V. Comparision Doses from Carbon-14 with Doses from Krypton-85

Figure 2 shows a comparision of the projected individual whole-body dose rates for the period 1970-2020 resulting from the release of carbon-14 and krypton-85 from the world nuclear industry. The krypton-85 dose rates were calculated using the procedure published by the Environmental Protection Agency (14) and assuming complete release of all krypton-85 produced. These data indicate that carbon-14 discharges would result in significantly greater dose rates than discharges of krypton-85.

An evaluation of the environmental impact from long half-life radionuclides such as carbon-14 depends to a large extent on the time frame over which their impact is considered. While for such isotopes as krypton-85 ($T_{1/2} \approx 10.7$ years) most of the impact will be within a generation or two following its release, carbon-14 effluents will persist in the biosphere for millennia. One way to characterize the public health implication of long-life isotopes is in terms of their "environmental dose commitment" which has been defined as the sum of all doses to individuals over the entire period the material persists in the environment in a state available for interactions with humans (15). In the case of carbon-14 where the naturally produced activity has acted as a historical tracer, the individual dose to humans over the long term can be predicted. However, because of its extremely long half-life it is impossible to sum the individual doses unless the world population can be predicted for tens of thousand years into the future. Therefore, in the population dose estimates given below, we have confined our prediction to the next 100 years using the U.N. formula for world population growth (16). Table II presents a comparision of the estimated "100-year population dose commitment" from carbon-14 discharges with that produced from krypton-85 discharges. The "100-year population dose commitment" per gigawatt-year of electric power is about a factor of 30 greater for carbon-14 than for krypton-85.

TABLE 1

PROJECTED ACCUMULATION OF CARBON–14 IN THE TROPOSPHERE FROM DISCHARGES FROM THE NUCLEAR INDUSTRY

YEAR	NUCLEAR POWER Generation–GWe	CUMULATIVE DISCHARGE Megacuries	TROPOSPHERIC INVENTORY Megacuries	$\frac{p\ Ci\ ^{14}C}{9\ Carbon}$
1970	8	5.6×10^{-4}	2.7×10^{-4}	4.8×10^{-4}
1975	87	1.8×10^{-2}	9.4×10^{-3}	1.6×10^{-2}
1980	270	8.7×10^{-2}	4.1×10^{-2}	6.9×10^{-2}
1985	579	0.24	0.11	0.18
1990	1,146	0.57	0.24	0.37
1995	1,936.	1.1	0.45	0.69
2000	3,060	2.0	0.79	1.2
2005	4,500	3.4	1.3	1.8
2010	6,200	5.4	2.0	2.6
2015	8,000	7.9	2.9	3.5
2020	10,000	11	4.0	4.6

UNSCEAR model we have assumed that the specific activity of carbon-14 in the body closely follows that in the troposphere (13).

The whole-body dose rate due to the naturally produced carbon-14 decreases by about 20 percent during this period due to an increase in the carbon dioxide content of the troposphere from the burning of fossil fuels. The dose rate due to projected discharges of carbon-14 from the nuclear industry would increase steadily during this period to a dose rate of about 0.8 millirad/yr in the year 2020.

V. Comparision Doses from Carbon-14 with Doses from Krypton-85

Figure 2 shows a comparision of the projected individual whole-body dose rates for the period 1970-2020 resulting from the release of carbon-14 and krypton-85 from the world nuclear industry. The krypton-85 dose rates were calculated using the procedure published by the Environmental Protection Agency (14) and assuming complete release of all krypton-85 produced. These data indicate that carbon-14 discharges would result in significantly greater dose rates than discharges of krypton-85.

An evaluation of the environmental impact from long half-life radionuclides such as carbon-14 depends to a large extent on the time frame over which their impact is considered. While for such isotopes as krypton-85 ($T_{1/2}$ = 10.7 years) most of the impact will be within a generation or two following its release, carbon-14 effluents will persist in the biosphere for millennia. One way to characterize the public health implication of long-life isotopes is in terms of their "environmental dose commitment" which has been defined as the sum of all doses to individuals over the entire period the material persists in the environment in a state available for interactions with humans (15). In the case of carbon-14 where the naturally produced activity has acted as a historical tracer, the individual dose to humans over the long term can be predicted. However because of its extremely long half-life it is impossible to the sum the individual doses unless the world population can be predicted for tens of thousand years into the future. Therefore, in the population dose estimates given below, we have confined our prediction to the next 100 years using the U.N. formula for world population growth (16). Table II presents a comparision of the estimated "100-year population dose commitment" from carbon-14 discharges with that produced from krypton-85 discharges. The "100-year population dose commitment" per gigawatt of electric power is about a factor of 30 greater for carbon-14 than for krypton-85.

FIGURE 1

PROJECTED INDIVIDUAL WHOLE BODY DOSE RATES FROM CARBON-14

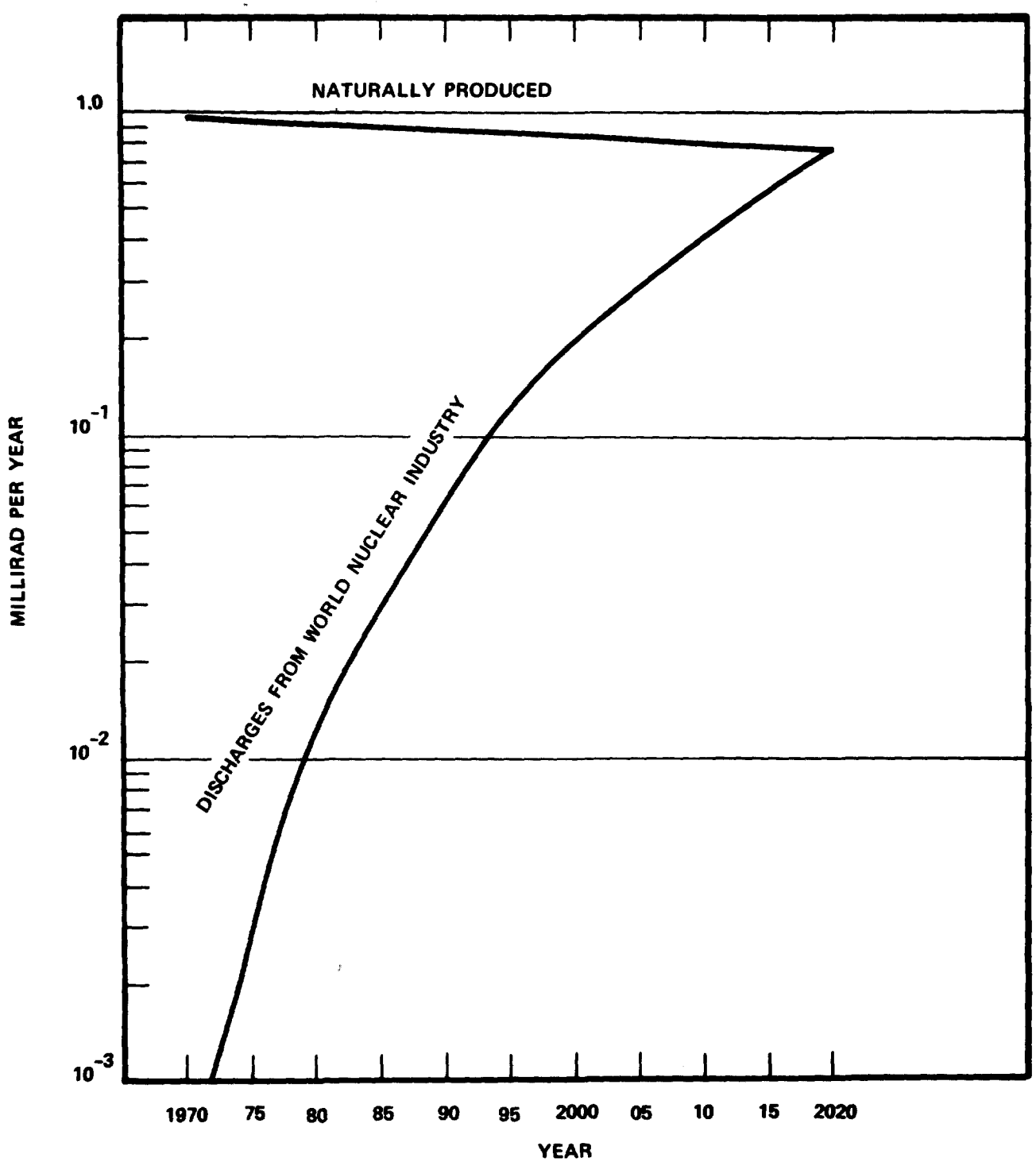

FIGURE 2

COMPARISON OF PROJECTED INDIVIDUAL WHOLE BODY DOSE RATES FROM CARBON-14 AND KRYPTON RELEASE BY THE WORLD NUCLEAR INDUSTRY

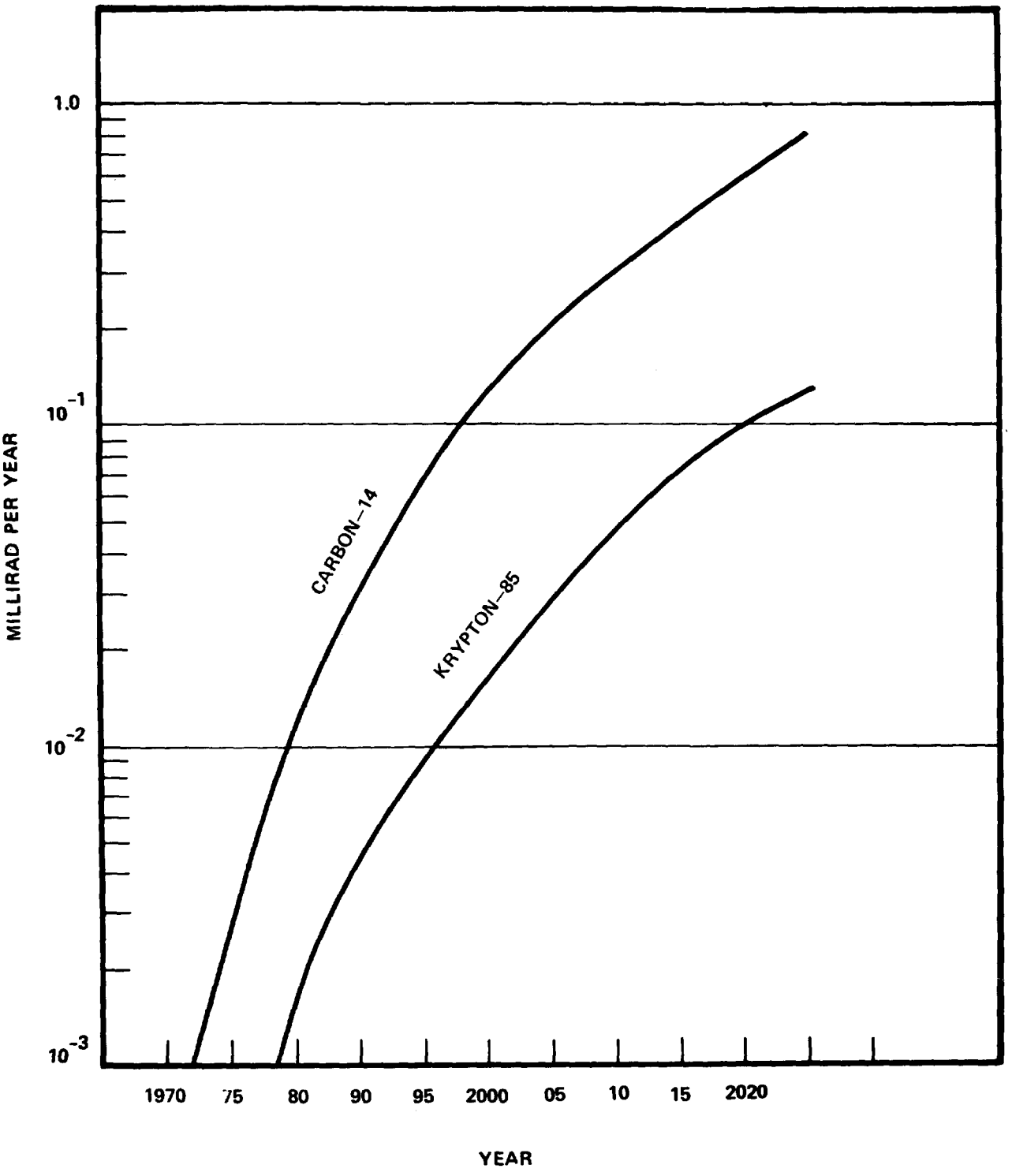

VI. Conclusions

This analysis, although based on limited data regarding production rates, indicates that discharges of carbon-14 from the nuclear power industry require our careful consideration. In order to better evaluate the significance of these discharges we need to improve our knowledge concerning this subject. This would include the following:

(1) measurements of the production rate of carbon-14 in nuclear reactors, the mechanisms which affect this production and the chemical form of carbon-14 produced,

(2) determination of how much of the carbon-14 produced is discharged at the reactor or fuel reprocessing plant,

(3) an evaluation of technology for control of carbon-14 at both reactors and reprocessing plants and the cost of this control,

(4) an evaluation to determine if carbon-14 control is necessary.

It is hoped that this discussion will provide the incentive and stimulus for initiation of studies to develop these information needs.

Table II

Population Dose Commitments
for Carbon-14 and Krypton-85

Radionuclide	Production Rate Ci/GWe-yr	Population Dose Commitment* person-rem/Ci	person-rem/GWe-yr
Carbon-14	70	4×10^{1}	3×10^{3}
Krypton-85	3.8×10^{5}	3×10^{-4}	1×10^{2}

* 100-yr population dose commitment from releases in 1980.

References

1. Bonka, H., et.al., "Unweltbelastung durch Radiokohlenstaff aus kerntechnischen Anlagen", Reaktortagung, Berlin, April (1974).

2. Rublevskiy, V. P., et.al., "Atomic Electric Power Stations as Sources of Carbon-14 Discharge", Presented at the Third International Congress of the International Radiation Protection Association, Washington, D.C. (1973).

3. Bonka, H., et.al., "Contamination of the Environment by Carbon-14 Produced in High Temperature Reactors", Kerntechnik 15, Nr 7, Jahrgang, January (1973).

4. Martin, A., and Fry, T. M., "Population Dose Commitments from Releases of Tritium, Carbon-14 and Krypton-85", Presented at the International Symposium on Radiation Protection, Aviemore, Scotland, June (1974).

5. Snider, J. W. and R. E. Leuze, "An Estimate of the Process Decontamination Factors Required to Meet Federal Effluent Regulations for the Burning of HTGR Fuel Elements", Proceeding of the Twelfth AEC Air Cleaning Conference, CONF-720823, Vol. II, August (1972).

6. United States Atomic Energy Commission, "Draft Environmental Statement for HTGR Fuels Reprocessing Facilities at the National Reactor Testing Station", WASH-1534, January (1974).

7. Personal Communication from B. Kahn, National Environmental Research Center, U.S. Environmental Protection Agency, Cincinnati, Ohio (1974).

8. Machta, L., "Prediction of CO_2 in the Atmosphere", Carbon and the Biosphere, G. M. Woodwell and E. V. Pecan editors, Technical Information Center, Office of Information Services, U.S. Atomic Energy Commission, August (1973).

9. Oscarson, E. C., et.al., "Considerations Regarding Timing of Krypton-85 Control Implementation". Presented at the International Symposium on Radiation Protection, Aviemore, Scotland, June (1974).

10. Hofmann, P. L., "U.S. Civilian Nuclear Power Cost-Benefit Analysis", Fourth United Nations International Conference on the Peaceful Uses of Atomic Energy, Geneva, Switzerland, A/CONF-49/p/072, September (1971).

11. U.S. Atomic Energy Commission, "Nuclear Power 1973-2000", WASH-1139 (1972), U.S. Government Printing Office, Washington, D.C., December (1972).

12. United Nations Scientific Committee on Effects of Atomic Radiation, "Ionizing Radiation, Levels and Effects", Vol. I paragraph 67, United Nations, New York (1972).

13. United Nations Scientific Committee on Effects of Atomic Radiation, "Ionizing Radiation, Levels and Effects", Vol. I paragraph 210, United Nations, New York (1969).

14. Office of Radiation Programs, "Environmental Analysis of the Uranium Fuel Cycle, Part III - Nuclear Fuel Reprocessing", EPA-520/9-73-003D, U.S. Environmental Protection Agency, Washington, D.C., October (1973).

15. Office of Radiation Programs, "Environmental Radiation Dose Commitment: An Application to the Nuclear Power Industry", EPA-520/4-73-002, U.S. Environmental Protection Agency, Washington, D.C., February (1974).

16. United Nations Statistical Office, "World Population Prospects as Assessed in 1963", Population Studies No. 41, United Nations, New York, (1966).

DISCUSSION

DEMPSEY: Krypton has not been considered there? Have you given any thought to the relative biological effect?

MAGNO: Yes, I listed the individual whole body dose rates. Supposedly, one would be able to equate the dose rate, or the health effect, on the whole body dose rate comparison. Those were not skin doses. Krypton would be considerably greater in terms of potential health effects and I think whole body dose would have to be considered.

LASER: I think the statement has very great importance for the HDF fuel cycle. I cannot see a way to retain it. I think one must start to handle this problem with a new design of the fuel. Reprocessing cannot solve this problem.

MAGNO: I agree. I think you must start to consider the necessity for control early enough that you might get to it before the design is too far along.

RESPIRATORY QUALITY ASSURANCE PROGRAM AT ROCKY FLATS*

C. D. Skaats
Dow Chemical U.S.A.
Rocky Flats Division
P.O. Box 888
Golden, Colorado 80401

Quality assurance testing of all respiratory equipment was initiated at Rocky Flats in July 1972. Since the first day we started testing respiratory equipment, it has become more and more evident that quality assurance testing is necessary. The program has advanced from a single Q127 to two Q127's plus all of the related equipment that's necessary. All operations are now located in one building in a nonexclusion area.

Two salaried technicians work full time in the current program. Additional effort by employees in support groups such as Laundry, Trucking and Health Physics is comparable to having 2-1/2 more full-time people in the program.

A program of this nature cannot be successful unless you have full support from management. Fortunately, we have this support.

Respiratory manufacturers will state that all particulant cartridges are DOP checked, but it is not uncommon at Rocky Flats to have a reject rate of two to three percent. In one instance, we encountered a 20% reject rate. In this particular instance, the rejected cartridges were dismantled, the cause determined, and the manufacturer notified.

This experience has taught us not to issue new full-face masks and respirators, as received from the manufacturer, until we wash, visually inspect, and test them. Our records prove that 75 to 80% of the units have leak rates over reject rate of .03%. These leaks are usually the result of factory dirt, mold release, and poor assembly. Actual part failure is rare. We now have all units washed and visually inspected prior to testing.

Since July 1972, we have assisted several manufacturers in correcting problems that we have detected during testing. Some of these could have seriously affected the user. The response from the manufacturers has been excellent, and most of them quickly take corrective actions. Time does not permit a detailed discussion on the problems that were discovered.

High efficiency cartridges are tested and date-coded following each time they are used. After four uses, the cartridges are discarded. The reasons for the discard are mechanical damage and high resistance. Actual penetration values do not show a significant change from the initial test.

*Work performed under USAEC Contract AT(29-1)-1106

Leak-checking half mask

Leak-checking Full-Face Mask

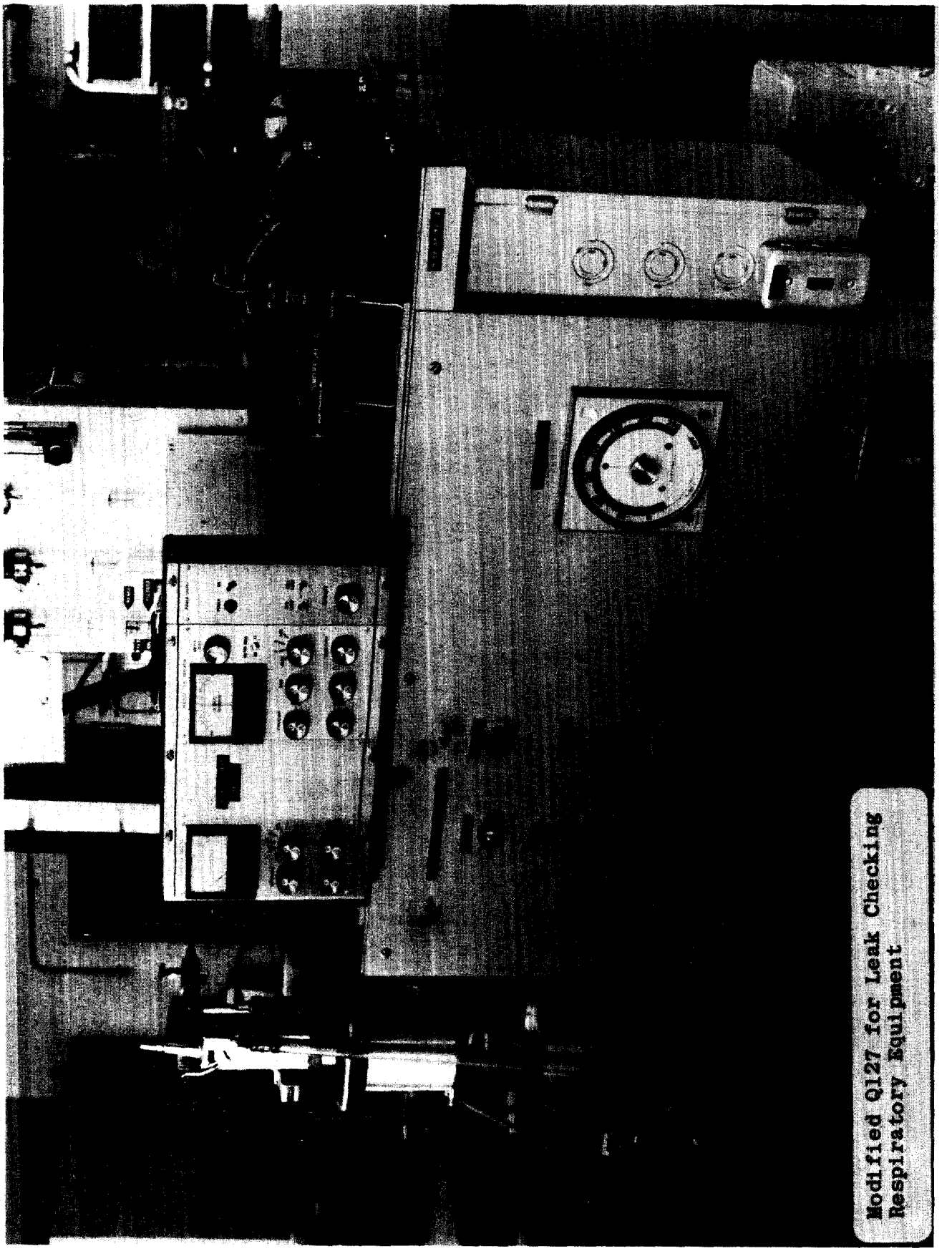
Modified Q127 for Leak Checking
Respiratory Equipment

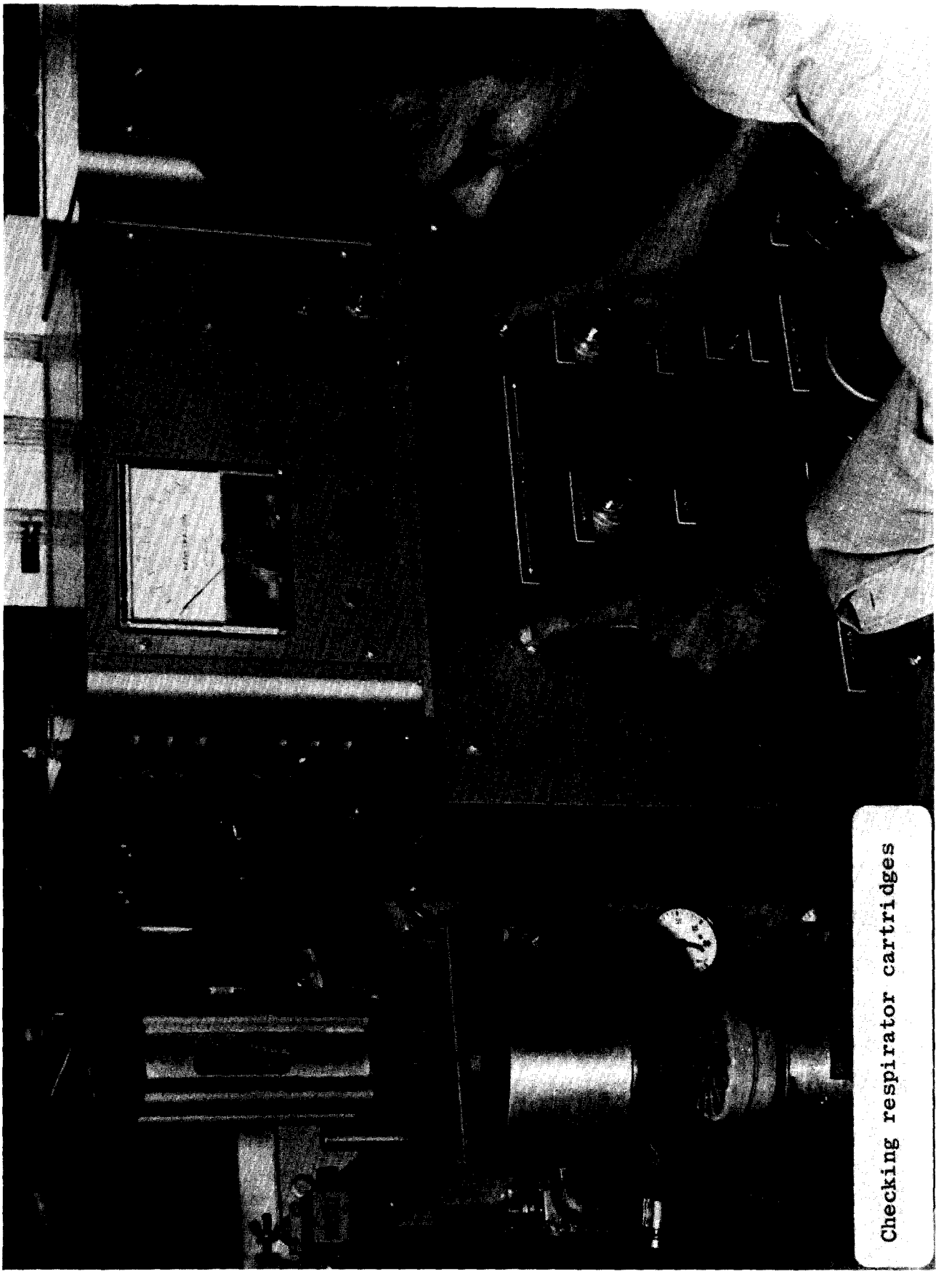

Checking respirator cartridges

Used full-face masks and half-mask respirators are washed, dismantled, inspected, provided with new parts when necessary, and sent to the Certification Laboratory for testing. The frequency depends on equipment usage. Technicians at the Laboratory perform minor adjustments and mark all areas where leaks are detected. The masks and respirators are then sent to the Laundry where highly trained individuals do the major repair work. Their efforts result in an average of only three to five respirators out of 100 being returned by our technicians to the Laundry for repair.

Our program involves each cartridge being checked twice--once in the Q127 chuck and again with the assembled unit.

During calendar year 1973, we tested:

114,000 cartridges of which 28,500 were new
35,000 full-face masks
12,000 half masks

We maintain an inventory of tested units available for any emergency. A monthly rotation keeps up-to-date respiratory equipment available.

On a request basis, we test all of the Fire Department's Surviv-Air units. We have found very few defective masks since our first test of all their units.

Dividends from a good quality assurance program are many. The most important I feel is knowing that the units meet all the required specifications and will protect the individual if worn properly.

We have a motto at the Test Lab, "A nonleaker is worth a million dollars." That may be a conservative figure because it's impossible to place a price tag on the health and well-being of individuals needing respiratory protection.

One last comment. Believe what your testing equipment tells you, and correct every problem.

DISCUSSION

CAREY: Could you tell me if the 28,000 cartridges represent your purchase that year?

SKAATS: No, the 28,000 would be the replacements for our throwaways. We maintain as high as a 10 to 15,000 inventory that has not been tested.

OLSON: Do you also have a program for testing filters on people; that is, testing for fit?

SKAATS: Yes. We have recently initiated one. I'm not in the program, but associated with the individual who is. We recently built a new test chamber in one of the buildings; it is quite sophisticated. We work very closely together on new equipment. I think, to date, he has tested and sized something in the neighborhood of 1,500 employees around the plant. I won't mention the manufacturer, but Monday morning we disqualified a brand new respirator because of defects and we found this defect through our tests.

FIRST: Are you using DOP or sodium chloride in your tests, Mr. Skaats?

SKAATS: DOP.

THE BEHAVIOR OF FISSION GAS HOLDUP BEDS DURING NORMAL STARTUP, ACCIDENTAL LOSS OF REFRIGERATION, AND SPILLAGE OF CHARCOAL

Dwight W. Underhill
Harvard School of Public Health
Department of Environmental Health Sciences
665 Huntington Avenue
Boston, Massachusetts 02115

Abstract

Charcoal adsorption beds are an important adjunct in reducing the exposure of the public to fission produced noble gases. Despite the fact that we can conceive of mishaps in the operation of these beds, nonetheless, these beds can serve to retain fission gases even after conditions such as spillage of the charcoal. It is the purpose of this paper to give calculations of fission gas releases under conditions other than simple steady state operation, and thus give further assurances of the protection offered by use of these beds.

I. Introduction

The use of adsorption beds for the holdup and decay of fission gas radionuclides creates a remote but still creditable new type of accident to consider: a malfunction in which a large quantity of stored radioactive gases is released. For the purpose of facilitating safety analyses, as well as design improvements, this paper presents calculations concerning the transient behavior of fission gas holdup beds under both normal and abnormal conditions.

Three situations are analyzed in the discussions which follow. First is the analysis of the behavior of an initially clean adsorption bed which is being loaded with radionuclides. Second is the development of equations for the analysis of the behavior of an adsorption bed in which the temperature is rising due to a loss of the refrigeration system. Lastly, equations are presented for describing the release to the air of fission gases from a pressurized charcoal bed which is assumed to have ruptured and discharged the charcoal onto the floor of the room in which the bed is located.

II. Startup Analyses

Calculations of the releases expected from an initially clean bed which is being loaded with radioactive gases should be helpful in determining the performance of a bed during the startup period. To make this analysis, we start with the partial differential equation for mass transfer in a fission gas holdup bed and solve it with the boundary conditions of an initially isotope free bed into which a constant input of a radioactive isotope is begun at time, t = 0. This equation is:

$$D\frac{\partial^2 C}{\partial x^2} - V\frac{\partial C}{\partial x} - \lambda\left(k\left(\frac{1-\varepsilon}{\varepsilon}\right) + 1\right)C = \left(k\left(\frac{1-\varepsilon}{\varepsilon}\right) + 1\right)\frac{\partial C}{\partial t} \qquad (1\text{-}1)$$

with the boundary conditions

$$C(t = 0) = 0 \tag{1-2}$$

$$C(t > 0, x = 0) = 1 \tag{1-3}$$

where

C = Concentration of fission gas in the interparticle void volume, $\mu Ci/cm^3$

x = Axial distance from inlet, cm

t = Time following introduction of fission gas, sec

V = Interparticle carrier gas velocity, cm/sec

D = Interparticle diffusion coefficient, cm^2/sec

ε = Fractional interparticle void volume, dimensionless

k = Partition coefficient for fission gas between equal volumes of adsorbent and carrier gas, dimensionless

λ = Isotopic decay constant, sec^{-1}

Taking the Laplace transform with respect to time reduces the above equations to the following ordinary differential equation:

$$\frac{D\partial^2 C^2}{\partial x^2} - \frac{V\partial \tilde{C}}{\partial x} - (\lambda + s)\left\{k\left(\frac{1-\varepsilon}{\varepsilon}\right) + 1\right\} C = 0 \tag{1-4}$$

with the boundary conditions

$$\tilde{C}\ (x=0) = 1/s \tag{1-5}$$

$$\tilde{C}\ (x=\infty) = 0 \tag{1-6}$$

which has the solution

$$\tilde{C} = \frac{1}{s} e^{\left\{V - \sqrt{V^2 + 4D(\lambda+s)\left\{k\left(\frac{1-\varepsilon}{\varepsilon}\right)+1\right\}}\right\}\frac{x}{2D}} \tag{1-7}$$

Inversion of the last equation gives the desired breakthrough equation:

$$C(x,t) = 1/2\left\{ e^{\left\{V - \sqrt{V^2+4\lambda D\left\{k(\frac{1-\varepsilon}{\varepsilon})+1\right\}}\right\}\frac{x}{2D}} \right.$$

$$\text{ERFC}\left\{ x/2\sqrt{\frac{k(\frac{1-\varepsilon}{\varepsilon})+1}{Dt}} - \sqrt{t(\lambda + \frac{V^2}{4D\left\{k(\frac{1-\varepsilon}{\varepsilon})+1\right\}})} \right\} +$$

$$e^{\left\{V + \sqrt{V^2+4\lambda D\left\{k(\frac{1-\varepsilon}{\varepsilon})+1\right\}}\right\}\frac{x}{2D}} \quad \text{ERFC}\left\{ \frac{x}{2}\sqrt{\frac{k(\frac{1-\varepsilon}{\varepsilon})+1}{Dt}} + \right.$$

$$\left. \left. \sqrt{t(\lambda + \frac{V^2}{4D\left\{k(\frac{1-\varepsilon}{\varepsilon})+1\right\}})} \right\} \right\} \qquad (1\text{-}8)$$

This equation agrees with the model derived by Glueckauf[1] for the case of a stable isotope (as can be shown by setting $\lambda = 0$) and also agrees with the steady-state breakthrough predicted by Madey[2] by setting $t = \infty$

$$C(x,t=0) = e^{\left[V - \sqrt{V^2+4D\lambda\left\{k(\frac{1-\varepsilon}{\varepsilon})+1\right\}}\right]\frac{x}{2D}} \qquad (1\text{-}9)$$

but for reasons not understood, the transient part of the equation derived here is somewhat different from that given by Madey.

Some of the factors used in Equation (1-8) can be redefined with the result of making them easier to determine. The interparticle diffusion coefficient can be looked on as giving the sum of the effects of molecular and eddy diffusion, viz.

$$D = \gamma D_m + \lambda_p d_p V \qquad (1\text{-}10)$$

where γ = tortuosity factor for molecular diffusion, dimensionless

D_m = molecular diffusion coefficient, cm^2/sec

λ_p = coefficient for eddy diffusion, dimensionless

d_p = mean sorbate particle diameter, cm

and for design purposes, values of γ and λ_p of 0.6 and 1.2 seem appropriate. The interparticle velocity, V, is related to the superficial velocity, V_s, as

$$V = V_s/\varepsilon \qquad (1\text{-}11)$$

and the bulk adsorption coefficient, K, and the partition coefficient, k, are related as

$$K = \left[\varepsilon + (1-\varepsilon)k\right]/\rho \qquad (1\text{-}12)$$

where K = bulk adsorption coefficient, cc/gm

ρ = bulk density of charcoal, gm/cc

The equations derived above can be used to calculate the time required for the effluent radionuclides to reach a fixed fraction of their final concentration. If, as will almost always be the case, Vx/D >>10, the second term on the right hand side of Equation (1-8) is negligible. Assuming this to be the case, then by setting the argument of the remaining ERFC function equal to 0, -0.91%, and -1.66, respectively, we can determine the time required for the effluent radionuclide concentration to reach 50%, 90%, and 99%, respectively, of the steady-state value. In this way, we can obtain a detailed analysis of the startup period for a fission gas holdup bed.

III. The Effect of Loss of Refrigeration

It is well known that adsorption beds operate more efficiently at reduced temperatures and that the use of refrigeration can reduce considerably the required weight of adsorbent. This leads us to consider how a fission gas holdup bed behaves in the time period following a malfunction which permits the bed to warm up. For evaluation of this situation, two cases will be analyzed. The first is that in which it is assumed that the bed is continued in operation as it warms up; the second is that in which it is assumed that the inlet to the bed is shut off when the refrigeration is lost but that the outlet remains open.

Case One

Let us assume first that the input of fission gases into the bed continues even after refrigeration is lost. This problem can be analyzed in a very simple manner by considering the input to the fission gas holdup bed to be a series of short pulses such as shown in Figure 1. For the sake of simplicity, let us further assume that each pulse consists of 0.01 μCi of a fission gas isotope and that there are 100 pulses per minute. This is equivalent to a constant input of 1 μCi/minute into the bed.

Figure 2 shows the effluent fission gas pulses before, during, and after the temperature rise caused by loss of refrigeration. Before the accident occurred, we find a set of effluent pulses, each spaced 0.01 minute apart and containing $0.01\, e^{-\lambda t_i}$ Ci of fission gas,

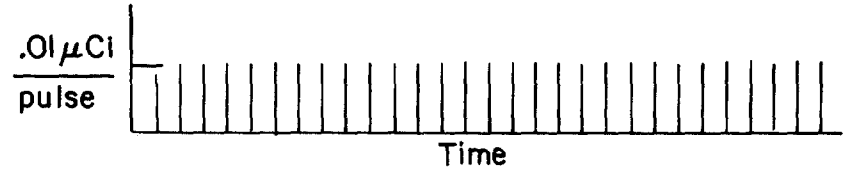

FIG. 1 INPUT PULSES

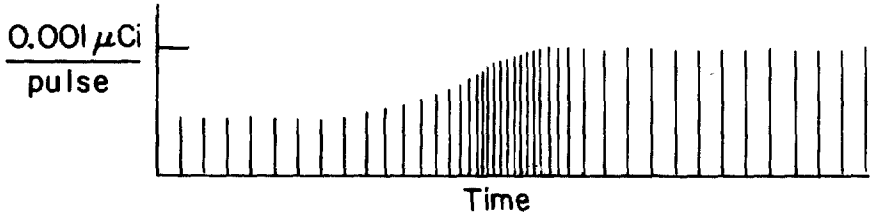

FIG. 2 "EFFLUENT" PULSES

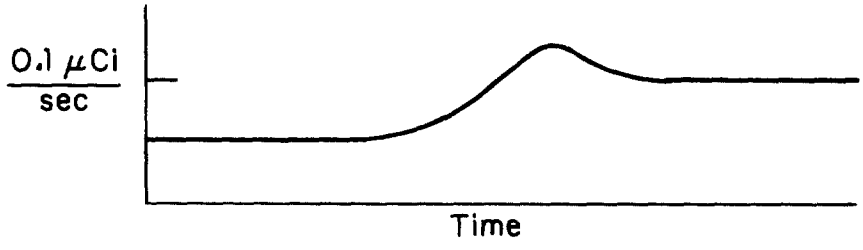

FIG. 3 EFFLUENT FISSION GAS RELEASE

where t_i is the passage time through the bed of the i^{th} pulse. After the bed has warmed up and steady state operation has again been attained, a set of effluent pulses, each spaced 0.01 minute apart and carrying $0.01\, e^{-\lambda t_i}$, will be found, but due to the fact that the holdup time, t_i, is now considerably shorter, the magnitude of these pulses is larger than before.

The most interesting portion of this analysis concerns the transient time period during which the bed is warming up. Here the highest releases of fission gases may occur. Figure 2 shows clearly the effects under consideration. As the bed warms up, the t_i are being constantly reduced and the time between pulses, $t_{i+1} - t_i$, is now shorter. This increases the effluent concentration of fission gas. Let us suppose for example, that $t_{i+1} - t_i$ for a short period of time is equal to 0.005 seconds. The effluent pulses are now twice as close together as they were before and the effluent fission gas concentration is increased by a factor of 2 over what would be calculated on the basis of radioactive decay. The formula for the effluent concentration is

$$C/C_o = \lim_{\Delta t \to 0} \left\{ \frac{\Delta t}{\Delta t + t_i - t_{i-1}} \right\} e^{-\lambda t_i} \qquad (2\text{-}1)$$

where C/C_o = the ratio of effluent to input fission gas

t = the time between pulse inputs

Figure 3 shows the effluent fission gas flow calculated from the above equation. As previously stated, for the case examined here, the highest rate of fission gas release can be found in this period. Given the large number of curies of fission gas which may be held in a bed, this phenomenon is worth consideration.

Case 2

Let us assume that following the loss of refrigeration, the inlet valve to the bed is shut, but that the outlet valve remains open. The question is how much activity will be swept out by the desorbing carrier gas as the bed warms up. The equations outlined below provide the basis for calculations which can be carried out quickly by a digital computer.

We start out with some basic definitions:

k = adsorption coefficient for carrier gas, cc(STP) per cc of bulk adsorbent

k' = k at 0^oC

β = temperature coefficient for k, $^oC^{-1}$. It is assumed

$$k = k' \quad -\beta t \qquad (2\text{-}2)$$

a = ratio of adsorption coefficient of fission gas to adsorption coefficient for carrier gas

a' = a at $0^{o}C$

γ = temperature coefficient for a. It is assumed

$$a = a' - \gamma t \tag{2-3}$$

The next step is to find a differential equation for the mass transport of carrier gas. In the bed shown below, x = distance of an atom of carrier gas from the inlet

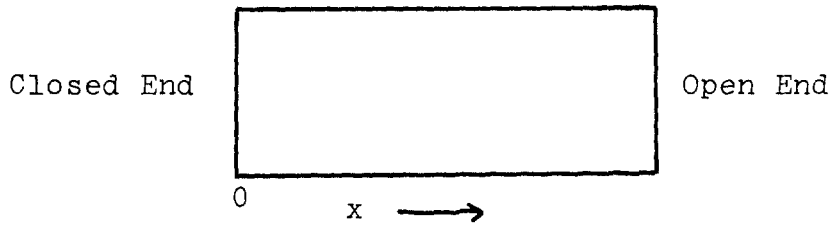

By the conservation of mass

$$xk = C \tag{2-4}$$

$$\ln x + \ln k = \ln C \tag{2-5}$$

$$dx/x + dk/k = 0 \tag{2-6}$$

but $$k = k' e^{-\beta t} \tag{2-7}$$

Then $$dk = -\beta k' e^{-\beta t} dt \tag{2-8}$$

$$dx/x = \beta dt \tag{2-9}$$

If now y is the distance of an atom of fission gas from the inlet,

$$dy = 1/a \; dx \tag{2-10}$$

So that $$dy/y = \beta dt/a \tag{2-11}$$

or $$dy/y = \frac{\beta e^{\gamma t}}{a'} dt$$

On integration

$$\ln \frac{y}{y_o} = \frac{\beta}{a' \gamma} \left[e^{\gamma t} - e^{\gamma t_o} \right] \tag{2-12}$$

Let L = the length of the bed and assume that at t_2, y = z. Then at t_1, the fission gas swept out of the bed at t_2 would be at y_1, where

$$y_1 = z e^{\beta/a' \gamma \left[e^{\gamma t_1} - e^{\gamma t_2}\right]} \tag{2-13}$$

The remainder of this analysis uses a digital computer. The bed is divided into small strips, and from the equation given for the warmup of the bed as a function of time, the time is calculated for each strip to reach the end of the bed. The rate of fission gas release is then

$$R = \frac{\left\{\begin{matrix}\text{quantity of fission gas between} \\ y_i \text{ and } y_{i+1} \text{ at start of warmup}\end{matrix}\right\} e^{-\lambda(\tau_i + \tau_{i+1})/2}}{\tau_i - \tau_{i+1}} \tag{2-14}$$

where τ_i is the time required for y_i to reach L, the end of the bed

Of the two cases considered here, the one which has the greatest potential for release and subsequent population dose is the first case, in which fission gas continues to feed into a bed no longer capable of a sufficient holdup time. In the second case, only the fission gases contained within a fraction of the bed are expected to be released, and the time required for the bed to warm up reduces still further the total quantity of radioactivity released.

IV. Retention of Fission Gases in Spilled Charcoal

Theoretical Model

Presented in this section is a mathematical analysis of the effect of the spillage of charcoal from a holdup bed through which there has been a continuous flow of fission gases. Obviously the quantity of fission gas released to the air depends on how much of the charcoal is brought into equilibrium with the air. But the "obvious" conclusion that the more charcoal that is released, the higher the fission gas content of the air, is not true. To illustrate this, let us suppose that we have a radioactive gas whose half-life is such that this gas is contained entirely within the first half of the bed. It is apparent that a rupture releasing only the charcoal in the first half of the bed will result in the release of more fission gas than a rupture in which the gases in the air are brought into equilibrium with the fission gases adsorbed on the charcoal.

The final concentration also depends on the order in which the charcoal is brought into contact with the air in the room. The procedure for investigating this problem is to bring the charcoal into contact with the air in such a way that the final concentration of fission gas in the air will be a maximum. Assume a bed with a concentration gradient such as shown here:

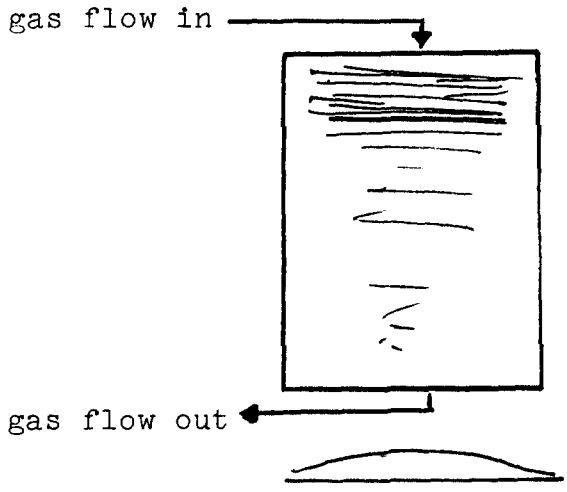

The charcoal will be released from the bed in such a way that the least contaminated charcoal is brought into equilibrium with the air first, and the release of charcoal will be continued until the entire bed is emptied. This gives the maximal release of fission gases into the room.

Derivation of the Basic Equation

The differential equation given below states that the quantity of fission gas released from the charcoal equals that gained by the air in the room. In addition to the mass balance, equilibrium is assumed between the air in the room and the charcoal released from the differential bed length, dx.

Mass Balance During Release

$$\underbrace{\text{Fission Gas Increase in Air}}_{Vdc} = \underbrace{\text{Fission Gas Released from Charcoal}}_{(C_i = ks)\,Adx} \qquad (3\text{-}1)$$

where V = free void volume in room, ft^3

c = concentration of fission gas in the air, $curies/ft^3$

C_i = concentration of fission gas in the charcoal being released, $curies/ft^3$

A = cross sectional area of bed, ft^2

dx = differential bed length, ft

k = partition coefficient of fission gas between equal volumes of bulk charcoal and air, dimensionless. This factor is equal to the bulk adsorption coefficient, cm^3/gm, times the bulk density of charcoal, gms/cm^3.

Assuming an initial exponential distribution of fission gas across the bed, the parameter, C_i, is given by:

$$C_i = C_o e^{-(L-x)\alpha} \tag{3-2}$$

where C_o = maximum concentration of fission gas in the charcoal, curies/ft^3

L = length of bed, ft

α = linear decay constant, ft^{-1}. The linear decay constant determines how sharply the initial concentration of fission gas dropped off with distance from the inlet during normal operation of the bed.

Then

$$Vdc = (C_o e^{(x-L)\alpha} - kc)\ Adx \tag{3-3}$$

and at $x = 0$, $c = 0$, so that on integration

$$c = \frac{C_o A}{V\alpha + kA}\left[e^{(x-L)\alpha} - e^{-(\frac{kAx}{V} + L\alpha)}\right] \tag{3-4}$$

If the release involves the entire charcoal bed, $x = L$, and

$$c = \frac{C_o A\ (1 - e^{-(\frac{kA}{V} + \alpha)L})}{+\ \frac{kA}{V}} \tag{3-5}$$

The quantity of fission gas contained within the bed is

$$\frac{C_o A}{\alpha}\ (1 - e^{-\alpha L}) \tag{3-6}$$

so that the fraction released is

$$f = \frac{1 - e^{-(\frac{kA}{V} + \alpha)L}}{(1 + \frac{kA}{\alpha V})\ \ (1 - e^{-\alpha L})} \tag{3-7}$$

But

$$\alpha = \frac{k\lambda A}{Q} \tag{3-8}$$

where λ = isotopic decay constant, sec^{-1}

Q = flow of gas into the bed during normal operation, ft^3/sec

Then

$$f = \frac{1 - e^{-kV_b\left(\frac{1}{V} + \frac{\lambda}{Q}\right)}}{\left(1 + \frac{Q}{\lambda V}\right)\left(1 - e^{-\frac{kV_b\lambda}{Q}}\right)} \qquad (3\text{-}9)$$

where V_b = volume of charcoal bed

The above equation gives the maximum fission gas release under equilibrium conditions.

Sample Calculations

Given

$Q = 109$ cfm $= 1.80\ ft^3/sec$

$V_b = 1000\ ft^3$

$V = 49{,}000\ ft^3$

$k = 225$ for Xe

Then for xenon-131^m, $\lambda = 6.67 \times 10^{-7}$ and based on the previous formula, the fraction released, $f = 0.22$. For xenon-135, $\lambda = 6.7 \times 10^{-4}$ and $f = 0.95$. If we had assumed the simpler process of complete equilibrium between the charcoal and the air, $f = V/(V + kV_b) = 0.18$ for all isotopes of xenon. However, for reasons stated at the beginning of this section, this calculation does not give the maximum possible release. The equation derived here is not difficult and it does give an upper limit to the release of fission gas, and for this reason we recommend its use.

Summary

One current practice in the operation of nuclear power reactors is to hold up the fission gases in pressurized tanks, and one of the accident situations which must be hypothesized in the safey evaluation reports is a rupture of one of these tanks. If such a tank contains no charcoal, the release of fission gases would be nearly 100%. The calculations presented here show that, even under the worst possible conditions, the release of gas from such a tank filled with charcoal would be but a fraction of this amount. The exact amount would depend upon the quantity and adsorption coefficient of the charcoal, the decay constant of the adsorbed gas, the free volume within the room housing the storage tank, and the initial distribution of fission

gases across the charcoal bed. On the basis of this study, we believe that serious consideration should be given to utilizing the retention effects of charcoal in limiting releases of fission gases from storage tanks under accident conditions.

References

1. Glueckauf, E., Theory of Chromatography, Part 9, Trans. Faraday Soc., 51 (1955) p. 34.

2. Madey, R. A., Physical Theory of Adsorption of a Radioactive Gas, Trans. Am. Nuclear Soc., 4 (1961) p. 354.

Acknowledgement

The author gratefully acknowledges that the work reported herein was supported by Cosmodyne Corporation. The most difficult part of this study - presentation of the problem in such a way that it could be analyzed simply - was done by Ashwin Desai and Clint Brooks of Cosmodyne Corporation.

HEPA FILTERS FOR OFF-GAS SYSTEMS OF BWR UNITS

Robert Avery
Cambridge Filter Corporation
Syracuse, New York

Background

An off-gas system for a boiling water nuclear power station (BWR) vents to the atmosphere gases which are generated or released as the water is used in the closed loop between the reactor and the turbine. The off-gas system itself is located in the return from the turbine to the reactor.

From an environmental point of view the off-gases of major interest are radioactive Krypton and Xenon, Iodine-131 and Tritium. In addition, there are quantities of oxygen and hydrogen from the thermolytic decomposition of water. The primary purpose of the off-gas system is to contain or to delay the passage of the radioactive gases to the atmosphere until they have significantly decayed into nonradioactive daughters. Because of the purpose of the off-gas system, it must be protected as much as possible from any accidents which might damage it. One source of accidents requiring shut-down of the system has been explosions of various intensities caused by the uncontrolled recombination of hydrogen and oxygen to form water.

In investigating these uncontrolled recombinations, different items have been listed as possible initiators of these events. One such item has been the HEPA filter used to remove airborne particulates from this off-gas.

Design of HEPA Filters

A HEPA filter is built by pleating a continuous sheet of filter media (paper). In order to prevent the media from collapsing on itself and to allow the passage of air thru the filter, corrugated separators are used to keep the pleats apart. The combination of media and separators, known as the filter pack, is then sealed into a filter frame. In the classic method of assembly, the exposed edge of the pack is coated with a heavy sealant before the pack is put into the frame. This sealant is a neoprene base material and is an electrical insulator. Additional sealant is used to prevent leakage between the pack and the filter fram.

For nuclear power stations the HEPA filter is usually built with aluminum foil corrugations and a cadmium plated steel frame. Although it has not been demonstrated, the theoretical possibility exists for a HEPA filter to become a large capacitor and accumulate an electrical charge if there is no electrical continuity between the filter frame and all of the aluminum corrugations or if the electrical connection has such high resistance that the charge cannot be bled off at the same rate as it is generated. It has been hypothesized in the case of some unexplained recombinations

that the HEPA filter did act as a capacitor, building up a static charge which led to a spark which in turn initiated the recombination.

Experimental Data

Based on the background data listed above, an investigation was undertaken to determine:

(a) If there was normally any electrical continuity between the aluminum corrugations and the metal frame.

(b) If there was any way that such continuity could be achieved or improved.

A sample HEPA (Cambridge Absolute) filter was selected at random from the production line. The model chosen was a 1E-200 unit 12" X 12" X 11 1/2" deep. A Triplett Model 630 V.O.M. meter was used to check electrical continuity. One lead was clipped to the metal frame, and the other probe was contacted to each corrugation. The electrical resistance of this circuit was read. The lower the resistance, the better the continuity. Thirty-two (32) separators on one side ("downstream") and thirty-one (31) on the other side ("upstream") were checked. The results of this procedure are listed below:

Measured Resistance	Percent of Separators
0 - 200 Ohms	17
200 - 8000 Ohms	29
8000 + Ohms	14
Infinite resistance	40

After all the readings had been made, a proprietary electrical conducting paint was applied over the sealant on the "downstream" side so that it bridge the space between the aluminum corrugations and the filter frame. After the paint dried, a continuity test was again made on this side of the filter and every separator now read zero (0) resistance.

Discussion

The test data indicates that normally there is poor electrical continuity between the aluminum corrugations and the steel frame. An effective current flow path can be developed by the use of suitable electrical conducting paint, applied to bridge between these two elements.

In order to eliminate any remote possibility of building up a charge, conducting paint should be applied on both the upstream and downstream faces of the filter.

If the filter is gasketed on both edges and clamped between two flanges, either electrical conducting gaskets or (more

preferably) a positive electrical connection between the filter housing and the rest of the equipment should be employed, to prevent any electrical isolation of the filter.

Most electrical conducting paints incorporate metallic powders such as silver or copper. Since both these metals react with iodine and since iodine may be present in the off-gases, provisions should be made to protect the paint from iodine corrosion which might cause the paint to fail. While this report covers only the use of electrical conducting paint, other methods of securing continuity also suggest themselves.

When a HEPA filter is to be used in an off-gas system it may be desirable to include in the specifications that there must be electrical continuity between the corrugations and the filter frame. If such a feature is included in the specifications, certification of electrical continuity whould be required and it is recommended that it include a report of tests on each corrugation.

Conclusions

Tests have shown that normally there is very little or no electrical continuity between the aluminum corrugations and metal frame of a HEPA filter.

Where such continuity is required, one method of achieving it is by use of electrical conducting paints.

DISCUSSION

RIVERS: We use a rig for determining charge density which consists of a HEPA filter mounted on a Teflon insulator and about six inches of clear plastic from the filter to ground. We connect this with a electrometer to ground. You can monitor the collection of charge on a filter from charged aerosols. You can also ground the case of the filter, from the Teflon insulator to dry ground, and if the filter maintained a charge after you grounded the case, you would get a voltage from the suspended filter. However, you never do. I don't know what kind of conductivity meter you use in measuring the conductivity of the separators.

AVERY: To answer your question directly, and I would rather take it as a comment, we used a Triplet type meter. It is not anywhere near as precise as a laboratory meter. The investigation was intended to be a practical application of a theoretical problem. All we can say is, yes, we can ground and we can make an electrical connection between the aluminum corrugations and that filter can be grounded. How effective it is, I do not know. Hopefully, it would be effective enough to allow a charge to be dissipated and the theoretical spark that causes a theoretical accident will not occur.

A STUDY OF MOISTURE SEPARATORS FOR FINE PARTICLE WATER-AIR-STREAM SERVICE*

Wayne L. Smith
Mine Safety Appliances Company
Evans City, Pennsylvania

Abstract

The need to remove 1-10 micron water particles from an air stream prompted the search for, and evaluation of, commercially available moisture separators that could best meet this requirement. An environmental test facility was designed, built, and used to test water particle filtering performance. Additional testing was done using NBS dust and DOP smoke. Five different commercially available units were evaluated.

I. Introduction

The objective of this effort was to determine the availability and performance of entrained moisture separators which are efficient in removing water droplets in the 1-10 micron size range from an air stream. The MSA acceptance criteria for moisture separators operating at PWR post-accident (incident) conditions were: 99+% removal of water particles in the 1-10 micron range as determined by measurement and visual observation, a rated flow of at least 1,000 SCFM, and a pressure drop of approximately 1 in. water column at rated flow. Many applications exist for separators with this kind of performance capability, such as: separating entrainment from steam to the low pressure turbine of nuclear-powered naval ships; removal of moisture from gas to catalytic recombiners and similar systems of this type in nuclear power plants; and one of the most publicized current applications, to protect the air-cleaning systems in the containment of boiling or pressurized water reactors.

In reactor air cleaning the moisture separator protects the high efficiency particulate air filters, charcoal adsorbers, and other components in those systems. Although anticipated PWR system incident containment conditions, under which entrained separators must operate, vary somewhat over the many installations, Table I illustrates some of the maximum levels expected. The 47 PSIG pressure- and 271°F. temperature values for Indian Point-2 reactor were selected as typical for testing on this project.

Five commercial separators were purchased for test performance evaluation particularly in the 1-10 micron size range. These units were the MSA type G-5, AAF type T, York type 321 SR, Farr type 68-44MZZ, and a Monsanto standard baffle-type separator. Of these, two exhibited satisfactory efficiency in the 1-10 micron range: the AAF and MSA units.

The separators were evaluated for response to 0.3, 0.6, and 1.1 micron DOP smoke; and water particles in the 2.5-10 micron size, measurement of water entrainment collected within and downstream of the separator, and by visual observation of the challenge and effluent stream.

*Work performed under USAEC Contract AT(45-1)-2145

II. Apparatus

Standard conventional test facilities existed for DOP testing. A special test facility was designed and built to test full size separators, high efficiency particulate filters, charcoal cells, and other components over a wide range of ambient and incident conditions.

This test facility consisted of a containment vessel 18 ft. long and 4 ft. in diameter with a 2 ft. square inner duct test chamber with recirculation of the entrainment atmosphere in the annular space. The vessel was rated at 100 PSIG @ 400°F. See Figure 1.

A variable speed fan takes gas from the inner duct and directs it through the annular space for return to the inner duct at the opposite end. The gas stream passes over the condensate pool in the annulus where it is heated by mixing with steam from the supply pipe and by the pool which is held at temperature by the same steam addition to maintain a high relative humidity. It then passes through the heat exchanger in the annulus and picks up fine (10 micron MVD and less) entrainment from pneumatic atomizing sprays just before entering the inner duct. Flow passes through the inner duct heat exchanger and can be viewed through the sight glasses (SG-1) at the heat exchanger outlet. Passage through the hydraulic spray section permits addition of larger (100 micron MVD) particle size entrainment which can be viewed through sight glasses (SG-2) just before entering the entrainment separator. The entrainment-laden gas steam then passes through the entrainment separator undergoing test. It can be viewed at the outlet sight glasses (SG-3) before entering the HEPA filter which serves to monitor the efficiency of the test separator. Effluent gas is then returned to the fan through the gas-flow metering nozzles for recirculation.

Auxiliary provisions include plant steam and water for heating and cooling; treated water, recirculated and measured in the entrainment section; instrumentation for measurement and control of system gas flow, pressure, and temperature. Sampling provisions across the separator permit analysis for separator efficiency measurements of the small (2.5-10 micron) particle size fraction.

The only practical approach for water particle analysis in the 1-10 micron size range readily adaptable to separator efficiency tests was the cascade-impaction method. Pneumatic atomizing nozzles offered the best hope for generating appreciable bulk quantities of 1-10 micron particle size entrainment for test purposes.

Submicron particles penetrating the separator were captured by the HEPA for measurement by weight gain. Larger particles resulting from re-entrainment generally dropped out of the gas stream and were collected for measurement in the separator penetration sump (16). The major portion of entrainment was removed by the separator for collection and measurement from the separator case drain sump (14).

III. Procedure

The final test plan included initial measurements at ambient conditions to establish the "normal" descriptive and operating functions of each separator in the "as received" condition. One separator of each type was then tested for actual

entrained moisture-removal characteristics in the test vessel at ambient conditions. Tests included variations in flow, in entrainment loading and entrainment size. Measurements included: resulting pressure drop of the separator and its downstream monitoring HEPA; visual observation of entrainment; mass measurements of entrainment removed by the separator, by the downstream duct, and by the downstream HEPA; and impactor sampling to identify particle size fractions. The final "normal" performance properties of each separator and the HEPA filter used with it were rechecked following ambient entrainment testing. Repeat testing with a duplicate separator or variations of test conditions were performed when indicated by data obtained. Only separators indicating good entrainment removal efficiency in the 1-10 micron particle size range at ambient conditions were selected for additional testing at PWR incident conditions of elevated temperature and pressure, and for extended performance properties and limits.

As mentioned, the response of the moisture separators to liquid particles of various sizes included: 0.3 - 0.6 - 1.1 micron DOP penetration measurements; 2.5 - 10 micron impactor fraction sampling; manufacturer's rating of entrainment generating nozzles; measurement of entrainment removed within the separator, collected in the downstream duct, collected by the downstream HEPA, and by visual observation of the challenge and effluent streams. DOP, or other calibrated stable particle tests, particularly in the 0.6 - 1.1 micron size, served as a rapid index to expected separator efficiencies in the lower particle size range. Impaction sampling offered the best known currently available method for characterizing 1-10 micron particles.

IV. Results

Test results of the five commercially available separators are summarized in Table II.

The MSA type G-5 moisture separator was greater than 99% efficient in removing water particles in the 1-10 micron range at mixed entrainment loadings up to 6.7 lbs/1000 cu. ft., from near-saturated air streams, ranging from ambient to elevated conditions of 271F. and 47 PSIG. No penetration was visible or measured in the 2.5 - 10 micron range; 0.6 micron DOP penetration was 80% and 0.3 micron DOP penetration was 96%.

The AAF type T separator was greater than 99% efficient in removing water particles in the 1-10 micron range at mixed entrainment loadings up to 6.5 lbs/1000 cu. ft. No penetration was visible or measured in the 2.5 - 10 micron fraction; DOP penetration was 93% for 0.6 micron and 95% for 0.3 micron. Removal of the bulk of large particles, without appreciable increase in differential pressure, is attributed to the baffled inlet section. The upper temperature limit is not known; however, at 251F, the binder in the glass was observed to darken the glass and color the water droplets clinging to fiber streamers in the effluent air stream.

On the York type 321 SR separator no fine entrainment penetration was visible or measured in the 2.5 - 10 micron range at ambient conditions. The DOP penetration was 69% for 0.6 micron and 93% for 0.3 micron, but the differential pressure was 1.29 in. WC at rated flow at ambient conditions which exceeds the Savannah River specifications of 0.95 ± 0.05 in. WC. Penetration measurements of 1.1 micron DOP for twelve layers of Teflon media at the same inlet velocities and pressure loss

were 56% for this media. This separator was not selected for testing at incident conditions since in the ambient, horizontal gas-flow tests with fine entrained particles, the separated liquid flowed to the downstream face of the separator and was blown off or re-entrained from the lower two-thirds of the downstream separator face. Two modes of re-entrainment were observed. The pool which accumulated in the bottom of the frame simply overflowed the frame and the air sheared some large drops from the top surface of the pool. These fell rapidly but had some horizontal motion imparted by the air flow. Other drops -- also larger than the entering droplets -- fell from points higher up on the downstream face of the separator. Only a small portion of the removed water was contained within the separator case and drained through the two 1/4 NPS nozzles provided in the bottom of the separator case. The percentage of water removed from within the separator case varied from 36% at 0.24 lb/1000 cu.ft. entrainment loading to 15% at 1.23 lb/1000 cu.ft.

The Farr type 68-44MZH separator allowed penetration of visible entrainment which was also detectable by impactor measurements. DOP penetration measurements gave 99% at 0.6 micron, indicating very little attenuation and essentially complete penetration of 100% at the 0.3 micron size. Removal efficiencies greater than 99% were found for 100 micron mean volume distribution particles up to a loading of 6.5 lb/1000 cu.ft. Some re-entrainment lowered this to 90% with 10 micron MVD loading at 0.03 lb/1000 cu.ft. This separator is rated primarily for solids, with slightly lower efficiencies ranging from 99% at 20 micron to 40% at 2.5 micron size particles. Since this separator gave measurable penetration in the 1-10 micron range at ambient conditions, no tests were made at incident conditions.

On the Monsanto baffle-type separator appreciable entrainment penetration was visible and detectable by impactor measurements when using the 10 micron MVD challenge stream. DOP penetration values were 99% at 0.6 micron and 100% at 0.3 micron. Overall entrainment-removal efficiencies ranged from 99% at 6.6 lb/1000 cu.ft. loading with 100 micron MVD entrainment to 85% at 0.04 lb/1000 cu.ft. loading with 10 micron MVD size entrainment. Since 1-10 micron response was poor, no tests at incident conditions were made on this separator.

V. Discussion

Atomizing nozzles proved to be a satisfactory method of generating controlled quantities of water particles of known sizes. Condensing steam at elevated conditions did not generate comparable bulk quantities. Using extended surface cooling of steam did not generate measurable amounts of small particles and decreased the wet-bulb temperature under MSA test conditions.

Humidity approaching saturation values is difficult to control, not accurately measurable at incident conditions with currently available equipment, and may influence small particle life to a greater degree than anticipated by calculations. Actual PWR incident conditions, however, would rarely approach saturation conditions except in the immediate vicinity of the pressurized water release. Cooling by containment structure, equipment and sprays, together with pressure-drop changes, contributes to lowering the humidity of the air entering the moisture separators to a value below saturation.

Figure 2. Figure 2 shows the predicted performance of the separators based on the test data. Three of the five separators tested exhibited satisfactory efficiency in the 1-10 micron range.

The MSA type G-5 moisture separator was greater than 99% efficient in removing water particles in the 1-10 micron range from ambient to elevated conditions of 271F. and 47 PSIG; 0.6 micron DOP penetration was 80% and 0.3 micron DOP penetration was 96%. In addition, its basic non-combustible construction makes this separator suitable to function as a prefilter under the requirements of AEC Regulatory Guide #1.52.

Figure 3. Figure 3 shows a typical installation of a moisture separator in a BWR ventilation system. In these illustrations one can see how the moisture separator could also conveniently serve as a prefilter.

TABLE I

MAXIMUM INCIDENT OPERATING CONDITIONS
TYPICAL PWR NUCLEAR REACTOR CONTAINMENTS

ITEM	SAVANNAH RIVER	CONNECTICUT YANKEE	INDIAN POINT-2	TURKEY POINT-3, 4
Temperature, F	212	261	271	283
Pressure, PSIG	Atmos. + System ΔP	40	47	59
Pressure Surge	7-8 times rated flow		14 in. WC	
Entrainment:				
Loading, lb/1000 CF	1.0	8.0	0.35	1.0
Type	Condensed Steam	Sprays plus Condensed Steam	Sprays plus Condensed Steam	Sprays plus Condensed Steam
Separator Duty:	For HEPA Protection	For HEPA Protection	For HEPA Protection	For HEPA Protection
Removal Efficiency	99.9%		99.9%	99.9%
Droplet Diameter	1-10 μ (calculated)		(Not specified)	1 μ
Test Method	Steam Condensed in Air	Hydraulic Sprays 2400 μ MVD	Hydraulic Sprays 580 μ MVD	Hydraulic Sprays 580-70 μ MVD
Separator Used	York 321 SR	AAF Type T	MSA Type G-3	MSA Type G-5

TABLE II

COMPARISON OF SEPARATORS

Manufacturer	Monsanto	Farr	York	AAF		MSA		MSA	
Separator Model Serial Number	Baffle Type 1	Type 68-44 M2H 7010	Type 321 SR TY-5	Type T 491-118		Type G 1234-2		Type G 1234-1	
Size, inches SF/MCF Weight - lbs	24 x 24 x 2 2.22 26	24 x 24 x 4 2.24 32	24 x 24 x 2.6 2.5 20	24 x 24 x 24 3.5 111		24 x 24 x 5 2.5 30		24 x 24 x 5 2.5 30	
Rated Flow, CFM ΔP at Flow, in. WC	1800 0.32	1785 0.27	1600 1.24	1140 0.78		1600 0.90		1600 1.03	
0.3 μ DOP-Penetration % 0.6 μ DOP-Penetration %	100 98	100 99	93 69	95 93		96 80		- 78	
ETF Run Number Temp °F - Pressure psig	T-18 100 - 0	T-19 96 - 0	T-20 96 - 0	T-21 88 - 0	T-24 271 - 47	T-22 100 - 0	T-23 271 - 47	T-14A 80 - 0	T-14 271 - 47
Entrainment									
100 μ Removal, lb/hr Penetration, lb/hr Efficiency, %	613 0.37 >99	566 0 ~100	33.4 94.2 26	311 0 ~100	50, 100 0 ~100	486 0 ~100	28, 55 0 ~100	112 0 100	22, 47 0 ~100
70 + 10 μ Removal, lb/hr Penetration, lb/hr Efficiency, %	717 0.37 + Mist >99	738 0.29 + Fog >99	18 100.2 16	444 0 ~100	0 - -	651 0 ~100	0 - -	0 Flow Test to 2100 CFM only, at constant	56 0 ~100
10 μ Removal, lb/hr Penetration, lb/hr Efficiency, %	3.66 0.37 + Mist <91	2.9 0.29 + Fog <91	.81 1.44 36	6.4 0 ~100	<1 0 ~100	2.5 0 ~100	<1 0 ~100	loading of 560 μ and 110 μ MVD	0 Not Available
Separator ΔP, in. WC ETF Ambient ETF Maximum Increase % Other Changes	0.35 0.42 20 None	0.26 0.35 35 None	1.29 2.22 72 None	0.80 1.20 50 Fibers Loosened	0.89 1.89 115 Fibers Darkened, Binder Loss	0.93 1.40 51 None	0.88 1.88 114 None	1.00 1.30 30 None	1.00 1.73 73 None
HEPA ΔP, in. WC ETF Ambient ETF Maximum Increase %	1.81 1.97 20	1.77 2.02 33	1.57 1.79 14	1.08 1.31 21	1.08 1.40 30	1.52 1.76 16	1.55 2.20 42	Not used; visible observation only.	1.40 2.30 64
Water Gain, lbs	0.94	0.63	0.88	0.94	-	0.63	-		0.50
0.3 μ DOP Change	None	None	None	None	None	None	None	None	None

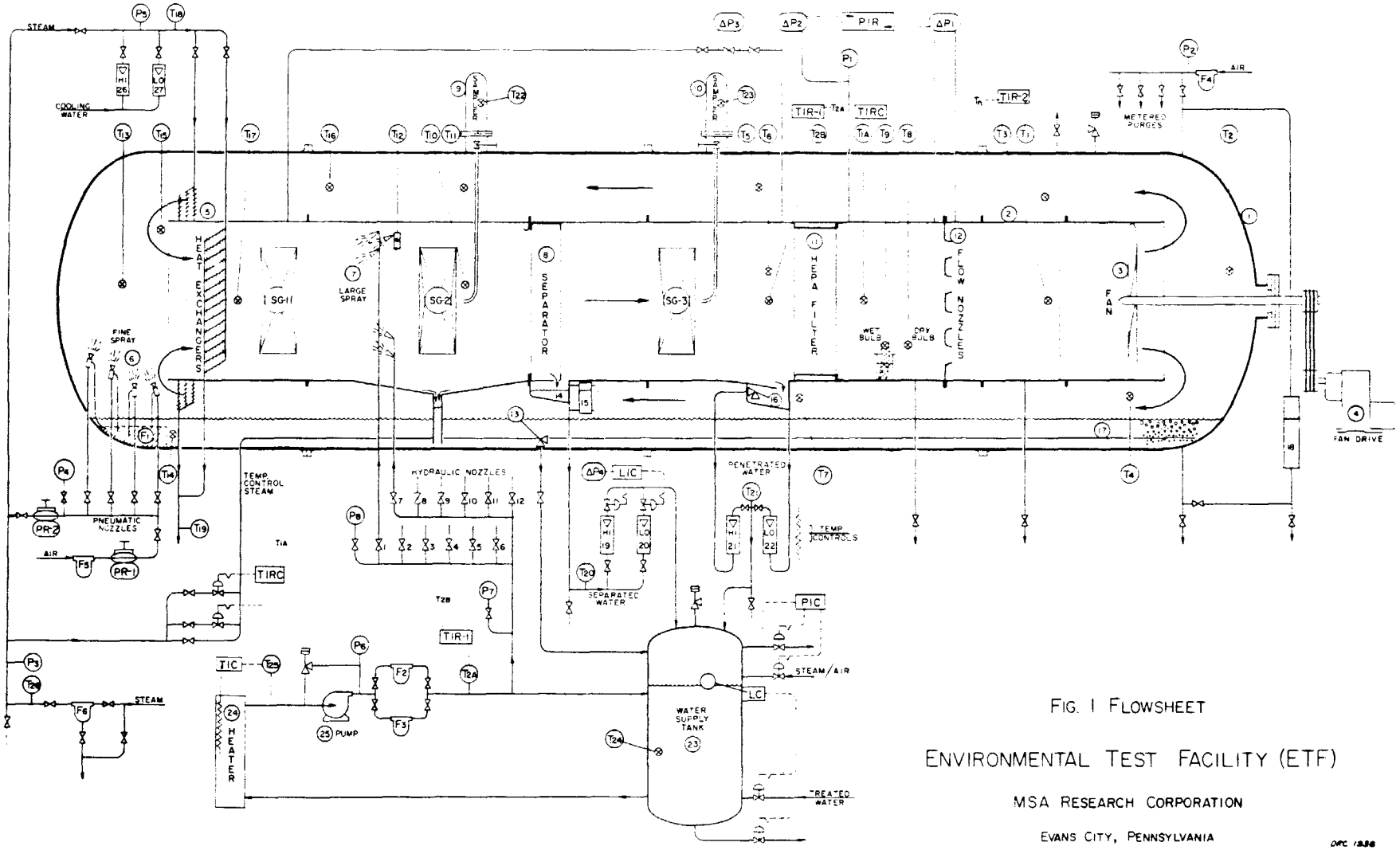

FIG. 1 FLOWSHEET

ENVIRONMENTAL TEST FACILITY (ETF)

MSA RESEARCH CORPORATION

EVANS CITY, PENNSYLVANIA

AK-2516-34

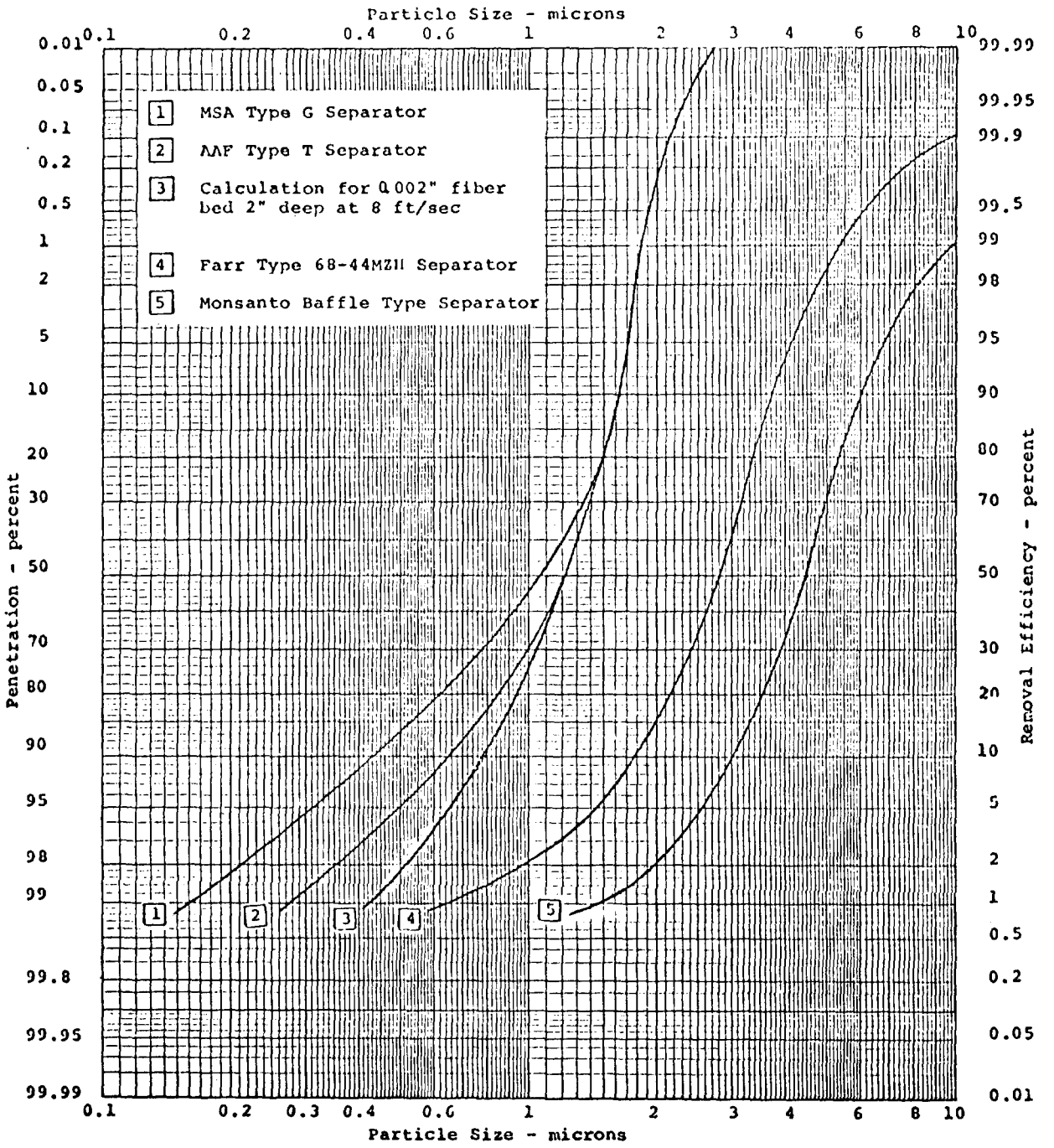

PREDICTED PERFORMANCE OF SEPARATORS

FIGURE 2

Typical Ventilation Systems for Boiling Water Reactor Containment

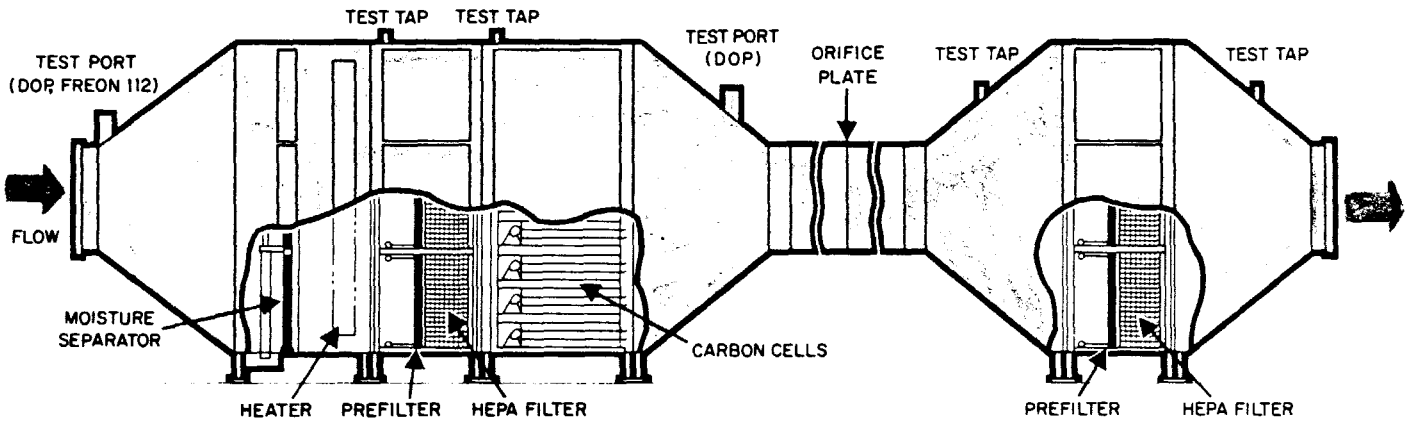

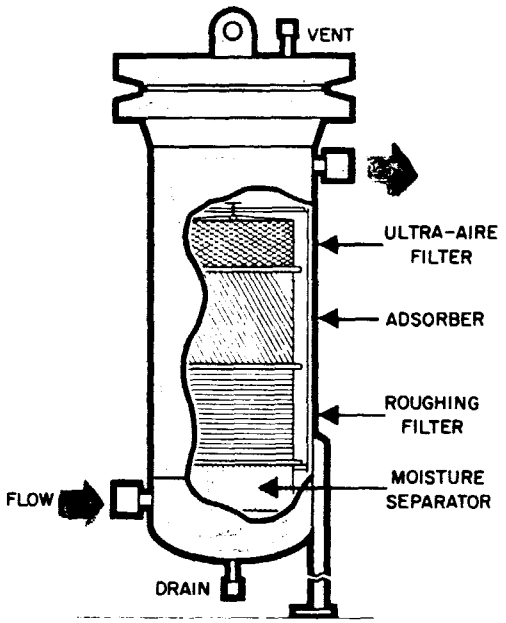

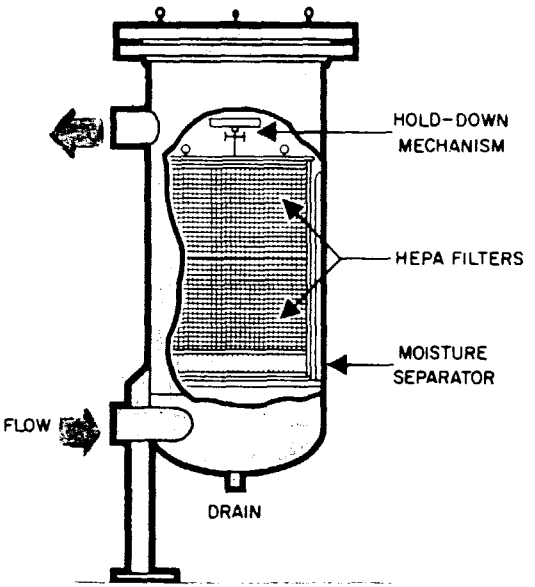

MSA FILTER DIVISION
MINE SAFETY APPLIANCES COMPANY • 201 N. BRADDOCK AVE. PITTSBURGH PA 15208

FIGURE 3

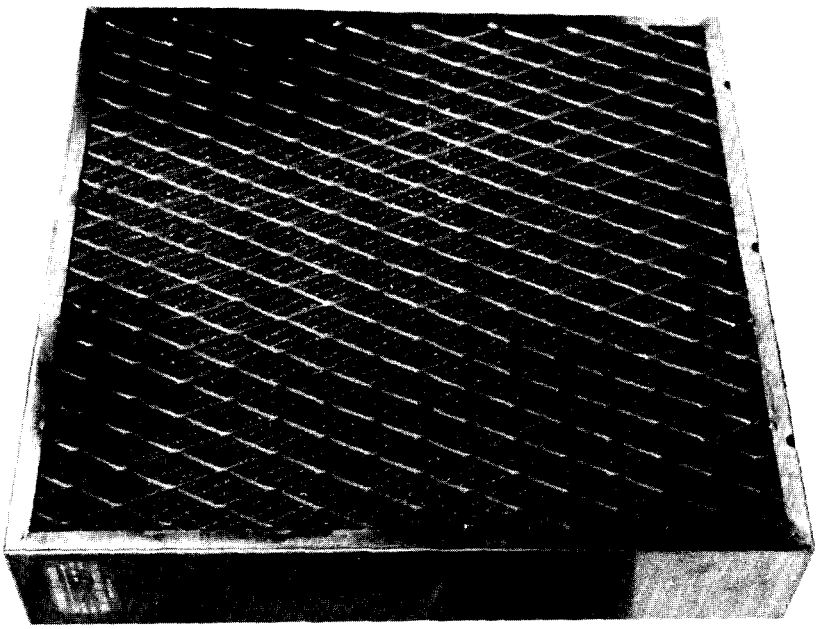

FIGURE 5 - MSA SEPARATOR OUTLET

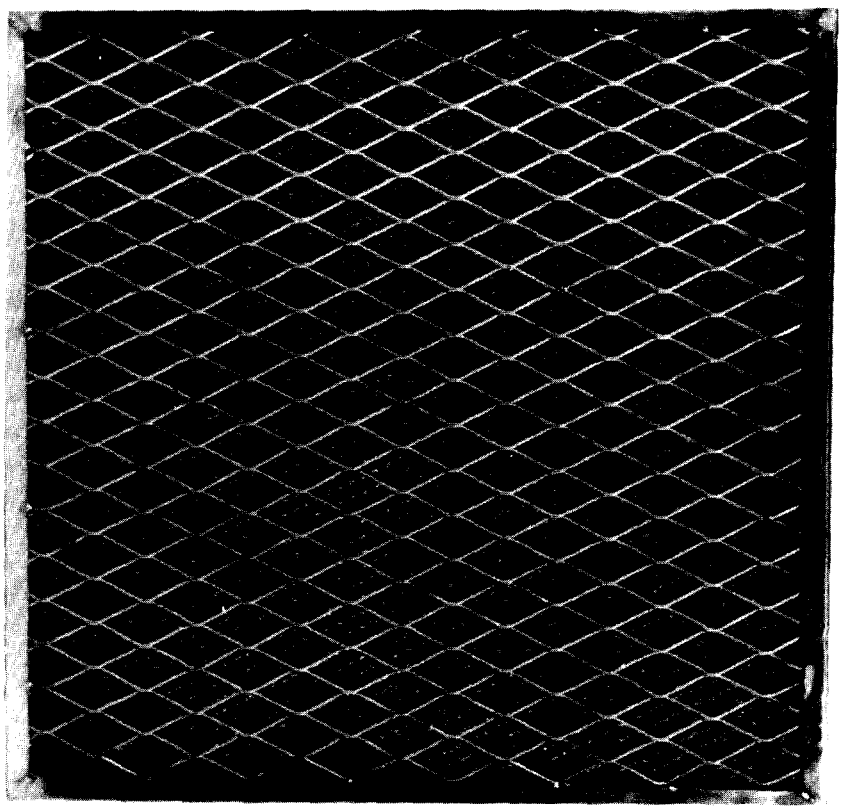

FIGURE 4 - MSA SEPARATOR INLET

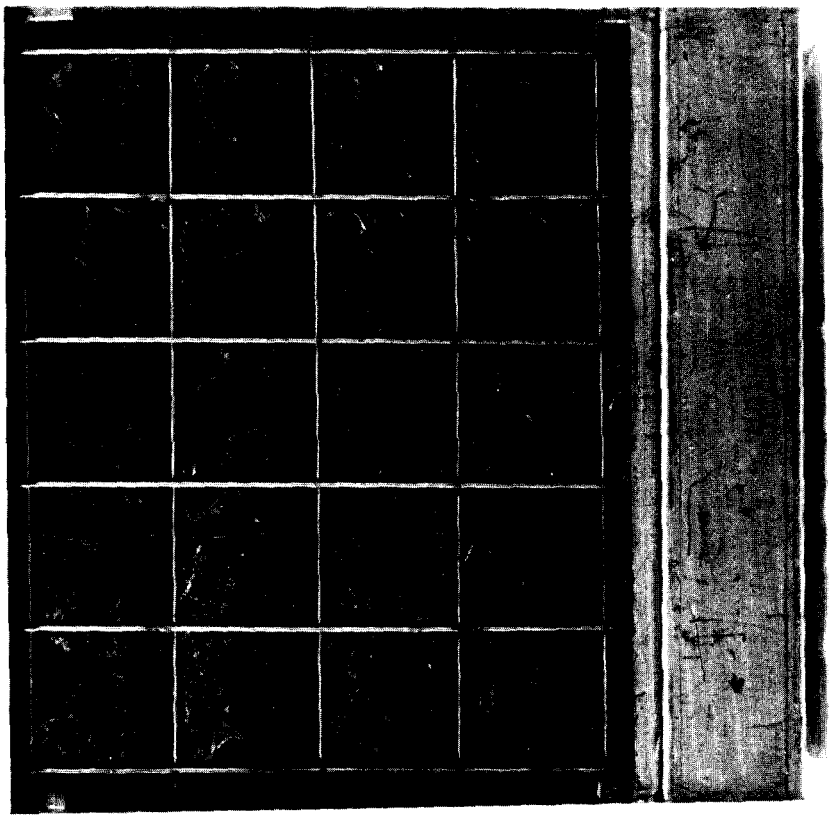

FIGURE 7 - AAF SEPARATOR OUTLET

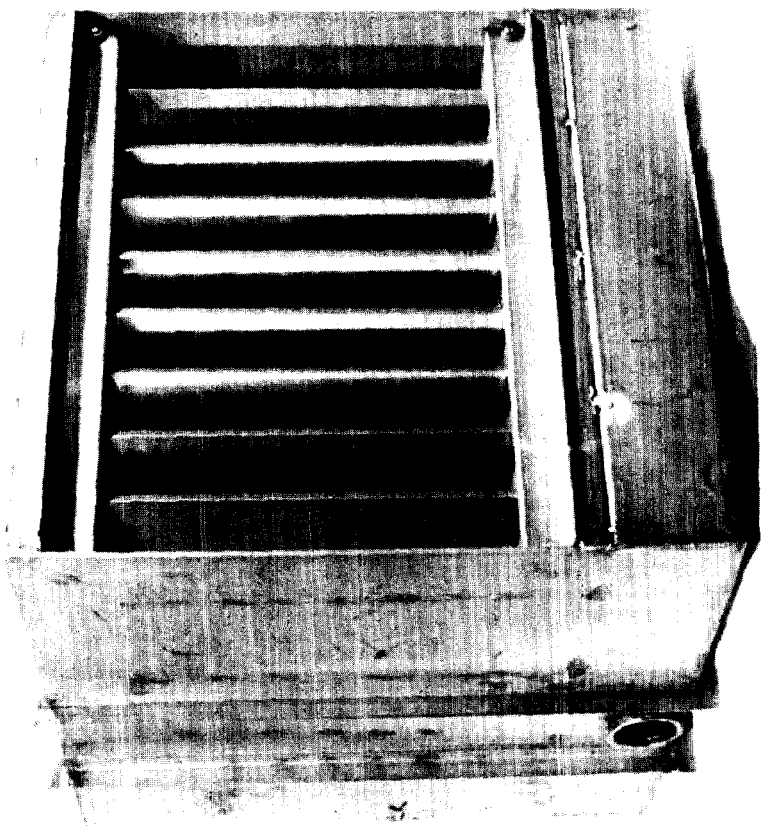

FIGURE 6 - AAF SEPARATOR INLET

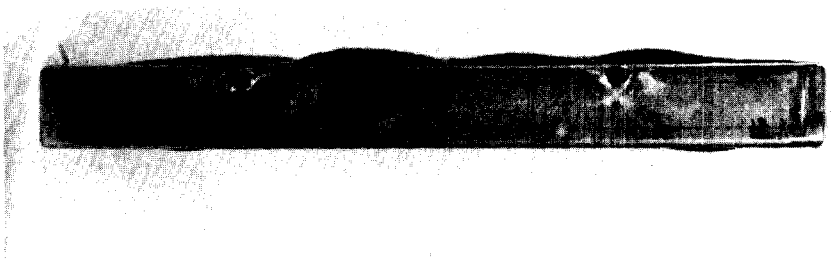

FIGURE 9 - YORK SEPARATOR SHOWING BOTTOM DRAINS - OUTLET ON RIGHT

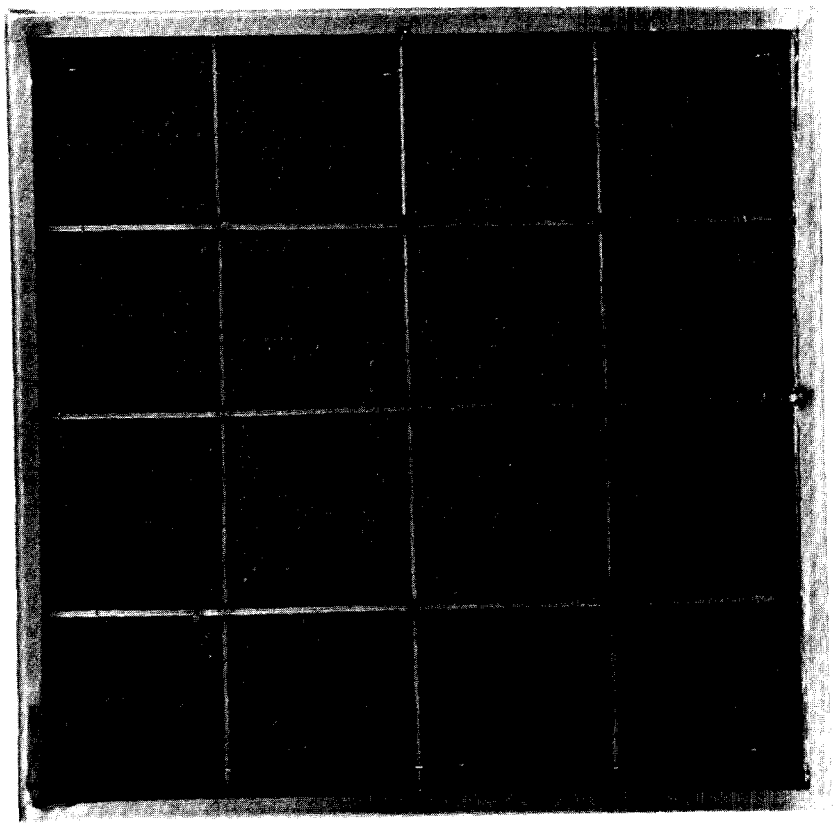

FIGURE 8 - YORK SEPARATOR OUTLET

FIGURE 11 - FARR SEPARATOR OUTLET SHOWING BOTTOM DRAINS

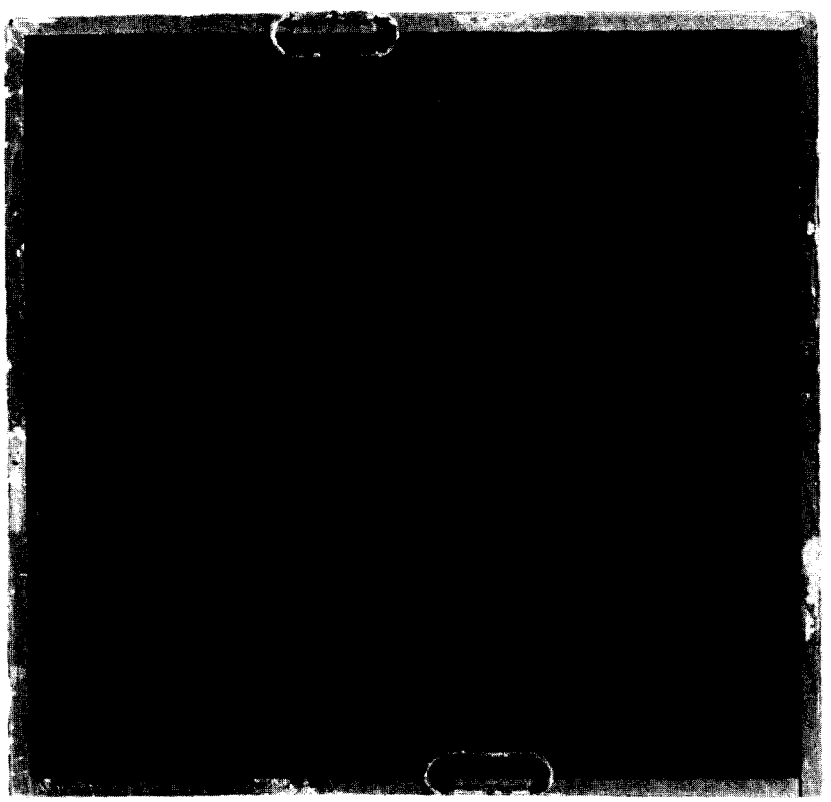

FIGURE 10 - FARR SEPARATOR INLET

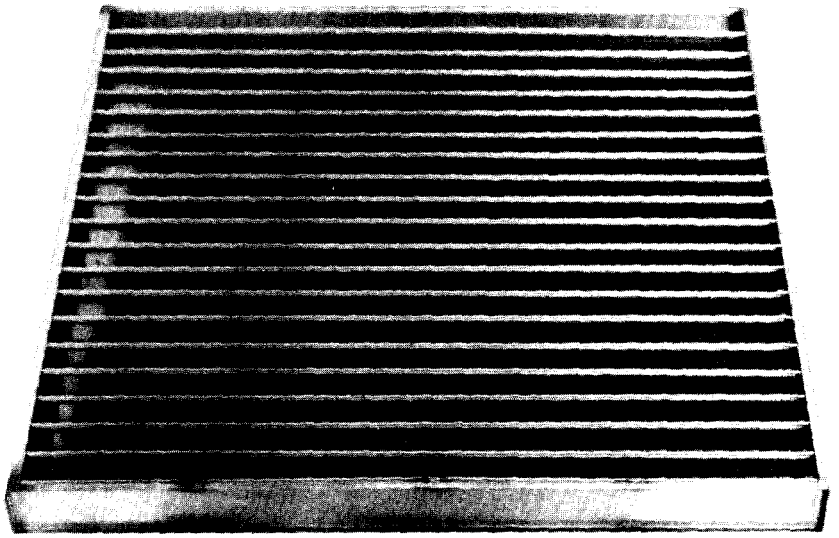

FIGURE 13 - MONSANTO SEPARATOR OUTLET

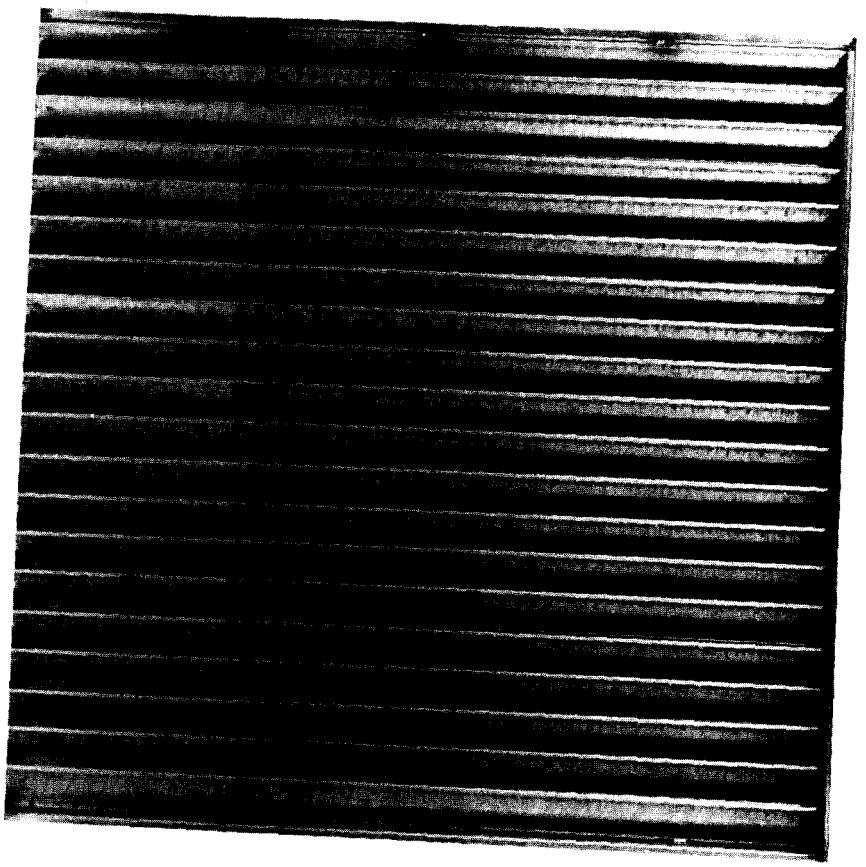

FIGURE 12 - MONSANTO SEPARATOR INLET

RADIOIODINE SORPTION ON ACTIVE CARBONS FROM LIQUID PHASE

Z.Vuković, O.Janković, Lj.Knezević, A.Svabić
Boris Kidric Institute of Nuclear Sciences, Beograd - Vinča - Yugoslavia

Abstract - Résumé

The results of investigation of the efficiency of various kinds of active carbons to the sorption of iodine species from solution with relatively low impurity content under static and dynamic conditions are given. The effects of pH, temperature, impurity concentration, flow rate and particle size were studied. The physical and chemical parameters of the pressurized water reactor's primary and secondary coolant system were simulated during the study. Under dynamic conditions the effects of pH, temperature, particle size, flow rate is explicit, whereas under static conditions most of these parameters have no significant effect.

Operation of nuclear facilities, especially nuclear power plants, generates large quantities of water contaminated with iodine which, if released, could have an important environmental impact. If the iodine can be controlled before it is volatilized to the atmosphere or to the gas phase, the total plant releases of iodine will be reduced proportionately.

The goal of the work was to evaluate the use of active carbon for adsorption of iodine species from large quantities of contaminated water, with relatively low impurity content. Some of the results are presented here.

The experiments were performed under static and dynamic conditions. In static conditions adsorption from solution was studied for 25°C, 45°C and 70°C, using stoppered pyrex flasks. The weight of carbon varied from 0.05 to 0.50 g in 25 cm . Aqueous solutions of I and KI were used. Iodine concentrations were determined by titration with standard sodium thiosulphate solutions. Diluted solutions of iodine and iodide were tagged with I-131 as an extremely diluted solution of potassium iodide in sodium bicarbonate. A well-type, scintillation counter was used for monitoring of radioactive iodine.

The apparatus used for the dynamic flow studies is shown on Figure 1. By doser pump (1) the solution from the vessel (2) was taken through the column (3) which was filled with the activated carbon. The effluent flowed through the magnetic valve to the collection vessel (4) from which the samples for analysis were taken. The flow rate was regulated by a manostat (6).

The active carbons used were (C_1) Nuchar WV-W 12x40 Mesh, (C_2) Nuchar WV-W 8x30 Mesh, (C_3) Nuchar MW-H 6x16 Mesh, (C_4) Nuchar WV-L 8x30 Mesh, (C_5) Nuchar WV-G 12x4 Mesh, (C_6) Nuchar C-190 plus 30 Mesh, (C_7) C-190-N-powder.

Figures (2-4) show sorption isotherms for iodide and iodine for each carbon at temperatures of 25°C, 45°C and 70°C. Carbons (C_1 - C_5) have similar adsorption characteristics whereas carbons C_6 and C_7 are not suitable adsorbent for iodine as compared to the former.

According to the data obtained for the impurity contents[1] in the primary and secondary coolant in several power plants, the following conditions were selected as "typical." The maximum concentration of chloride was 75 ppm. "Synthetic coolant" contained LiOH (as Li), H_3BO_3 (as B), and KCI in the ratio 5ppm: 20ppm; 75 ppm respectively.

The pH of the carbon extract was 8.4 + 0.4. Owing to buffer properties of carbon, the following reaction of hydrolysis is favorable[2]:

$$I_2 + H_2O = H^+ + I^- + HOI$$

Hypoiodous acid is present in our experiments. Since hypoiodous acid and iodide are weakly adsorbed on active carbon, impregnation is a necessary step in order to improve the sorption charecteristics of carbon. Impregnation with silver salts give the best results in comparison with other procedures (Figure 5).

Table 1 shows bed volumes for inlet concentrations decreasing to 1% (K =100) at a flow rate of 16.5 cm/min. Particle size and flow rate have important effects on the sorption efficiency.

In dechlorination processes the half-length value is used as a measure of efficiency. The half length is a characteristic value of the carbon bed length required to decrease the inlet concentration to one half[3]. In decontamination processes, i.e., in the iodine sorption process, the arbitrary standard factor is assumed to be that bed volume value at which the inlet concentration decreases to 10% or to 1% that is the desired decontamination factor is 10 to 100. Figures (6-7) show the dependence of the 10% length value on particle size and flow rate. As expected, the efficiency decreases with particle size but increases with flow rate. The longitudinal distribution along the bed length shows that only a small part of the carbon capacity is exhausted (Figure 8).

The results indicate the dominant role of three parameters for selective adsorption of iodine on carbon from the liquid phase; pH of the solution, column geometry, and impregnation condition.

References

1. W.N. Thomasson, Private communication (1972)

2. F.O.Carton, H.R.Beard, F.A. Duce, J.H.Keller Evidence for the Existence of Hypoidous Acid, "Proceedings of the Tenth Air Cleaning Conference," New York (August 1968).

3. M.Smisek, S.Cerny, Active Carbon, Elsevier Publishing Company, Amsterdam -London - New York 1970.

TABLE I.

BED VOLUME FOR K = 100; FLOW RATE = 16.5 CM/MIN.

IODINE SPECIES	TEMP.	25°C		45°C				75°C	
	CARBON (ppm)	20	100	10	20	50	100	10	100
I_2	ACTIVE C	1300	220	750	100	80	50	—	—
I^-	ACTIVE C	300	<100	<250	100	80	50	—	<100
I^-	IMPREGNATED	>9500	6000	9500	>9000	9000	5800	<250	<250

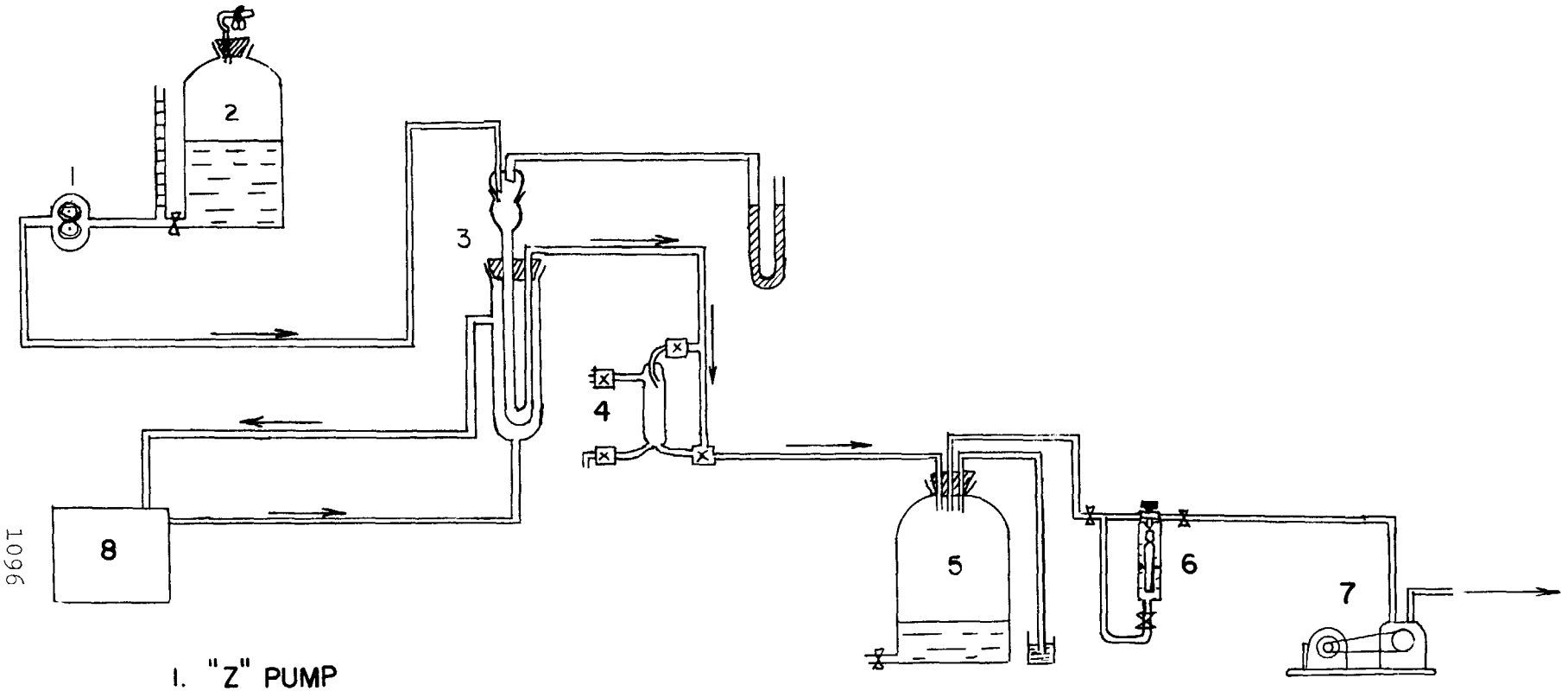

1. "Z" PUMP
2. VESSEL
3. COLUMN
4. SAMPLING
5. VESSEL
6. MANOSTAT
7. VACUUM PUMP
8. THERMOSTAT

FIGURE 1.

SCHEMATIC DIAGRAM OF TEST APPARATUS

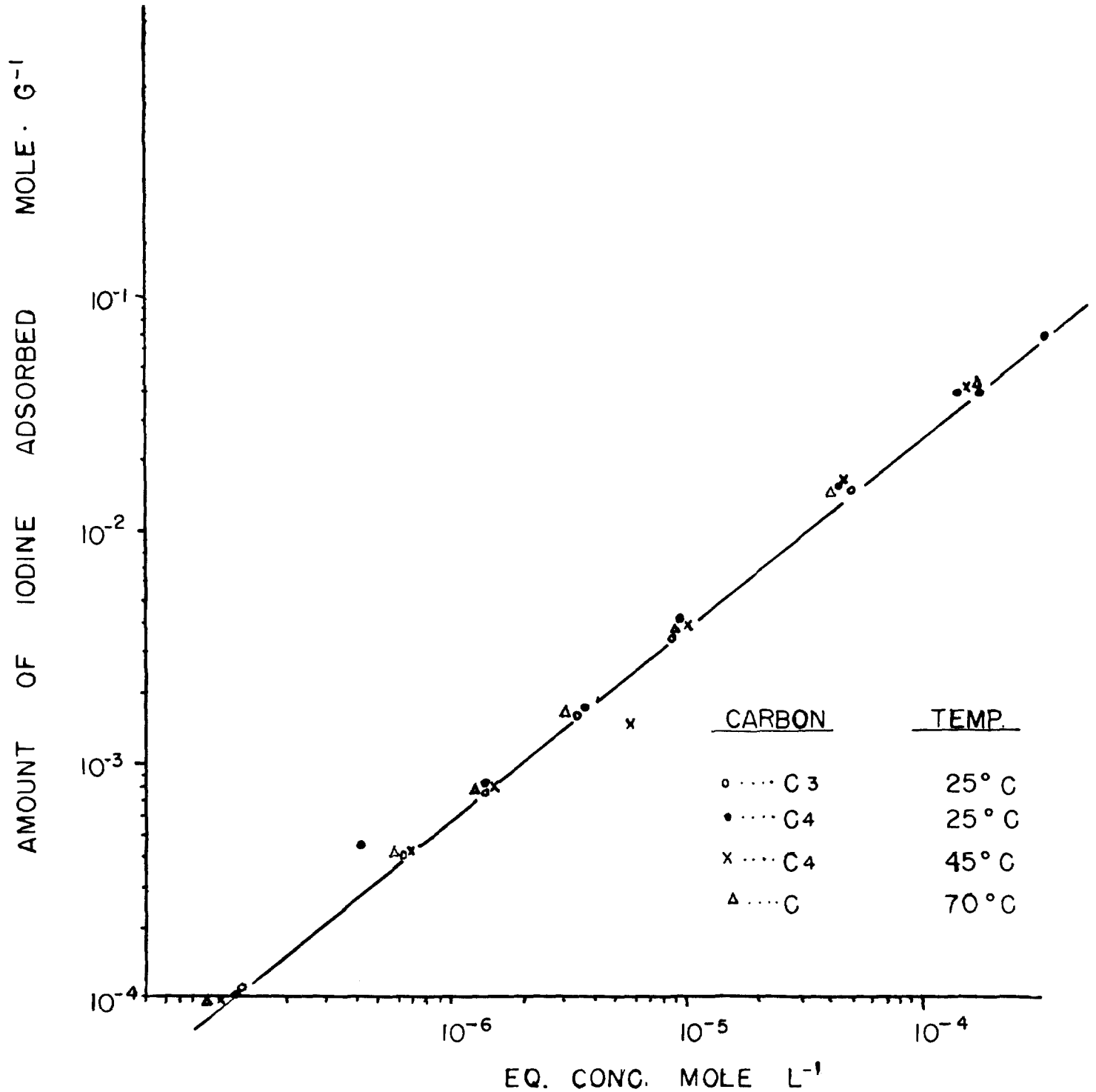

FIG. 2 SORBED AMOUNT OF IODINE AT 25°C, 45°C, 70°C

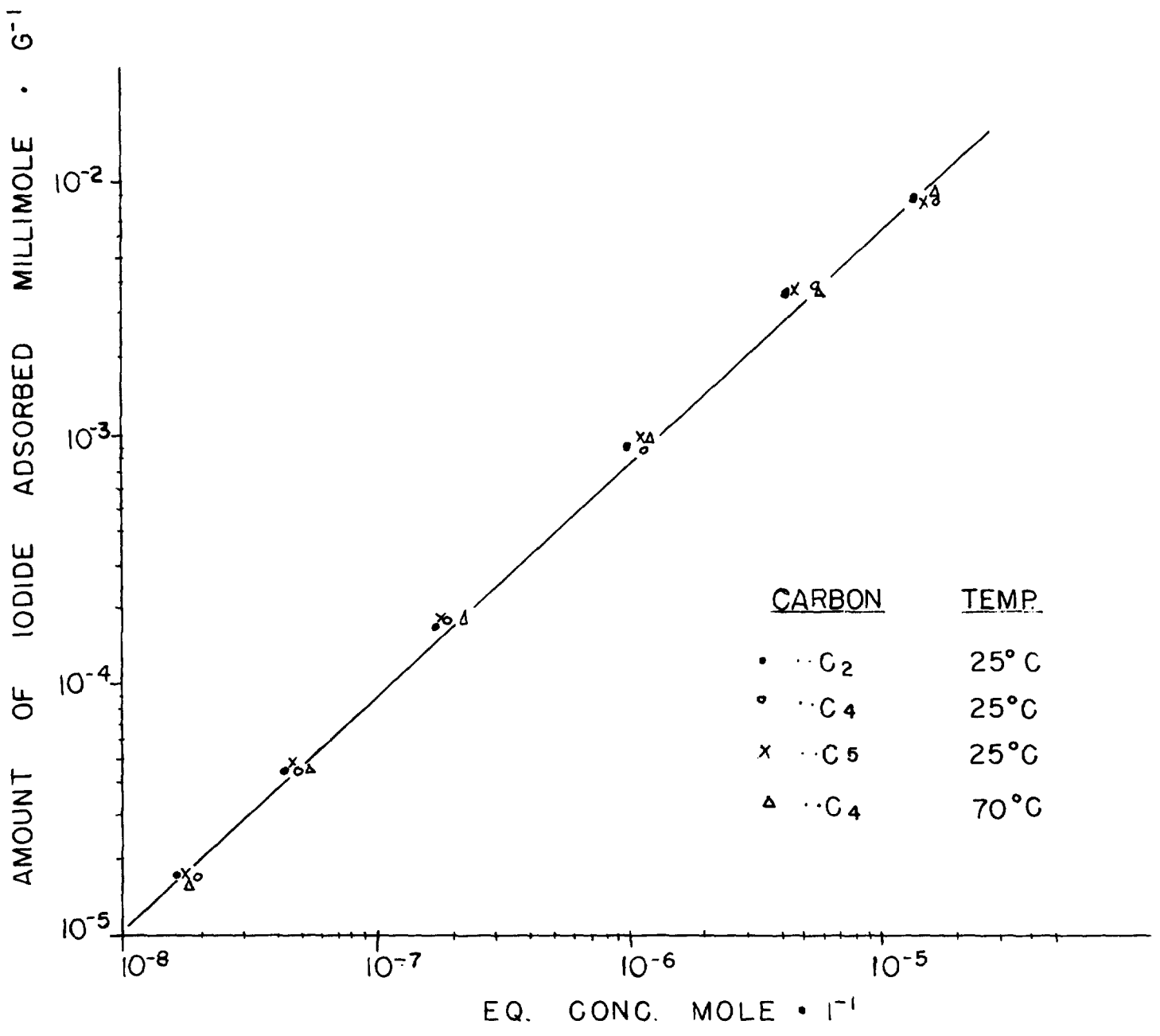

FIG. 3 SORBED AMOUNT OF IODIDE.

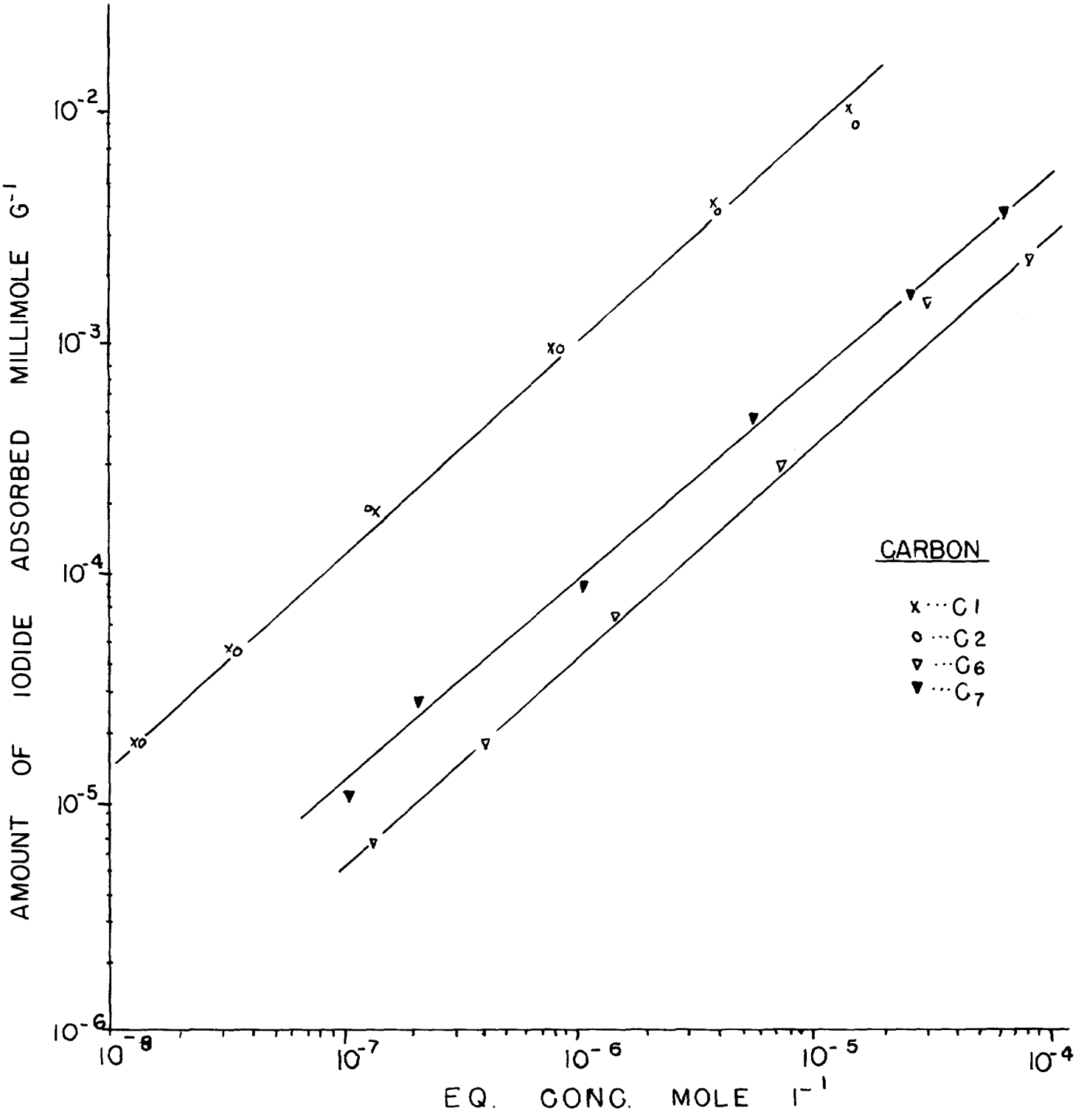

FIG. 4. SORBED AMOUNT OF IODIDE AT 25°C

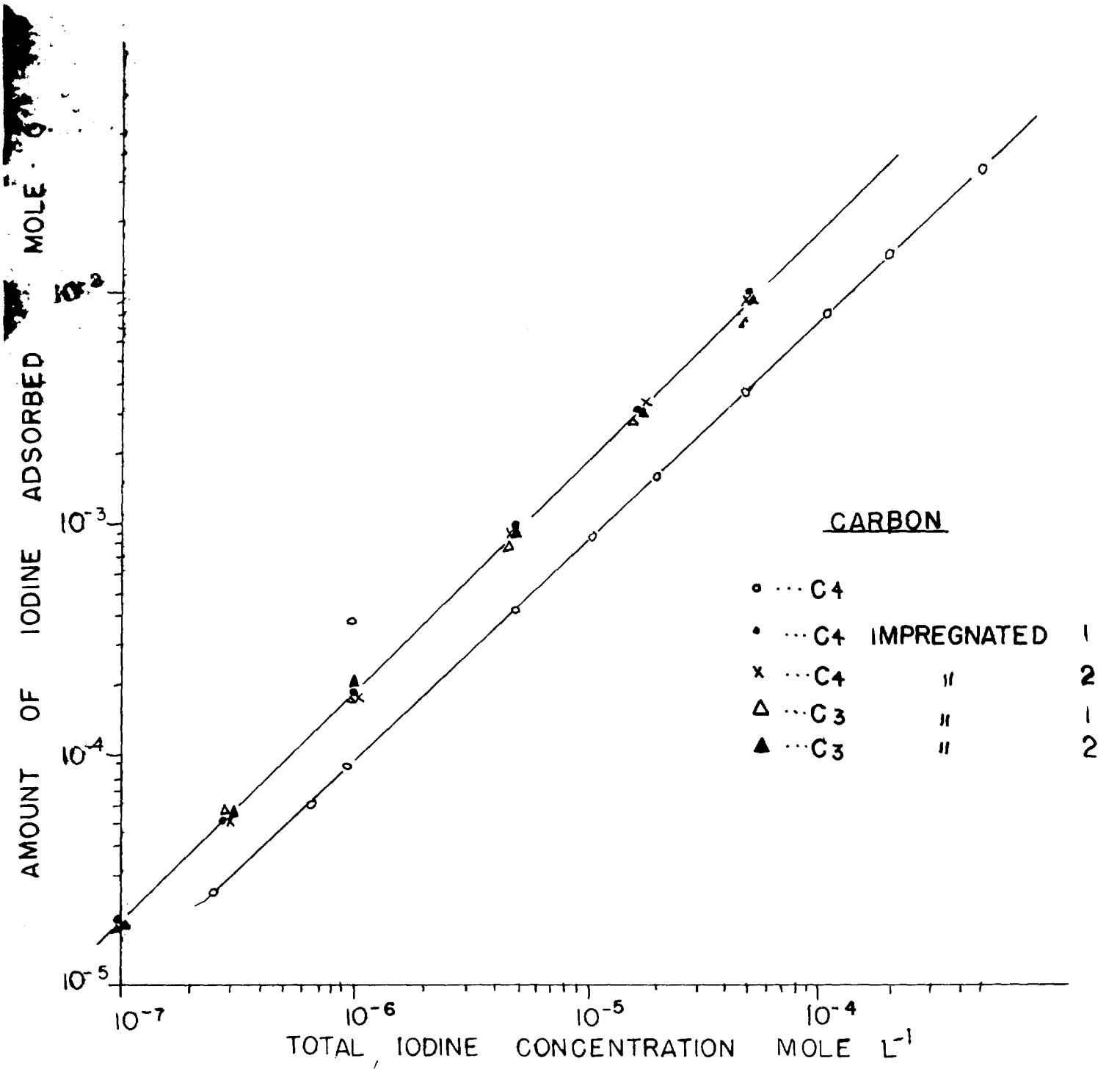

FIG. 5. DEPENDANCE OF ADSORBED AMOUNT OF IODINE OF TOTAL IODINE CONCENTRATION.

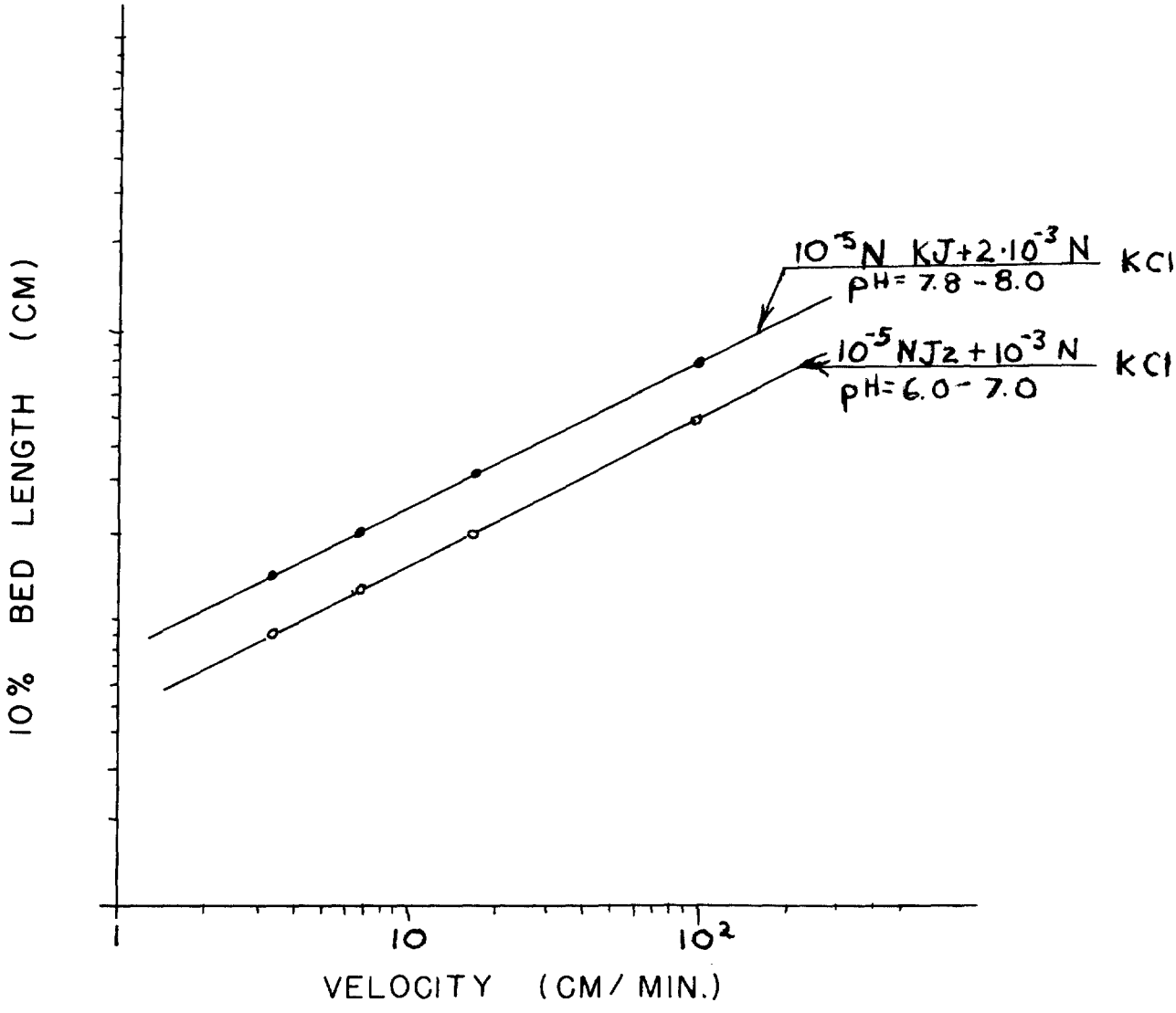

FIG. 6. SORPTION EFFICIENCY OF IODINE AND IODIDE VERSUS SOLUTION FLOW RATE, CARBON C_2

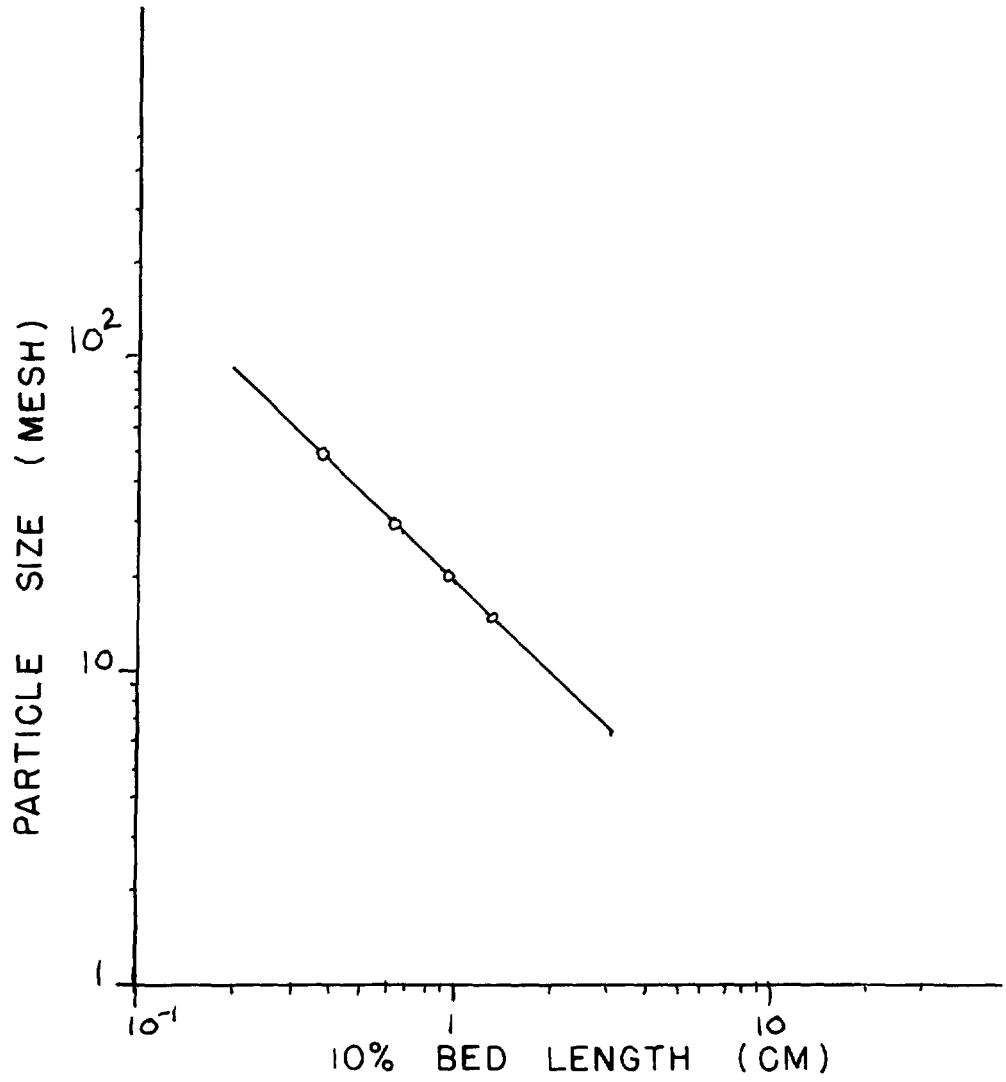

FIG. 7. THE EFFECT OF CARBON PARTICLE SIZE ON SORPTION EFFICIENCY FOR IODINE (VELOCITY 3.3 CM / MIN.)

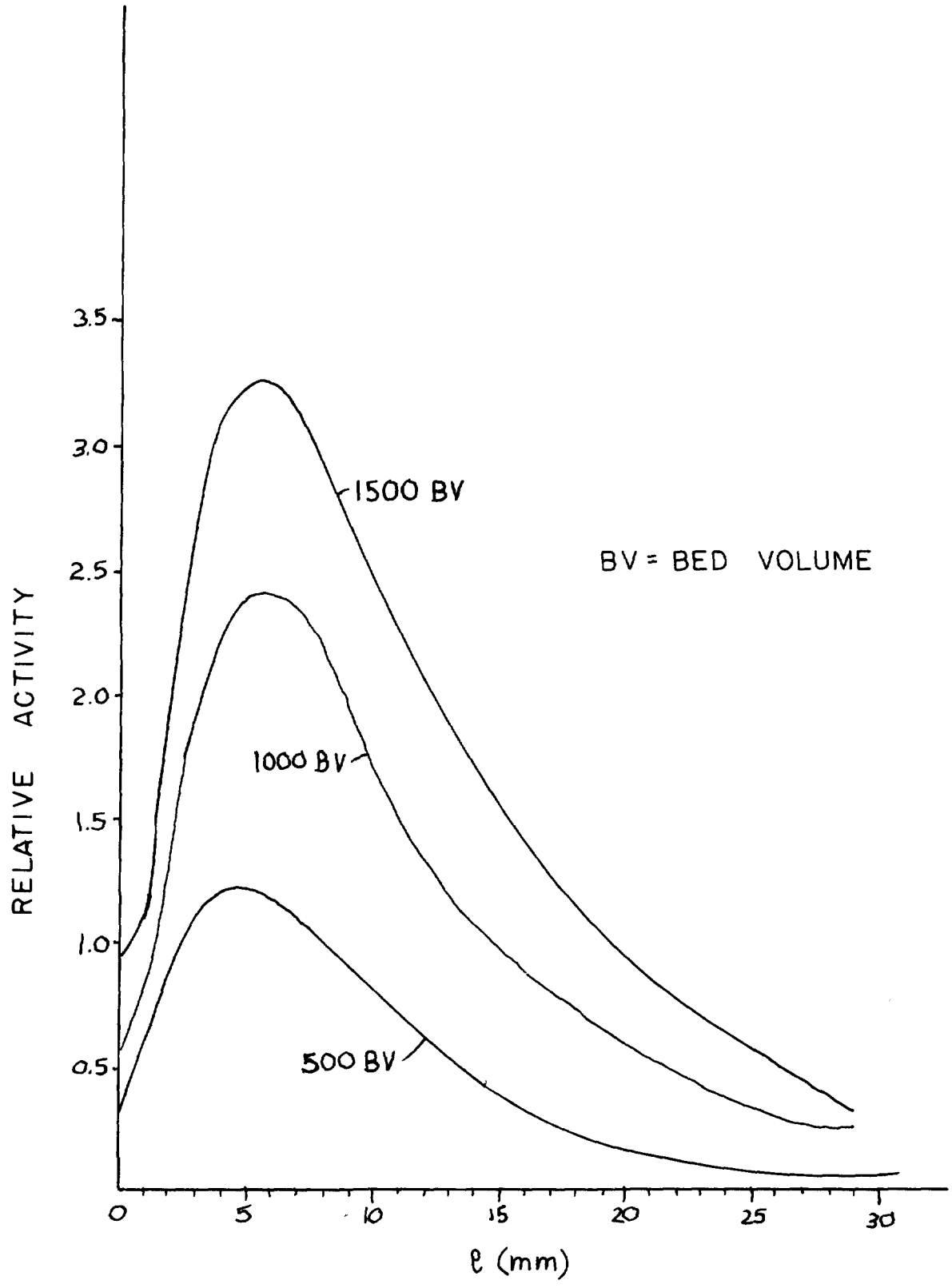

FIG. 8. LONGITUDINAL DISTRIBUTION OF IODINE ACTIVITY.